

**ASSESSING BUILDING VULNERABILITY TO TSUNAMI HAZARD
USING INTEGRATIVE REMOTE SENSING AND
GIS APPROACHES**

Dissertation
der Fakultät für Geowissenschaften
der Ludwig-Maximilians-Universität München



eingereicht von

Sumaryono

im September 2010

1. Gutachter: Prof. Dr. Ralf Ludwig

2. Gutachter: Prof. Dr. Günter Strunz

Datum der Disputation: 9. Dezember 2010

ACKNOWLEDGMENTS

First of all, I would like to express my sincere gratitude and appreciations to my supervisors Prof. Dr. Ralf Ludwig and Prof. Dr. Günter Strunz for their constant helps, encouragements and invaluable suggestions during my Ph.D study. They inspire me very much how to express my ideas and showed me different paths to approach research problems and to accomplish final goals. I also express my special thanks to Dr. Joachim Post, Dr. Kai Zoßeder, Dr. Torsten Riedlinger, Matthias Mück, Stephanie Wegscheider and Dr. Jörg Szarzynski for invaluable daily supports, sharing ideas and fruitful discussions that enrich my knowledge and experiences not only about technical things but also about things that make living in Germany enjoyable.

I convey my honest thanks to Prof. Stefan Dech and Dr. Harald Mehl for having opened the doors of DLR-Oberpfaffenhofen for my Ph.D work and also to Ir. R.W. Matindas, M.Sc., Dr. Asep Karsidi M.Sc., Dr. Aris Poniman, Drs. Sukendra Martha, M.Sc., Dr. Cecep Subarya, M.Sc., Ir. Agus Hermawan Atmadilaga, M.Sc., Drs. Suwahyuono, M.Sc and Drs. Adi Rusmanto, M.Sc. for giving me invaluable supports and opportunities to study in Germany.

Many thanks to Dr. Thomas Zschocke and Evalyne Katabaro for managing administrative matters and also many thanks to all GITEWS Ph.D students of United Nations University, Institute for Environment and Human Security (UNU-EHS) for mutual collaboration and warm togetherness in carrying out the research.

My heartfelt thanks to my dear parents, my parents-in-law, my brothers and my sisters for their love, affection, advice, suggestions, consoling talks and so on.

Lastly but not the least, I would like to express my gratefulness and my appreciation to my beloved wife Rani, my lovely children, Khansa, Hasby, Alfi and Kaureena for their supports, love, encouragement and care during the period of my studies.

Financial Support of this work is provided by United Nations University, Institute for Environment and Human Security (UNU-EHS) in close-collaboration with German Aerospace Center (DLR). Finally, I convey my thanks to all individuals and institutions, who have assisted me during my study.

SUMMARY

Risk and vulnerability assessment for natural hazards is of high interest. Various methods focusing on building vulnerability assessment have been developed ranging from simple approaches to sophisticated ones depending on the objectives of the study, the availability of data and technology. In-situ assessment methods have been widely used to measure building vulnerability to various types of hazards while remote sensing methods, specifically developed for assessing building vulnerability to tsunami hazard, are still very limited. The combination of remote sensing approaches with in-situ methods offers unique opportunities to overcome limitations of in-situ assessments.

The main objective of this research is to develop remote sensing techniques in assessing building vulnerability to tsunami hazard as one of the key elements of risk assessment. The research work has been performed in the framework of the GITEWS (German-Indonesian Tsunami Early Warning System) project. This research contributes to two major components of tsunami risk assessment: (1) the provision of infrastructure vulnerability information as an important element in the exposure assessment; (2) tsunami evacuation modelling which is a critical element for assessing immediate response and capability to evacuate as part of the coping capacity analysis.

The newly developed methodology is based on the combination of in-situ measurements and remote sensing techniques in a so-called “bottom-up remote sensing approach”. Within this approach, basic information was acquired by in-situ data collection (bottom level), which was then used as input for further analysis in the remote sensing approach (upper level). The results of this research show that a combined in-situ measurement and remote sensing approach can be successfully employed to assess and classify buildings into 4 classes based on their level of vulnerability to tsunami hazard with an accuracy of more than 80 percent. Statistical analysis successfully revealed key spatial parameters which were regarded to link

parameters between in-situ and remote sensing approach such as size, height, shape, regularity, orientation, and accessibility. The key spatial parameters and their specified threshold values were implemented in a decision tree algorithm for developing a remote sensing rule-set of building vulnerability classification. A big number of buildings in the study area (Cilacap city, Indonesia) were successfully classified into the building vulnerability classes. The categorization ranges from high to low vulnerable buildings (A to C) and includes also a category of buildings which are potentially suitable for tsunami vertical evacuation (VE).

A multi-criteria analysis was developed that incorporates three main components for vulnerability assessment: stability, tsunami resistance and accessibility. All the defined components were configured in a decision tree algorithm by applying weighting, scoring and threshold definition based on the building sample data. Stability components consist of structure parameters, which are closely related to the building stability against earthquake energy. Building stability needs to be analyzed because most of tsunami events in Indonesia are preceded by major earthquakes. Stability components analysis was applied in the first step of the newly developed decision tree algorithm to evaluate the building stability when earthquake strikes. Buildings with total scores below the defined threshold of stability were classified as the most vulnerable class A. Such the buildings have a high probability of being damaged after earthquake events. The remaining buildings with total scores above the defined threshold of stability were further analyzed using tsunami components and accessibility components to classify them into the vulnerability classes B, C and VE respectively.

This research is based on very high spatial resolution satellite images (QuickBird) and object-based image analysis. Object-based image analysis is chosen, because it allows the formulation of rule-sets based on image objects instead of pixels, which has significant advantages especially for the analysis of very high resolution satellite images. In the pre-processing stage, three image processing steps were performed: geometric correction, pan-sharpening and filtering. Adaptive Local Sigma and

Morphological Opening filter techniques were applied as basis for the subsequent building edge detection. The data pre-processing significantly increased the accuracy of the following steps of image classification.

In the next step image segmentation was developed to extract adequate image objects to be used for further classification. Image classification was carried out by grouping resulting objects into desired classes based on the derived object features. A single object was assigned by its feature characteristics calculated in the segmentation process. The characteristic features of an object - which were grouped into spectral signature, shape, size, texture, and neighbouring relations - were analysed, selected and semantically modelled to classify objects into object classes. Fuzzy logic algorithm and object feature separation analysis was performed to set the membership values of objects that were grouped into particular classes. Finally this approach successfully detected and mapped building objects in the study area with their spatial attributes which provide base information for building vulnerability classification. A building vulnerability classification rule-set has been developed in this research and successfully applied to categorize building vulnerability classes.

The developed approach was applied for Cilacap city, Indonesia. In order to analyze the transferability of this newly developed approach, the algorithm was also applied to Padang City, Indonesia. The results showed that the developed methodology is in general transferable. However, it requires some adaptations (e.g. thresholds) to provide accurate results.

The results of this research show that Cilacap City is very vulnerable to tsunami hazard. Class A (very vulnerable) buildings cover the biggest portion of area in Cilacap City (63%), followed by class C (28%), class VE (6%) and class B (3%). Preventive measures should be carried out for the purpose of disaster risk reduction, especially for people living in such the most vulnerable buildings.

Finally, the results were applied for tsunami evacuation modeling. The buildings, which were categorized as potential candidates for vertical evacuation, were selected and a

GIS approach was applied to model evacuation time and evacuation routes. The results of this analysis provide important inputs to the disaster management authorities for future evacuation planning and disaster mitigation.

TABLE OF CONTENTS

SUMMARY	i
TABLE OF CONTENTS	v
LIST OF FIGURES	ix
LIST OF TABLES	xii
LIST OF ACRONYMS	xiii
CHAPTER 1. INTRODUCTION	1
1.1. Motivation	1
1.2. Research Problems	4
1.3. Research Objectives	5
1.4. Main Benefit of The Research	5
1.5. Thesis Structure	6
CHAPTER 2. RESEARCH FRAMEWORK	8
2.1. The GITEWS Project.....	8
2.2. Risk and Vulnerability Assessment Framework of the Research	10
2.3. Study Area	12
2.3.1. Geographic and Demographic Conditions	13
2.3.2. Urban Structure and Economic Conditions	13
2.3.3. Tectonic Structures	14
CHAPTER 3. LITERATURE REVIEW AND STATE OF THE RESEARCH	16
3.1. Vulnerability: An Interdisciplinary Concept	16
3.2. Vulnerability Assessment Methods	18
3.3. Vulnerability Indicators.....	21

3.4.	In-situ Building Vulnerability Assessment	22
3.5.	Remote Sensing and GIS based Building Vulnerability Assessment.....	28
3.5.1.	Object-Based Image Analysis	28
3.5.2.	OBIA Applications for Building Analysis	31
3.5.3.	OBIA Applications for Building Vulnerability Assessment.....	35
CHAPTER 4.	METHODOLOGY	37
4.1.	Bottom-up Approach: Combining In-situ Survey and Remote Sensing Methods	37
4.2.	In-Situ Survey	39
4.2.1.	Sampling Techniques.....	39
4.2.2.	Building Vulnerability Parameters	40
4.2.2.1.	Building Stability Parameters	40
4.2.2.2.	Tsunami Component Parameters	41
4.2.2.3.	Accessibility Parameters	42
4.2.3.	The Concept of Building Vulnerability Classification.....	43
4.2.4.	Scoring Method	44
4.3.	Remote Sensing and GIS Approach: Object-based Image Analysis.....	45
4.3.1.	Pre-Processing	45
4.3.2.	Image Analysis	46
4.3.2.1.	Segmentation	46
4.3.2.2.	Image Classification	48
4.3.2.3.	Accuracy Assessment of the Building Detection	56
4.3.2.4.	Statistical Analysis.....	57
4.3.2.5.	Building Vulnerability Classification	57
4.3.2.6.	Accuracy Assessment of the Building Vulnerability	60

Classification	
4.3.3. Transferability Analysis.....	61
CHAPTER 5. RESULTS OF THE RESEARCH	62
5.1. In-situ Survey	62
5.1.1. Building Sample Selection	62
5.1.2. Building Samples Classification using Direct Field Measurements	63
5.1.3. Statistical Analysis	63
5.1.3.1. Boxplot Analysis of Building Area.....	64
5.1.3.2. Boxplot Analysis of Building Height.....	65
5.2. Remote Sensing Approach	65
5.2.1. Pan-Sharpning	65
5.2.2. Image Filtering	67
5.2.3. Image Segmentation	69
5.2.4. Building Detection Analysis	72
5.2.4.1. Object Features Selection	72
5.2.4.2. Building Detection	72
5.2.5. Remote Sensing Technique for Building Vulnerability Classification	75
5.2.6. Accuracy Assessment	75
5.2.7. Transferability Analysis.....	78
CHAPTER 6. APPLICATION OF THE RESEARCH: Tsunami Evacuation Modelling....	82
6.1. Introduction	82
6.2. Distribution of Vertical Evacuation Target Points	83
6.3. Accessibility Modelling	85

6.4.	Evacuation Modelling	86
6.4.1.	Evacuation Shelter Capacity and Time Area	87
6.4.2.	Evacuation Routes	89
CHAPTER 7. DISCUSSION	91
7.1.	Building Vulnerability Assessment Using Bottom up Approach.....	91
7.2.	Image Segmentation	99
7.3.	Building Detection	104
7.4.	Comparison of Building Detection Methods	105
7.5.	Transferability Analysis	106
7.6.	Research Application: Tsunami Evacuation Modelling	107
CHAPTER 8. CONCLUSIONS	109
REFERENCES	112
APPENDIX	128
CURRICULUM VITAE	133

LIST OF FIGURES

1.1.	Map of global tsunami hazard.....	2
1.2.	Tsunami Hazard Map of Indonesia.....	2
2.1.	The GITEWS Project Organization comprises several Work Packages conducted by a consortium of nine large German institutions	9
2.2.	The concept of the Tsunami Early Warning and Mitigation Centre	9
2.3.	Risk and vulnerability assessment framework	10
2.4.	Study Area	14
2.5.	Location of the study area and its distance from the last epicentre of the 17 July 2006 earthquake-tsunami	15
3.1.	Building vulnerability classification used in the European Macroseismic Scale (EMS).....	24
3.2.	Procedural steps of building-based damage analysis.....	33
4.1.	The general workflow of the combined in-situ survey and remote sensing approach.....	38
4.2.	The decision tree approach of building vulnerability assessment.....	43
4.3.	Multiple objects level of segmentation algorithm	48
4.4.	Flow chart of the building extraction algorithm.....	52
4.5.	Membership function of customized feature BR 7 for water classification	53
4.6.	Decision tree analysis for building vulnerability classification using object-based image analysis.....	58
5.1.	The distribution of building samples for in-situ assessment	62
5.2.	Building vulnerability classification using in-situ assessment	63
5.3.	Boxplot analysis of building size (area) and building vulnerability classes...	64
5.4.	Boxplot analysis of building height and building vulnerability classes.....	65

5.5.	The results of image pan-sharpening process.....	66
5.6.	Image filtering result using adaptive local sigma and morphology opening algorithms	67
5.7.	Horizontal pixel profile of red band of QuickBird image: (a) before filtering process, (b) after filtering process and (c) comparison before (red line) and after filtering (blue line)	68
5.8.	The results of multilevel image segmentation	70
5.9.	Segmentation level 4 is suitable for vegetation detection	70
5.10.	Level 2 is suitable for buildings segmentation.....	71
5.11.	The results of building detection process based on roof colour	73
5.12.	The result of building detection analysis.....	74
5.13.	Building vulnerability classification results	76
5.14.	Manually digitized buildings for a reference map of accuracy assessment	77
5.15.	The result of building extraction analysis of Padang city area using IKONOS.....	79
5.16.	The result of transferability analysis of building vulnerability classification in Padang	80
6.1.	Tsunami evacuation modelling concept.....	83
6.2.	Hazard zone map modelling using pre-calculated scenarios	84
6.3.	Hazard zone map for tsunami major warning level.....	84
6.4.	Vertical evacuation buildings distribution	85
6.5.	Workflow of accessibility modelling	86
6.6.	Evacuation shelter capacity and time area approach.....	87
6.7.	Workflow of evacuation shelter capacity and time area.....	88
6.8.	Evacuation shelter capacity and time area in Cilacap city.....	88
6.9.	Interactive evacuation routes	90

7.1.	Buildings classified as class A	92
7.2.	Typical small buildings which are vulnerable to tsunami hazard.....	93
7.3.	Detecting irregular buildings using elliptic fit value object feature.....	94
7.4.	Buildings classified as class B	96
7.5.	Buildings classified as class C	97
7.6.	Buildings classified as class VE	98
7.7.	Comparison of two adjacent building profiles before and after filtering.....	102
7.8.	Comparison of image segmentation results before filtering and after filtering ...	103

LIST OF TABLES

3.1.	Building Vulnerability Parameters.....	25
3.2.	Summary of various available building vulnerability assessment methods.....	28
4.1.	Building stability parameters, thresholds and their weight factors.....	40
4.2.	Tsunami component parameters.....	41
4.3.	Accessibility parameters.....	42
4.4.	Selected features for object classification.....	50
4.5.	Results of the Feature Separability analysis.....	56
4.6.	Confusion matrix for accuracy assessment of building vulnerability.....	60

LIST OF ACRONYMS

ADPC	: Asian Disaster Preparedness Center
AWI	: Alfred Wegener Institute
Bakosurtanal	: Badan Koordinasi Survey dan Pemetaan Nasional (National Coordinating Agency for Surveys and Mapping)
BAPPENAS	: Badan Perencanaan Pembangunan Nasional (Indonesian National Development Planning Agency)
BBC	: Bogardi-Birkmann- Cardona
BPS	: Badan Pusat Statistik (Central Bureau of Statistics – Indonesia)
BR	: Band Ratio
CWD	: Cost Weighted Distance
DFD	: Deutsches Fernerkundungsdaten-zentrum (German Remote Sensing Data Center)
DLR	: Deutsches Zentrum für Luft- und Raumfahrt (German Aerospace Center)
DTM	: Digital Terrain Model
EMS	: European Macroseismic Scale
ETM+	: Enhanced Thematic Mapper Plus
ETA	: Estimated Time Arrival
EWMC	: Early Warning and Mitigation Center
GEOBIA	: Geographic Object-Based Image Analysis
GIS	: Geographic Information System
GITEWS	: German-Indonesia Tsunami Early Warning System
GLCM	: Gray-Level Co-occurrence Matrices
GLDV	: Gray-Level Difference Vector

GPS	: Global Positioning System
GTZ-IS	: Deutsche Gesellschaft für Technische Zusammenarbeit (German Technical Cooperation- International Services)
InSAR	: Interferometric Synthetic Aperture Radar
ISDR	: International Strategy for Disaster Reduction
LIDAR	: Light Detection And Ranging
NDVI	: Normalized Difference Vegetation Index
NDWI	: Normalized Difference Water Index
OBIA	: Object-Based Image Analysis
PCA	: Principal Component Analysis
PMI	: Palang Merah Indonesia (Indonesian Red Cross)
PTVAM	: Papathoma Tsunami Vulnerability Assessment Model
RS	: Remote Sensing
SEaTH	: Separability and Threshold
SNN	: Standard Nearest Neighbour
SPOT	: Satellite Pour l'Observation de la Terre (Earth Observation Satellite)
TEBC	: Tsunami Evacuation Building Capacity
UNU-EHS	: United Nations University-Environment and Human Security
USA	: United States of America
USGS	: United States Geological Survey
VE	: Vertical Evacuation
VHRSI	: Very High Resolution Satellite Imagery
WCDR	: World Conference on Disaster Reduction
WP	: Work Package

CHAPTER 1

INTRODUCTION

1.1. Motivation

On 26 December, 2004, a massive earthquake registering 9.0 on the Richter scale, and the resulting giant tsunamis, affected or destroyed many cities along Indian Ocean rim including Banda Aceh, Aceh Besar, Meulaboh (Indonesia), Penang (Malaysia), Phuket (Thailand), Galle and Batticaloa (Sri Lanka), Andhra Pradesh and Tamil Nadu (India). The fast-moving tsunami killed an estimated 220,000 people and left 1.5 million people homeless in the region (The World Bank, 2006). According to Bappenas (2005), the massive human toll the earthquake and tsunami took on Indonesia was larger than in any other country in the region. The giant tsunami had destroyed also thousands of buildings, industries, bridges, and other man-made infrastructures, making it the most destructive tsunami as well as one of the largest natural disasters ever on a global scale.

In simply looking at the map of the world, it is clear that a large number of cities located near coastlines need to be monitored for tsunami hazard. Figure 1.1 features a global map of tsunami hazard areas, including the most urban areas along the Indian and Pacific Oceans as well as the Mediterranean Sea. It is obvious that, on a world scale, a large number of people, buildings, infrastructure and other human facilities are prone to tsunami hazard. Red lines indicate the most dangerous areas of tsunami hazard with tsunami wave heights of more than 5 m. Most of the areas located along the coastlines of the Pacific Ocean are classified as the most dangerous areas. Almost half of coastal areas of Indian Ocean are classified as the most dangerous areas including the west coast of Sumatra Island (Indonesia), Andaman and Nicobar Islands (Thailand), coastal area of Myanmar, east coast of India and east coast of Sri Lanka.

1. Introduction

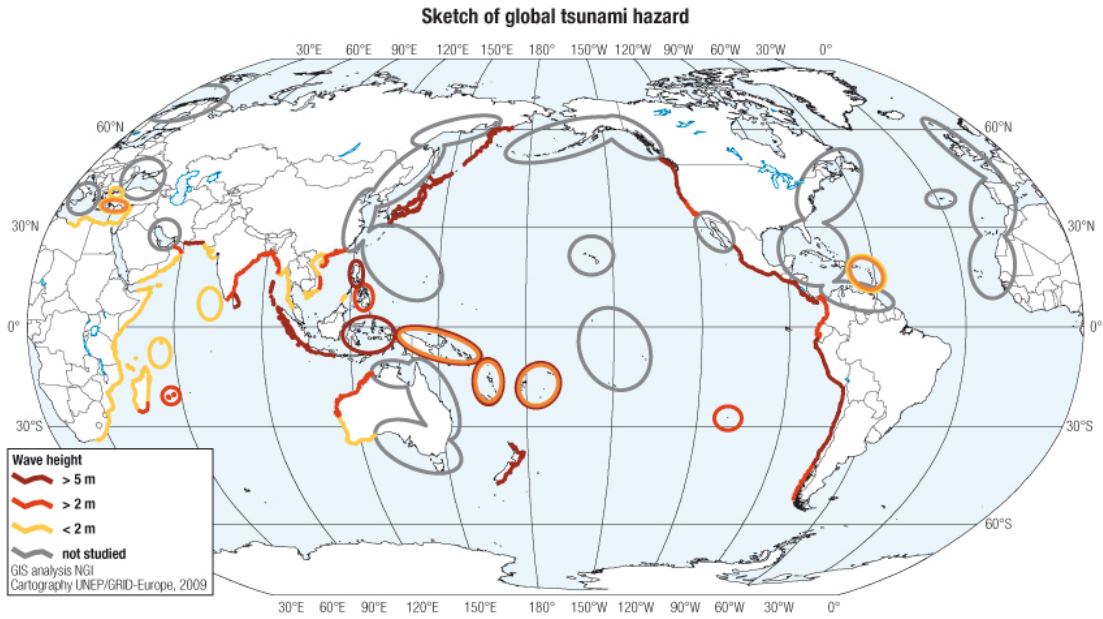


Figure 1.1. Map of global tsunami hazard (Source: ISDR, 2009)

Figure 1.2 is a more detailed view of the tsunami hazard map, focused on the coastal area of Indonesia. The west coast of Sumatra, south coast of Java, south coast of Maluku and many other Indonesian coastal areas are at high to very high risk of tsunami.

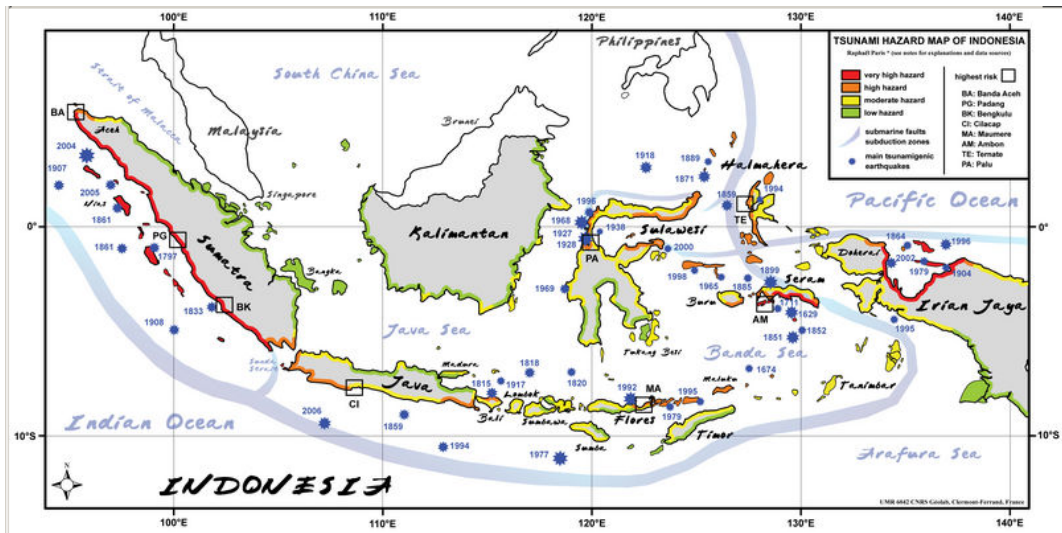


Figure 1.2. Tsunami Hazard Map of Indonesia (Source: Paris, 2008)

A detailed tsunami risk assessment is therefore an important task in order to provide a sound basis for disaster risk reduction and mitigation measures in these coastal areas.

ISDR (2004) defined risk as the probability of harmful consequences or expected losses (deaths, injuries, property, livelihoods, economic activity disrupted or environment damaged) resulting from interactions between natural or human-induced hazards and vulnerable conditions. This is simply expressed by the formula:

$$\text{Risk} = \text{Hazard} \times \text{Vulnerability}$$

According to Chambers (1989), risk assessment is two-dimensional: The assessment of shocks and stressors (hazard assessment, external), and the assessment of vulnerability (internal), which includes the measurement of the susceptibility of exposed elements and their degree of defencelessness (or coping capacity) against damaging loss. In this regard, we recognize that there are two important elements in the assessment of risk: hazard and vulnerability. In the context of natural hazard, hazard was defined as the probability of occurrence of a specified natural hazard at a specified severity level in a specified future time period (after Peduzzi et al., 2005).

In the framework of tsunami disaster risk reduction, the hazard component can be regarded as a given factor almost out of human control. Tsunami hazard can only be modelled and mapped but cannot be managed or reduced. Thus, vulnerability analysis plays an important role in tsunami disaster reduction. The term vulnerability covers a broad field of research, encompassing many techniques, applications and disciplines. Thywissen (2006) stated that the term vulnerability is an envelope for complex and interconnected parameters and processes. Villagran de Leon (2006) said a simple way to address vulnerability is found in a proposal by the International Strategy for Disaster Reduction. Vulnerability is defined by the ISDR as “the set of conditions and processes resulting from physical, social, economic, and environmental factors, which increase the susceptibility of a community to the impact of hazards” (ISDR, 2004). The physical factors encompass susceptibilities of location and the built environment, and can be

represented through such factors as population density, remoteness of a settlement, location, and construction materials and techniques employed to build infrastructure.

Because risk is a function of hazard and vulnerability, building vulnerability is one of the most important parameters in the framework of earthquake and tsunami disaster risk reduction. “Earthquakes don’t kill people, but buildings do” is a familiar sentence tossed about among seismic scientists. In the context of disaster reduction, tsunami scientists often consider buildings as potential vertical evacuation shelters. These common understandings view building vulnerability as an important parameter in disaster management.

The demand for a building vulnerability assessment is great: The places where people live can be the cause of fatalities when natural disaster strikes, but they can also provide evacuation shelter under certain conditions. Such information about buildings is usually derived from field measurements based on selected parameters that determine the level of vulnerability.

Given the fact that building vulnerability information so vital, up-to-date information is in high demand. However, relying only on such direct measurements requires resources beyond acceptable time and cost. The combination of in-situ building survey and remote sensing/GIS technology is a challenging yet promising approach expected to overcome this problem. This research aims to elaborate on the capability of integrative remote sensing and GIS approaches in the assessment of building vulnerability to tsunami hazard.

1.2. Research Problems

This research is designed to investigate and to find solutions for the following research questions:

1. Can we categorize built-up areas according to their vulnerabilities?
2. Can we develop a combined approach using in-situ building surveys and remote sensing in an efficient and cost-effective way?

3. Which parameters are necessary for the vulnerability assessment and how can we identify them using remote sensing?
4. Is it possible to determine which buildings are potentially well-suited for use as vertical evacuation buildings by using remote sensing technology?
5. Can the methods developed in the pilot area (Cilacap) be transferred to other coastal areas?
6. What kind of applications can be derived from the result of this research?

1.3. Research Objectives

Based on the research problems, the objectives of this research can be stated as follows:

1. To develop and evaluate the capability of an integrative remote sensing, GIS and in-situ survey approach in vulnerability assessment of buildings to tsunami hazard.
2. To develop a new concept and method for extracting the required information from very high resolution satellite images for the purpose of vulnerability analysis to tsunami hazard.
3. To recognize potentially affected buildings by tsunami hazard.
4. To recognize potential locations for vertical evacuation, for the purpose of tsunami evacuation modelling.

1.4. Main Benefits of the Research

The results of the research may benefit government, private sectors, researchers, society, non-governmental organizations (NGO) as well as international organizations in the following ways:

- as input for city spatial planning
- as contribution to earthquake and tsunami disaster mitigation planning as well as disaster risk reduction management
- in determining vertical evacuation buildings for tsunami evacuation planning
- as information used to develop better awareness among the general public and support better preparedness for possible future disasters.

1.5. Thesis Structure

The thesis is organized as follows:

Chapter 1 describes the general introduction and justification of the research. This chapter discusses the basic and principal motivation for this research. The key questions of this research are listed and the main research objectives are given.

Chapter 2 describes the framework of the research, the organization and the position and scope of the research as it pertains to the GITEWS project. This chapter also describes the wide spectrum of vulnerability definitions and concepts. In this respect, we select the most relevant conceptual framework of vulnerability as the basis of research theory and implementation. Finally, this chapter shortly describes the selected research areas including geographic and demographic profiles, urban structures, economic conditions and tectonic structures.

Chapter 3 reviews literature on state of current research studies, focussing on the theoretical, conceptual and practical backgrounds of the research topic. Closely-related topics discussed in this chapter include: vulnerability concepts, methods, and indicators; in-situ building vulnerability and object-based image analysis applications, including building detection and analysis, building vulnerability assessment, vegetation and environment analysis.

Chapter 4 discusses research methodology and explains all technical procedures and steps needed to achieve the ultimate goals of the study. Technical procedures include in-situ survey technique, sampling method, parameter definition, in-situ building vulnerability assessment and remote sensing and GIS approaches in building vulnerability assessment. Remote sensing and GIS approaches in assessing building vulnerability is a new method developed in order to answer the problems and difficulties in assessing building vulnerability using in-situ measurements. This method features some procedural steps of the object-based image analysis (OBIA) technique, including pre-processing, segmentation technique, building classification and building

vulnerability classification. Thus, this chapter presents the combined in-situ survey and remote sensing method used in assessing building vulnerability.

Chapter 5 presents the results of this research. The results are presented sequentially based on the procedural steps of the methodology. The results presented in this chapter comprise building sample selection, in-situ building classification, spatial parameter definition of building vulnerability, pre-processing of object-based image analysis, segmentation, building detection and building vulnerability classification.

Chapter 6 presents an application of the research in the area of tsunami evacuation modelling. Vertical evacuation buildings that were identified by the remote sensing technique provided valuable input for vertical evacuation planning. GIS techniques were used extensively in the generation of the tsunami evacuation map. The sub-chapters of this analysis include information on: inundation and safe areas identification, target points distribution for vertical evacuation, population distribution modelling, accessibility modelling and evacuation modelling.

Chapter 7 discusses the analysis of the results and findings of the study. The focus of the discussions are mainly in the context of in-situ survey of building vulnerability, pre-processing of image analysis, object-based image analysis for building vulnerability classification and the accuracy assessment.

Chapter 8 presents the conclusions of the research.

CHAPTER 2

RESEARCH FRAMEWORK

2.1. The GITEWS Project

This research is conducted as a part of the German-Indonesian Tsunami Early Warning System (GITEWS) project. GITEWS is a project funded by the German government to implement an effective tsunami early warning system for the Indian Ocean, mainly off-coast of Indonesia. The system integrates terrestrial observation networks of seismology and geodesy with marine measurement technique and satellite observations. As seen in Figure 2.1, GITEWS is designed as a large and comprehensive project comprising several Work Packages. GITEWS is being developed by a number of scientists and engineers of the Helmholtz Centre Potsdam GFZ German Research Centre for Geosciences (GFZ, Project Lead), the Alfred Wegener Institute for Polar and Marine Research (AWI), the German Aerospace Centre (DLR), the GKSS Research Centre (GKSS), the German Marine Research Consortium (KDM), the Leibniz Institute of Marine Sciences (IFM-GEOMAR), the United Nations University Institute for Environment and Human Security (UNU), the Gesellschaft für Technische Zusammenarbeit (GTZ) and the Federal Institute for Geosciences and Natural Resources (BGR). It is implemented in close cooperation with the Indonesian partner organizations and international partners.

Building vulnerability assessment research is a part of WP4200 (Vulnerability Analysis and Risk Modelling) under the umbrella of WP4000 (Early Warning and Mitigation Centre, EWMC), led by DLR. Figure 2.2 depicts the concept of the Tsunami Early Warning and Mitigation Center, an entity that will integrate all related components into one system to arrive at one main goal: assessment and decision support.

2. Research Framework

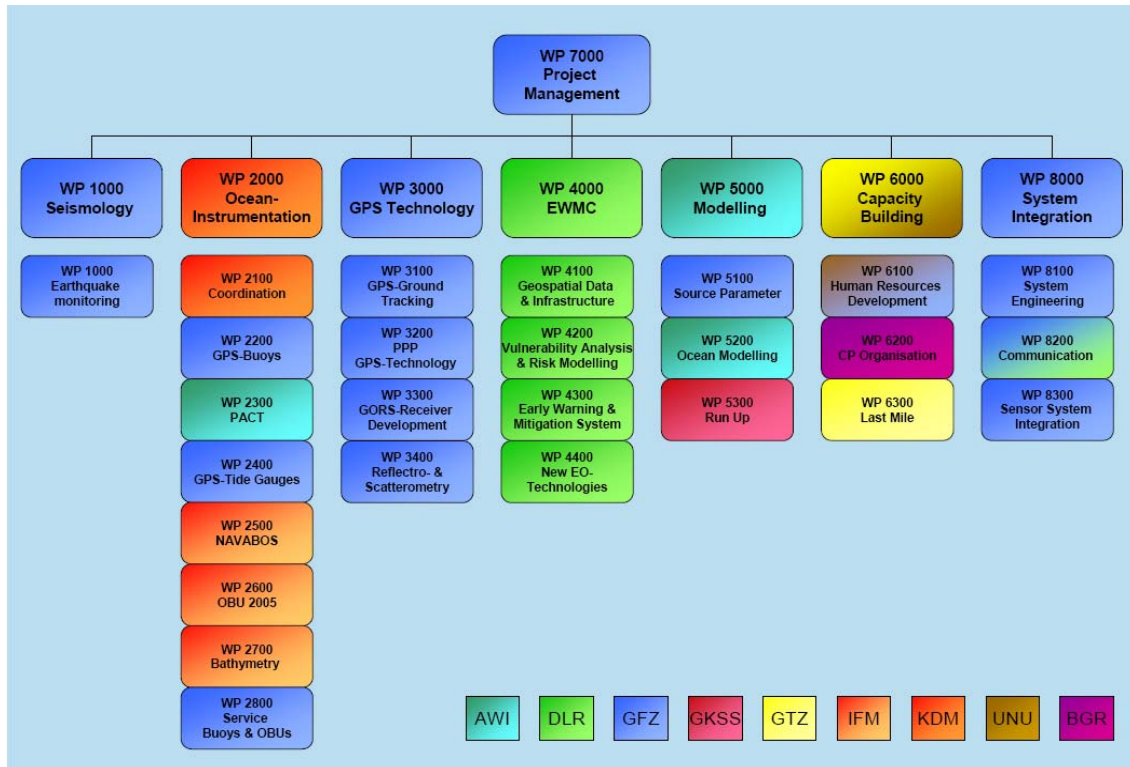


Figure 2.1. The GITEWS Project Organization comprises several Work Packages (WPs) conducted by a consortium of nine large German institutions

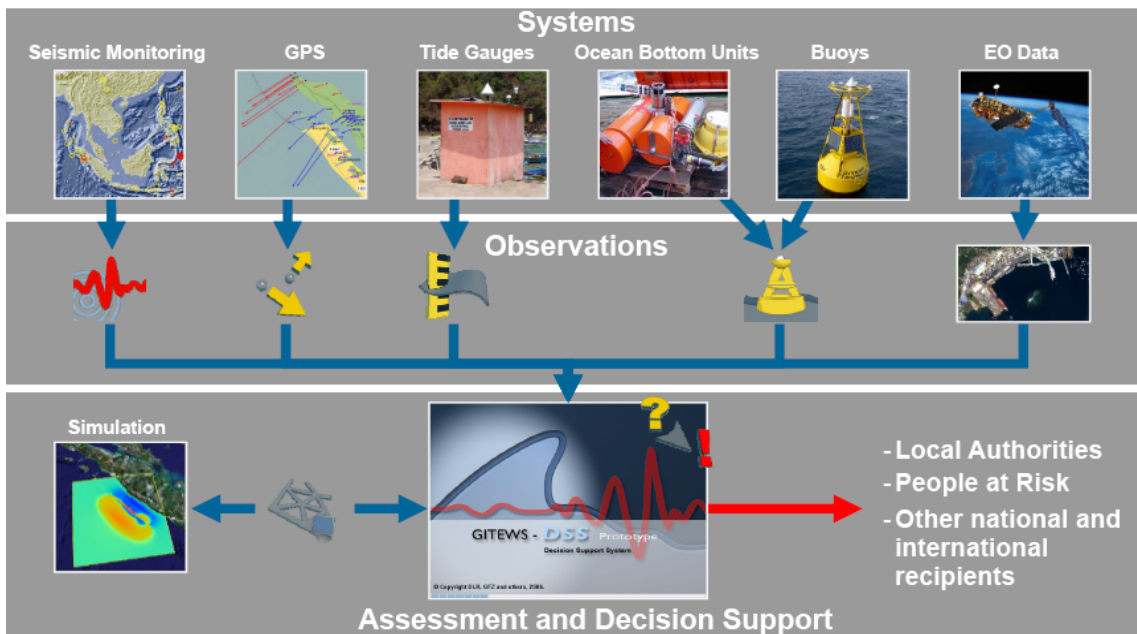


Figure 2.2. The concept of Tsunami Early Warning and Mitigation Centre

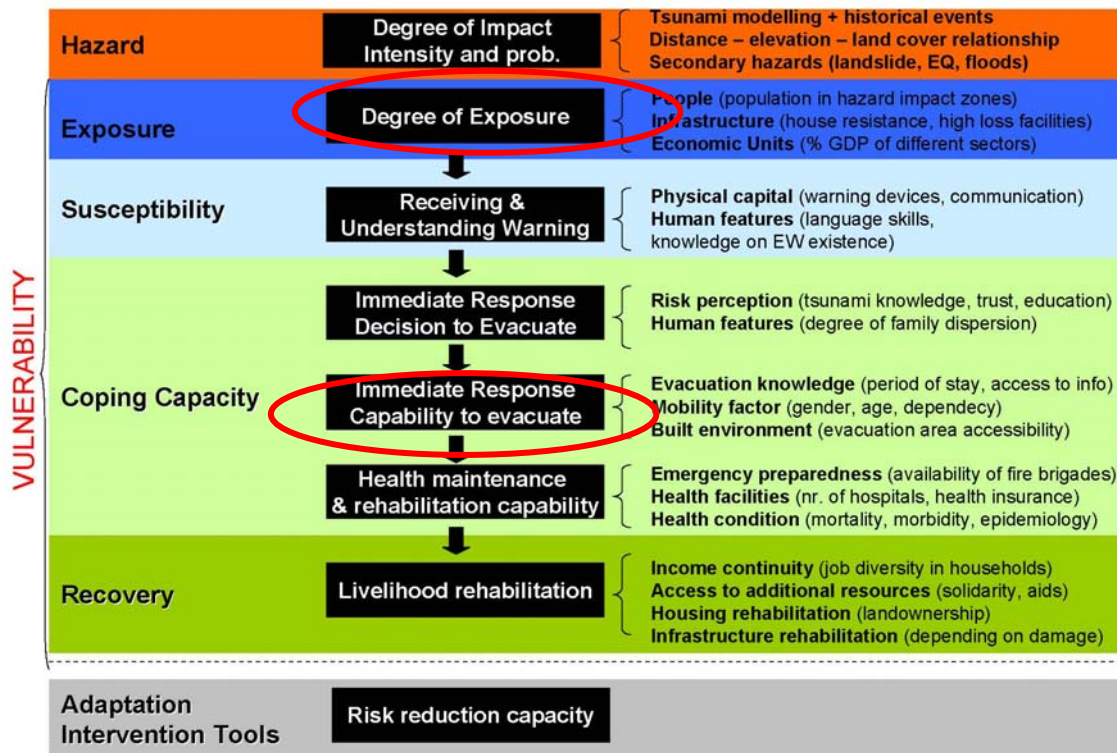


Figure 2.3. Risk and vulnerability assessment framework

As seen in Figure 2.3., the concept of the risk and vulnerability assessment covers several aspects. This research work focuses on building assessment which is relevant for the analysis of the exposure and the coping capacity.

2.2. Risk and Vulnerability Assessment Framework of the Research

As stated by ISDR (2004), ‘disaster reduction is based on a continuous strategy of vulnerability and risk assessment’, therefore being one component of risk management as proposed by ISDR. Risk and vulnerability assessment in the GITEWS context encompasses two main goals: Emergency assistance and crisis management capacity for early warning and disaster risk reduction – strategies developed within the frame of adaptation, mitigation and contribution to evacuation planning.

Overall, risk assessment is two-dimensional: The assessment of shocks and stressors (hazard assessment, external), and the assessment of vulnerability (internal), which includes the measurement of the susceptibility of exposed elements and their degree

of defencelessness (or coping capacity) against damaging loss (Chambers, 1989). This leads to three fundamental dimensions of vulnerability:

- the likelihood of being exposed to a stress situation (probability of occurrence, magnitude);
- the likelihood of not being able to respond to or withstand a stress event with suitable coping strategies;
- the likelihood that the stress has severe consequences for population groups, economy, physical spheres (build environment and infrastructure) and regions affected (extent of damage)

The assessment aims to disclose these dimensions, and to gain spatially distributed risk and vulnerability information that will serve as a precondition for risk management. Components of risk management are proposed by ISDR (2004) and serve as general guideline for developing disaster preparedness and adaptation measures based on the risk and vulnerability assessment.

In this respect, vulnerability is trans-disciplinary and multidimensional. It covers social, economic, physical, political, engineering and ecological aspects and dimensions. Vulnerability analyses should be capable of identifying specific problem situations and inherent vulnerabilities. The characteristics of the vulnerability between highly developed industrialized countries and developing countries, for example, are entirely different and must find consideration in the conception of local vulnerability analysis attempts. A comprehensive and critical analysis of different methods and indicators for the measurement of vulnerability and risk is found in Birkmann, 2006, and in the context of several expert working groups of UNU-EHS, discussed in Birkmann and Wisner, 2005.

The traditional disaster risk reduction community, for example, focuses more on engineering and natural science aspects, on event and exposure and on technical solutions (e.g. structural measures as flood embankments, more resistant buildings) than on social factors. Conversely, environmental, developmental and global change research places emphasis on environmental and socio-economic aspects of

vulnerability. The contemporary risk and vulnerability science communities recognize the need to develop a joint agenda on conceptualizing vulnerability (Thomalla et al., 2006). Thus, a holistic approach to integrate natural (including engineering science) and social (including economics) sciences is needed addressing the following questions:

- (1) Which drivers (perturbations, stressors) are considered?
- (2) Which regions are vulnerable?
- (3) Who or what is vulnerable?
- (4) How do regions compare?

The vulnerability assessment approach conducted and put into operation in this research is based on the BBC framework, elaborated by Bogardi and Birkmann (2004) and Cardona (2001). It aims at exploring various characteristics of the vulnerability in social, economic and environmental dimensions. This includes the identification and assessment of the vulnerability of the population exposed (different social groups), basic infrastructure services and physical structures within coastal communities. The BBC framework emphasizes the fact that vulnerability is defined, on the one hand, by exposed and susceptible elements, and by the coping capacities of the affected entities (e.g. social groups) on the other.

The framework stresses the importance of being proactive to reduce vulnerability before an event strikes the society, economy or environment. In contrast to other approaches, the framework clearly indicates the link between vulnerability assessment and sustainable development by taking into account the three pillars of sustainable development – the social, economic and environmental spheres (Birkmann, 2006).

2.3. Study Area

The study area for this research is Cilacap City, one of the vulnerable areas to tsunami hazard along the Indian Ocean rim. It is one of the pilot areas of the GITEWS project, in addition to Padang and Kuta.

2.3.1. Geographic and Demographic Conditions

Cilacap is a city located in the southern part of the Java Island, Indonesia. This is one of the most populated urban-coastal areas in the Province of Central Java, which has a total area of about 225 million hectares and is divided into 24 sub-districts and 284 villages. It is located between 108° 04' 30"E – 109° 30' 30"E and 7° 30' 00"S – 7° 45' 20"S. In the south, Cilacap is separated by the Indian Ocean. In the north, it neighbours the Banyumas district, in the East it borders the Kebumen district and its western border meets the Province of West Java. Cilacap's highest elevation is 198 meters above mean sea level and its lowest land is 6 meters above the surface of the sea. (BPS Cilacap, 2005).

According to BPS Cilacap (2005), the total population of Cilacap at the end of 2005 was about 1.7 million persons. During the last five years, the average population growth has measured 0.53 percent per year. As of 2005, the average Cilacap population density was 803/km² – of that, the most densely populated area is located in the sub-district of South Cilacap (about 8500/km²) and the lowest is 93/km² located in the sub-district of Kampung Laut. The population of people under 15 years old is about 28 percent.

The study area is mainly located in the South of Cilacap, an area that lies between 108° 59' 30"E – 109° 04' 40"E and 7° 39' 00"S – 7° 45' 00"S and covers 3 sub-districts and 20 villages with a total area about 60.5 km². Around 200,000 people live in the study area. The study area is shown in Figure 2.4.

2.3.2. Urban Structure and Economic Conditions

Cilacap's current urban structure comprises settlement, trade, commerce, industry, education, health services, green, office buildings, transportation, harbour and warehouses, mixed land uses, tourism, a special armed forces training area, agriculture, conservation, fisheries and a cemetery. Generally, the existing urban structure of Cilacap is developed under the influence of physical and natural conditions and points of access by transportation vehicles.



Figure 2.4. Study Area

Though the Cilacap district is well-known for its industrial area, its agricultural sector, especially its rice farms, is the largest contributor to Cilacap's gross domestic product. Another important source of income is won from the trade, hotel, restaurant and manufacturing sector.

In the study area, people mainly depend on rice cultivation, shrimp farming and fishing. Many industries, especially the oil-mining industries, are located on/near the coast.

2.3.3. Tectonic Structures

Tsunami occurrences in the southern coast of Java can be categorized as very frequent, as shown in Figure 1.2. The region of the plate boundary between the Australia plate and Sunda plate has a high seismic activity. Many destructive earthquakes were produced in the offshore region of Southern Java, some of which generated destructive tsunamis. The offshore seismic activity along the southern coast of Java is a result of oblique subduction: The Australia plate slides beneath the Sunda (Eurasian) plate with convergence rates between 66 and 71 ± 5 mm/year in north-north-eastward direction (Michel et al., 2000).

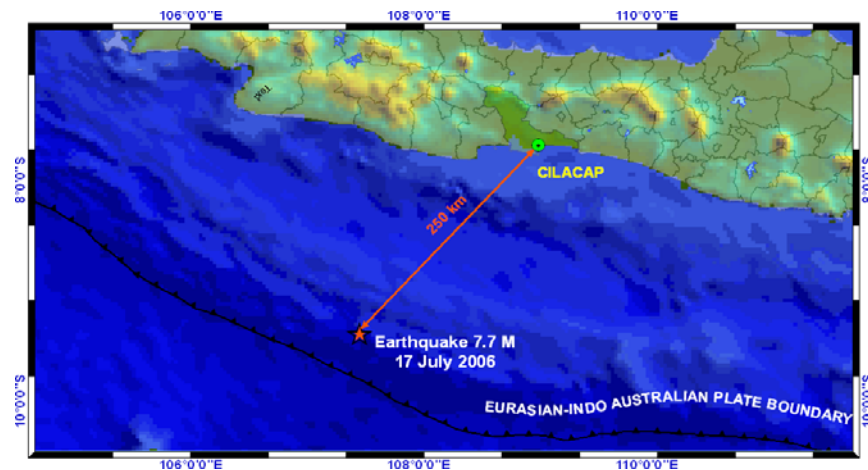


Figure 2.5. Location of the study area and its distance from the last epicentre of the 17 July 2006 earthquake-tsunami

The destructive earthquake on 17 July 2006, with its magnitude of 7.7, occurred as a result of thrust-faulting on the boundary between the Australian plate and the Sunda plate. The earthquake subsequently generated a three-meter-high tsunami, called Pangandaran tsunami, which struck the south coast of Java Island, Indonesia (USGS, 2006). The Pangandaran beach resort area and Cilacap city, were affected most. The most recent report from the Indonesian National Coordinating Agency for Disaster Management (BAKORNAS PBP), released in August 2006, indicates that 157 people were killed, 10 are missing, 8 were injured, and 306 people were displaced following the wave's destruction of poorly constructed buildings. The 17 July 2006 earthquake is thought to be similar to the earthquake of 2 June 1994, which produced a tsunami with a maximum run-up height of 13 meters and killed more than 200 people. That earthquake occurred in the South of Java and about 600 km east-southeast of 17 July's earthquake, also as a result of thrust faulting on the shallow plate boundary (USGS, 2006).

CHAPTER 3

LITERATURE REVIEW AND STATE OF THE RESEARCH

This chapter describes the current status of worldwide studies being conducted on the topic of determining building vulnerability to tsunami hazard using combined in-situ assessment and remote sensing/GIS approaches. This overview will reveal where there are gaps in current research, and how this study can contribute significantly to the filling of those gaps. This chapter can also be regarded as an overview of the state-of-the-art of studies on topics closely related to building vulnerability assessment. This particular overview is featured in the sub-chapters found here. The description begins with vulnerability concepts and is followed by analytical and technical aspects related to the procedural steps of assessing building vulnerability to tsunami hazard.

3.1. Vulnerability: An Interdisciplinary Concept

As a term and a concept, vulnerability, originally used in social sciences, has been applied in a wide range of multidisciplinary studies. According to Birkmann (2006), current literature encompasses more than 25 different definitions, concepts and methods to systematise vulnerability. A people-centred definition of vulnerability was defined by Wisner (2005) as “the characteristics of a person or group and their situation that influence their capacity to anticipate, cope with, resist and recover from the impact of a natural hazard (an extreme natural event or process)”. Cardona (2004) defined vulnerability as an internal risk factor of the subject or system that is exposed to a hazard and corresponds to its intrinsic predisposition to be affected, or to be susceptible to damage. In other words, vulnerability represents the physical, economic, political or social susceptibility or predisposition of a community to become damaged in the case of a destabilizing phenomenon of natural or anthropogenic origin. Coburn (1994) called vulnerability the propensity of things to be damaged by a hazard. Furthermore, he defined vulnerability as the degree of loss of a given element (or set of elements) at risk, resulting from a given hazard at a given severity level.

Vulnerability, as defined by ISDR, is “the set of conditions and processes resulting from physical, social, economic, and environmental factors, which increase the susceptibility of a community to the impact of hazards” (ISDR, 2004). The physical factors include susceptibilities of location and the built environment, and can be represented through such factors as population density, remoteness of a settlement, location and construction materials and techniques employed to build infrastructure.

Based on this broad spectrum of vulnerability definitions, the term of building vulnerability to tsunami hazard used in this research is defined as an internal risk factor of a building or a group of buildings that is exposed to tsunami hazard and corresponds to the building’s intrinsic predisposition to be affected, or to be susceptible to damage. In this research, vulnerability represents only the physical susceptibility or predisposition of a building or a group of buildings to become damaged in the case of tsunami hazard. The physical factors or parameters of building vulnerability are represented by 3 groups of parameters: building stability parameters, tsunami component parameters and building accessibility parameters (see section 4.2.2). In this case, social, economic and environmental factors are not taken into account in the vulnerability analysis.

Given the wide range and spectrum of vulnerability applications, the past decade has seen a huge rise in the number of studies being conducted on vulnerability assessment. The term ‘vulnerability’ covers a broad field of research encompassing many techniques, applications and disciplines. Scientists from a variety of disciplines – including social science, economics, health, environment, structural, disaster management, regional planning and many others – often bring with them their own conceptual frameworks in the vulnerability assessment. The growing body of literature on vulnerability and adaptation contains a sometimes bewildering array of terms: vulnerability, sensitivity, resilience, adaptation, adaptive capacity, risk, hazard, coping range, adaptation baseline and so on (Brooks, 2003). In the area of disaster management studies, vulnerability assessment topics have been carried out by many researchers. Fernandez (2009), Grünthal et al. (2006), Bou-Rabee and Van Marcke

(2001), Roca et al. (2006), Taubenböck et al. (2006), Oliveira et al. (2006), Madariaga (2002), Van Westen et al. (2002), Lamadrid (2002), Kappos et al. (1998), Fischer et al. (2002), Gomes et al. (2006), Coburn et al. (1994) and Wen et al. (2002) measured vulnerability to earthquakes using different approaches. Alkema (2007), Guarin (2008), Minciardi et al. (2006), Schmidt-Thome et al. (2006), Van Westen et al. (2002) and Gambolati and Teatini (2002), Forte et al. (2006), Grothmann and Reusswig (2006), Heiko et al. (2006), Schlerf (2000), UNCHS (2001) and Van der Sende et al. (2003) reported on their research of various methods of flood risk and vulnerability. Spence et al. (2004), Petrazzuoli and Zuccaro (2004), Pareschi et al. (2000), Pomonis et al. (1999) completed studies in volcano and pyroclastic flow risk and vulnerability. Studies focusing on the vulnerability to storm hazard have been conducted by Grünthal et al. (2006), Stewart (2003) and Khanduri and Morrow (2003). Kaplan et al. (2009), Dall’Osso et al. (2009), Dominey-Howes and Papathoma (2007), Birkmann (2006), Hwang et al. (2005), Papathoma et al. (2003), Sato et al. (2003), Evgueni et al. (2005), Wood and Stein (2001), Clark et al. (1998) published studies on tsunami risk and vulnerability in a variety of locations. Cannon et al. (2004), Cardona (2005), Downing et al. (2005), Turner et al. (2003), Downing et al. (2002), Dwyer et al. (2004), EEA (2005), El-Raey (1997), Gallopin (2006), Guenter (2005) and Kropp et al. (2006) studied social vulnerability as it pertains to different hazard types and areas of study. Thomalla et al. (2006), Yohe and Tol (2002), Zebisch et al. (2005), Freeman and Warner (2001), Füssel (2005), Füssel and Klein (2006), Metzger (2005), O’Brien et al. (2004), Pelling and Uitto (2001), Schröter et al. (2005), Sutherst et al. (2000) and Gwilliam, et al. (2006) investigated climate change vulnerability. In her comprehensive review, Thywissen (2006) concluded that the term vulnerability is an envelope for complex and interconnected parameters and processes. However, the goal is often to reduce any risk.

3.2. Vulnerability Assessment Methods

Vulnerability is complex, dynamic, compounding and cumulative (Anderson, 1995) and whatever function is selected to describe it should include these characteristics

(Fernandez, 2009). Vulnerability assessment constitutes its systematisation and evaluation in the contexts of a household, a group of people, a community, a province, a country, a sector or a system with respect to the different types of hazards (Villagran de Leon, 2006). Birkmann (2006) summarized various vulnerability models used by different scientists for different studies. The vulnerability models can be summarized as follows:

- a. Double structure of vulnerability, explaining the importance of coping and response capacity as the internal side of vulnerability, and exposure as the external side.
- b. Sustainable livelihood framework, in which the key elements are the livelihood assets or capitals (human, natural, financial, social and physical), and the vulnerability context is understood as shocks, trends and seasonality, and the influence of transforming structures.
- c. Risk-Hazard (RH) model, explaining the impact of a hazard as a function of exposure of a system to the hazard and the response of the system.
- d. PAR (Pressure and Release) model, explaining vulnerability as a series of levels of social factors called root causes and dynamic pressures. These, in combination with social, cultural and political processes, make for unsafe conditions. This is described as “progression of vulnerability or “chain of causation”.
- e. Onion framework, for which two axes are defined as the reality axis and the opportunity axis. The reality axis shows how an event disrupts the social sphere when a disaster occurs. The opportunity axis, on the other hand, compares the event to the hazard, the damage to the risk and the disaster to the vulnerability.
- f. BBC framework, as the combination of existing models, and is mainly based on the conceptual work of Bogardi and Birkmann (2004) and Cardona (2001). As mentioned in the previous chapter, this research uses the BBC framework as the basis for risk and vulnerability analysis.

Because the concept of vulnerability is multidimensional and often ill-defined, it is difficult – and perhaps even impossible – to define a universal measurement methodology or to reduce the concept to a single equation (Birkmann, 2006). However, Villagran de Leon (2006) found that in relation to the number of different definitions about vulnerability, the number of methods to assess vulnerability is relatively low. Studies conducted around the world are developing and testing methods to either evaluate, or at least represent in some kind of fashion, the degree of vulnerability of a system, a process, a community or an organization. Such approaches narrow down the definition of vulnerability to a format that allows for its assessment using data available, or data that can be acquired by different means. Polsky et al. (2003) proposed an eight-step method for vulnerability assessment. The eight steps are:

- a. Define the study area in tandem with stakeholders
- b. Become aware of the study area and its contexts
- c. Hypothesize who (or what) is vulnerable to what
- d. Develop a causal model of vulnerability
- e. Find indicators for the components of vulnerability
- f. Weight and combine the indicators
- g. Project future vulnerability
- h. Communicate vulnerability Creatively

These steps are applicable not only for social-oriented vulnerability analysis but also for various kinds of vulnerability analyses, including building vulnerability assessment. In the case of building vulnerability assessment using a combined in-situ survey and remote sensing approach, some steps need to be added as follows (see section 4.1):

- a. Define the study area
- b. Try to understand and become aware of building conditions and their contexts in the study area
- c. Develop hypotheses in the context of building vulnerability
- d. Develop a causal model of building vulnerability
- e. Find indicators or parameters for the components of building vulnerability

- f. Select building samples in the study area using appropriate sampling technique
- g. Weight and combine the parameters
- h. Find spatial parameters for remote sensing analysis
- i. Develop remote sensing rule sets incorporating the selected spatial parameters
- j. Regionalize vulnerability assessment to whole area of interest
- k. Compose building vulnerability maps
- l. Project future vulnerability
- m. Communicate vulnerability creatively.

3.3. Vulnerability Indicators

The World Conference on Disaster Reduction (WCDR), held in Kobe, Japan, in January 2005, defined a priority in the development of indicator systems for disaster risk and vulnerability as one of the key activities enabling decision makers to assess the possible impacts of disasters (Bogardi, 2006). Wisner et al. (2003) defined indicator as an easily accessible, comparable, repeatable item of information property judged to “indicate” or point to more complex states of affairs. Birkmann (2006) defined indicator for hazards of natural origin as a variable that is an operational representation of a characteristic or quality of a system able to provide information regarding the susceptibility, coping capacity and resilience of a system to an impact of an albeit ill-defined event linked with a hazard of natural origin. Furthermore, he defined standard criteria for indicator development as follows:

- a. Measurable
- b. Relevant: Represent an issue that is important to the relevant topic
- c. Policy-relevant
- d. Only measure important key-elements instead of trying to indicate all aspects
- e. Analytically and statistically sound
- f. Understandable
- g. Easy to interpret
- h. Sensitivity: Be sensitive and specific to the underlying phenomenon
- i. Validity/accuracy

- j. Reproducible
- k. Based on available data
- l. Data comparability
- m. Appropriate scope
- n. Cost effective

Hahn (2003) outlined the characteristics of disaster-risk indicators as listed below:

- a. Validity: Does the indicator measure the key element under consideration?
- b. Sensitivity: When the outcome changes, will the indicator be sensitive to those changes?
- c. Availability: Will it be easy to measure and collect information?
- d. Reliability: Is the measurement consistent over time?
- e. Objectivity: Can the data be reproduced under changing conditions?

In the context of vulnerability associated with natural disasters, validity is a crucial characteristic, which should be verified under disaster conditions. This means that what has been diagnosed as highly vulnerable should undergo major losses or damages once the hazard manifests itself as an event, while what has been diagnosed as low vulnerable should experience minimal losses or damages (Villagran de Leon, 2006).

3.4. In-Situ Building Vulnerability Assessment

The wide-range of vulnerability studies mostly encompassed the general aspects of vulnerability, only a few did specifically focus on buildings. Discussing building vulnerability mostly refers to the discussion of structural vulnerability because building structural components are regarded as internal risk factors of the building that are exposed to a hazard. Building vulnerability assessment studies on the general source of hazards have been conducted by several researchers, covering a variety of aspects. Grünthal et al. (1998) and other members of the European Commission on Seismology defined six classes of vulnerability related to different types of construction materials and techniques. The vulnerability terminology used in their research expresses the

differences in the way that buildings respond to earthquake tremors. If two groups of buildings are subjected to exactly the same earthquake tremors, and one group performs better than other, then it can be said that the buildings that were less damaged had lower earthquake vulnerability than the ones that were more damaged. Figure 3.1 depicts the differentiation of structures (buildings) put into vulnerability classes used in the European Macroseismic Scale (EMS).

Gomez and Queiroz (2006) studied seismic vulnerability of dwellings in the Sete Cidades Volcano area. In their work, dwellings were classified according to their vulnerability to earthquakes (Classes A to F), using the structure types table of the EMS (Grünthal et al., 1998), adapted to the types of constructions made in the Azores. Fischer et al. (2002) developed an integrated model for earthquake risk assessment of buildings in seismic regions. The model has five stages as follows:

- Characterization of earthquake motion for a specific site
- Construction of the building model
- Evaluation of the inelastic building response
- Structural damage assessment
- Risk evaluation

This study emphasized the evaluation of the inelastic building response and the structural damage assessment. Examples, including a large building inventory and two individual structures, were developed to show the potential use of the model.

Results showed that the model was capable of identifying different foundation soils, earthquake performance of shear-wall and frame buildings, asymmetries in height and plan, and to differentiate between conventional and seismically isolated structures. Such features may be useful for engineers working in city planning, emergency and risk management, and the insurance industry. Similar studies about building vulnerability to earthquake hazard were presented by Kappos, et al. (1998), Augusti et al. (2001), Karantoni and Bouckovalas (1997), Rocca et al. (2006) , Wen et al. (2002), Coburn et al. (1994), Lang and Bachmann (2004).

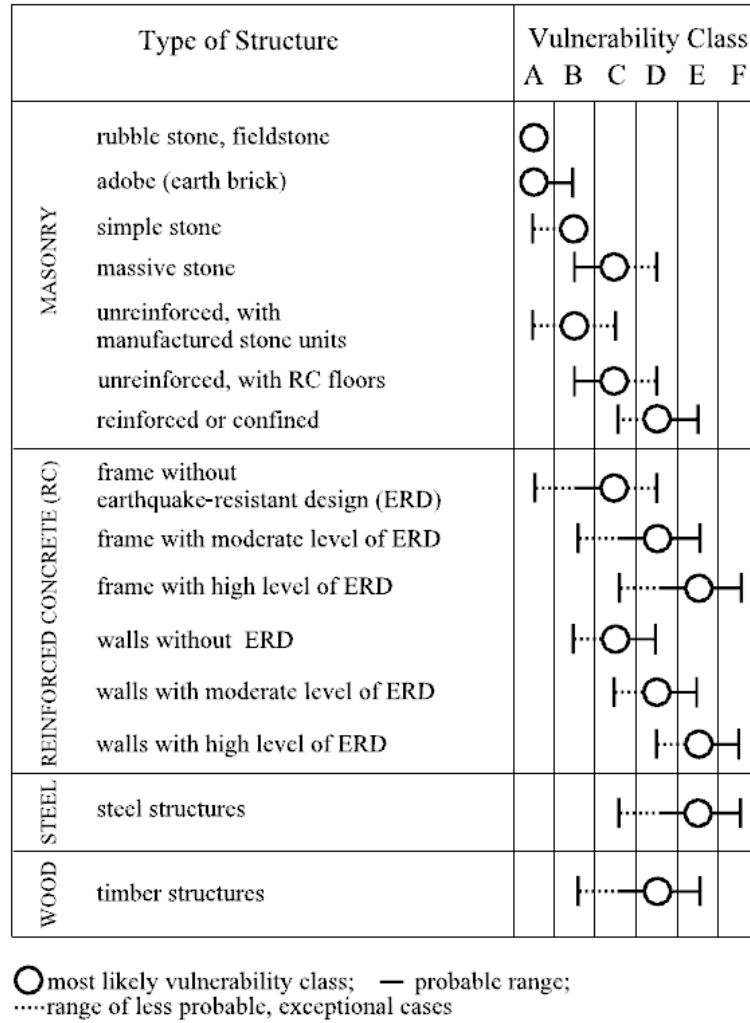


Figure 3.1. Building vulnerability classification used in the European Macroseismic Scale (EMS) (Source: Grünthal, 1998)

Papathoma et al. (2003) and Dominey-Howes and Papathoma (2007) intensively studied building vulnerability specifically to tsunami hazard using field measurements (in-situ survey) in the coastal areas of Greece and Maldives. In their studies, the analysis relates to individual buildings or open space rather than to blocks of buildings, cities or even entire regions. The data were collected during a ground-based, building-to-building survey, during which every unit was identified, coded and subject to assessment for each of the parameters listed in Table 3.1. Building vulnerability parameters were collected from 759 buildings. They were measured directly in the field; then attributes and spatial data were added and integrated into the GIS. Building vulnerability classes were derived by using a scoring method.

Table 3.1. Building Vulnerability Parameters

FACTORS	PARAMETERS	Classification	Vulnerability
1.The Built Environment	1.1.Number of Stories in each building	a. Only one floor	Vertical evacuation is impossible (high vulnerability)
		b. More than one floor	Vertical evacuation is possible (low vulnerability)
	1.2. Description of ground floor	a. open plan with movable objects e.g. tables and chairs	High vulnerability to injury/damage
b. open plan or with big glass windows without movable objects		Moderate vulnerability	
c. None of the above		Low vulnerability	
1.3. Building surroundings		a. No barrier	Very high vulnerability
		b. Low/narrow earth embankment	High vulnerability
		c. Low/narrow concrete wall	Moderate vulnerability
		d. High concrete wall	Low vulnerability
1.4. Building material, age, design		a. Buildings of fieldstone, unreinforced, crumbling and/or deserted	High vulnerability
		b. Ordinary brick buildings, cement mortar, no reinforcement	Moderate vulnerability
		c. Precast concrete skeleton, reinforced concrete	Low vulnerability
1.5. Movable objects		a. Movable objects (objects considered moveable are those that can cause injuries to people, damage to buildings or block evacuation routes. Such objects include old cars, barrels, refrigerators, containers, construction materials and car components etc.)	High vulnerability
		b. No movable objects	Low vulnerability

2. Sociological Data	Number of people per building:	High or low (high or low vulnerability).	
3. Economic Data	3.1. Land Use	a. Business (shops, storage rooms, taverns, hotels, etc.).	
		b. Residential	
		c. Services (schools, hospitals, power stations, etc.).	
4. Environmental /Physical Data	Physical or man-made barriers/sea defence	Natural (sandy beach or marsh)	low protection against flooding -high vulnerability
		Soil embankment	moderate protection against flooding-moderate vulnerability
		Concrete stone wall	high protection against flooding- low vulnerability
	Natural Environment	Wide intertidal zone	High protection against flooding- low vulnerability
		Intermediate intertidal zone	Intermediate protection against flooding- moderate vulnerability
		Narrow intertidal zone	low protection against flooding- high vulnerability
5. Land Cover	Vegetation	No vegetation cover	High vulnerability
		Scrub and low vegetation	Moderate vulnerability
		Trees and dense scrub	Low vulnerability

Van Westen et al. (2002) studied building vulnerability to multi-hazards (earthquake, landslide and flood) by using a GIS approach. The study focussed almost solely on direct tangible losses in its vulnerability assessment of the buildings and their contents. The basic method used was the application of damage-state curves, also known as loss functions or vulnerability curves (Smith, 1994). The cadastral database of the city was used in combination with the various hazard maps for different return periods, to generate vulnerability maps for the city.

Bücheler et al. (2006) mapped building risk to extreme floods in Baden-Wuerttemberg, Germany. They estimated building damage owing to flood hazard by using a GIS-based tool based on the following steps:

- Selection of the project area (spatial, postcodes or areas of communities)
- Identification and categorization of each building in the project area
- Estimation of the flood-sill for each structure (lowest damaging water level)
- Estimation of the ground-floor elevation (floor above the cellar).
- Estimation of the values for building-structure and contents (fixed/mobile inventory).
- Estimation of the stage-damage-functions, differentiated for different types of buildings, cellar/floor, building structure/contents.
- Calculation of the water-level for each object in the area.
- Estimation of the damages to buildings and contents for different water-levels based upon the type and use of each building.

In their study, the damage estimation was based on the general assumption that the monetary damage depends on the type and use of the building. Additionally, other topics of building vulnerability assessment were addressed by Khanduri and Morrow (2003), Petrazzuoli and Zuccaro (2004), Spence et al. (2004), Pomonis et al. (1999), and Stewart (2003) They focussed on vulnerability of buildings to windstorm, pyroclastic flows, volcanic activity and cyclones.

It is clear that there are various methods for in-situ assessment of the building vulnerability. Whatever the type of hazard, all vulnerability assessment methods

consider structural elements as the vulnerability parameters. Lang (2002) outlined available different methods in the order of increasing computational effort, type of application and the level of sensitivity as shown in Table 3.2.

Table 3.2. Summary of various building vulnerability assessment methods (Source: modified from Lang (2002))

Expenditure	Increasing computation effort ----->				
Application	Building stock			Individual building	
Methods	Observed vulnerability	Expert opinions	Simple analytical models	Score assignment	Detailed analysis procedures
Precision (Sensitivity)	Increasing precision ----->				

3.5. Remote Sensing and GIS based Building Vulnerability Assessment

The various studies focused on building vulnerability discussed here thus far have mostly dealt with individual building vulnerability based on direct measurements in the field (in-situ survey). Some of the studies utilized GIS technology for the purpose of data visualization and database modelling. None of them utilized remote sensing approaches for deriving building properties in the analysis of building vulnerability. However, such building vulnerability assessments conducted using in-situ survey methods provide important and fundamental basic information for those who conduct building vulnerability assessments using a remote sensing approach.

3.5.1. Object-based Image Analysis

Of the most recent studies on application of remote sensing for building extraction , most refer to object-based image analysis (OBIA) methods. Object-based image analysis has become an alternative approach in remote sensing analysis, especially for

the automatic image interpretation of very high spatial resolution satellite imagery such as IKONOS (launched in 1999 with 1 m spatial resolution), QuickBird (launched in 2001 with 0.6 m spatial resolution), and OrbView-3 (launched in 2003 with 1 m spatial resolution), WorldView-1 (launched in 2007 with 0,5 m resolution), GeoEye-1 (launched in 2008 with 0.41 m spatial resolution) or WorldView-2 (launched in 2009 with 0.46 m spatial resolution). It is clear that using a pixel-based image approach in high spatial resolution image analysis is not the appropriate approach. Blaschke and Strobl (2001) discussed the advantages of object-based versus pixel-based image analysis. There are huge amounts of meaningful information that cannot be included in pixel-based image analysis, such as object shape, area, orientation, relative position, etc. Many researchers increasingly apply object-based image analysis in analyzing very high-resolution satellite imagery. Moreover,, OBIA has been applied not only in high spatial resolution image but also in coarser spatial resolution image.

A comprehensive review of object-based image analysis in a wide spectrum of applications is given in Blaschke (2009). Benz et al. (2004), Xiaoxia et al. (2004) and Schiewe (2002) described the fundamental concepts of object-based image analysis and segmentation algorithms for remote sensing applications. They underlined the strength of object-based image analysis in remote sensing applications especially for high resolution image analysis. Yan et al. (2006) reported that the thematic mapping result using the object-oriented image analysis approach gave a much higher accuracy than that obtained using the pixel-based approach. Myint et al. (2008) compared 3 remote sensing image processing techniques to identify tornado damage areas from Landsat TM data. They employed the direct change detection approach using two sets of images acquired before and after the tornado event to produce a principal component, composite images and a set of image difference bands. Comparative techniques include supervised classification, unsupervised classification, and object-oriented classification approach with a nearest neighbour classifier. They concluded that the object-oriented approach exhibited the highest degree of accuracy. PCA and image differencing methods show comparable outcomes.

In studying riparian and forest ecosystem classification, Johansen et al. (2007) applied object-oriented classification algorithms to spectral and textural transformations of the QuickBird image data to map vegetation structural classes. The use of both spectral and textural image bands yielded the highest classification accuracy. Langanke et al. (2007) assessed the mire conservation status of a raised bog site in Salzburg using OBIA and structural analysis. Duveiller et al. (2008) studied deforestation in Central Africa, at regional, national and landscape levels, by using the OBIA technique. The combination of automated image processing and interactive labelling rendered this method cost-efficient. The approach was operationally applied to the entire Congo River basin to accurately estimate deforestation at regional, national and landscape levels. Desclee et al. (2006) analyzed forest change detection using a statistical, object-based method and concluded that the object-based change detection method proved to be very efficient in identifying forest land cover changes in both deciduous and coniferous stands. There are many other similar studies focussed on vegetation and ecosystem/environment analysis using OBIA techniques (see Ehlers et al., 2003; Blaschke, 2000; Chubey et al., 2006; Zhang et al., 2005; Bunting and Lucas, 2006; Dorren et al., 2003; Mathieu et al., 2007; Stow et al., 2008; Burnett and Blaschke, 2003; Walter, 2004; Conchedda et al., 2008; Laliberte et al., 2003; Mallinis et al., 2008; Wiseman et al., 2009; Radoux and Defourny, 2007; Wu and David, 2002; Giakoumakis, 2002; Kim et al., 2005; Kamagata et al., 2005).

Object-based image analysis algorithms have also been applied to study land cover and land use classification. Walker and Blaschke (2008) utilized OBIA in the development of two urban land cover classification schemes on high-resolution, true colour aerial photography of the Phoenix, Arizona metropolitan area in the USA. Their initial classification scheme was heavily weighted by standard nearest neighbour (SNN) functions generated by samples from each of the classes. A second classification was developed from the initial classification scheme, in which SNN functions were transformed into a fuzzy rule set. A comprehensive accuracy assessment revealed a slightly lower overall accuracy for the rule-based classification. They concluded that, for high-resolution data, per-pixel classifiers no longer perform adequately, and that

segmentation or other contextual tools will become the standard in urban land cover mapping with remotely sensed imagery. Lewinski (2006) presented results of object oriented classification of Landsat ETM+ satellite image using fused multispectral and panchromatic data. Using membership function and SNN classification, this research successfully classified 18 land use classes and concluded that image fusion does not significantly influenced the improvement of land use classes separation but it is useful for segmentation process. Similar studies in the area of land cover and land use mapping were conducted by Whiteside and Ahmad (2005), Van der Sende et al. (2003), Wei et al. (2005), Kim et al. (2005), Meinel et al. (2001) and Kong et al. (2006). Vu (2006) employed object-based image analysis to map tsunami-affected areas of Thailand by using land cover changes analysis. Objects were analyzed in a morphological scale-space to extract separately different types of land cover objects. He concluded that the results based on ASTER and Quickbird images show a good agreement with visual inspection results. Park and Chi (2008) performed a quantitative assessment of landslide susceptibility using high-resolution remote sensing data. An unsupervised change detection analysis, based on multi-temporal object-based segmentation and threshold analysis, was adopted to detect landslide-prone areas.

3.5.2. OBIA Applications for Building Analysis

In the field of building analysis, some studies have employed OBIA in their methods. Durieux, et al. (2008) developed a method for monitoring building construction in urban sprawl areas using object-based analysis of SPOT 5 images within a 2.5 m resolution and existing GIS data. Building extraction from Spot 5 images was done in three steps: creating a hierarchical network of image objects using the multi-resolution segmentation, classifying the derived objects by their physical properties and describing the semantic relationships of the network's objects in terms of neighbourhood relationships or being a sub- or super-object. Image objects resulting from the coarse segmentation used for cloud screening were used as the first level of the hierarchical network. A second level was created with a much finer multi-resolution segmentation to reach building objects' scale. A class hierarchy, which

defines the class descriptions, is built on this two-level hierarchical network. Class descriptors are a combination of fuzzy membership functions used to describe intervals of feature characteristics, wherein the objects do belong to a certain class or not by a certain degree of membership. A class is described by combining one or more class descriptors by means of fuzzy-logic operators and/or by means of inheritance. In the concluding remark, they stated that the bottom-up, region-growing algorithm used for segmentation gave satisfactory segments for a building extraction on 2.5 m resolution Spot 5 images. The limitation of the extraction came from the limit of the image resolution that makes it possible to identify only the brightest part of the buildings (mainly the white zinc roofs). Contextual and scale information was used to differentiate buildings from other bright objects such as coral sand beach or sugarcane mulch. The extraction methodology was adapted for urban sprawl change detection, using an existing GIS urban database.

Dutta and Serker (2004) demonstrated urban building inventory for Bangkok City with very high resolution remote sensing data. They developed four different segmentation levels to extract features of interest from different levels. The classification was done on the image objects using multi-level classification approach based on fuzzy methods. Membership functions were developed based on the spectral reflectance characteristics and shape properties of the image objects. To separate different urban features, spectral information based on image objects was used. Buildings were separated from roads based on their shape properties. Field survey data was used as the primary knowledge base and was combined with the spectral information obtained from the image objects to develop membership functions for different classes. Buildings were extracted from segmentation at levels 1 and 2. Buildings were classified as reinforced and non-reinforced concrete buildings depending on their roof materials and types. They concluded that with the OBIA scheme, an overall accuracy of 85% was achieved in detailed classification of urban land cover in the study area.

Turker and Sumer (2008) investigated building-based earthquake damage using watershed segmentation of aerial images taken after the event. The approach utilized

the relationship between buildings and their cast shadows. The cast shadows were detected through immersion-based watershed segmentation. The boundaries of the buildings were available and stored in a GIS as vector polygons. The vector-building boundaries were used to match the shadow casting edges of the buildings with their corresponding shadows and to perform assessments on a building-specific manner. For each building, a final decision on the damage condition was taken, based on the assessments carried out for that building only. The approach was implemented in Golcuk, one of the urban areas most strongly hit by the 1999 Izmit, Turkey earthquake. Figure 3.2 depicts the procedural steps of the methodology. Of the 284 buildings processed and analysed, 229 were correctly labelled as damaged and undamaged, providing an overall accuracy of 80%.

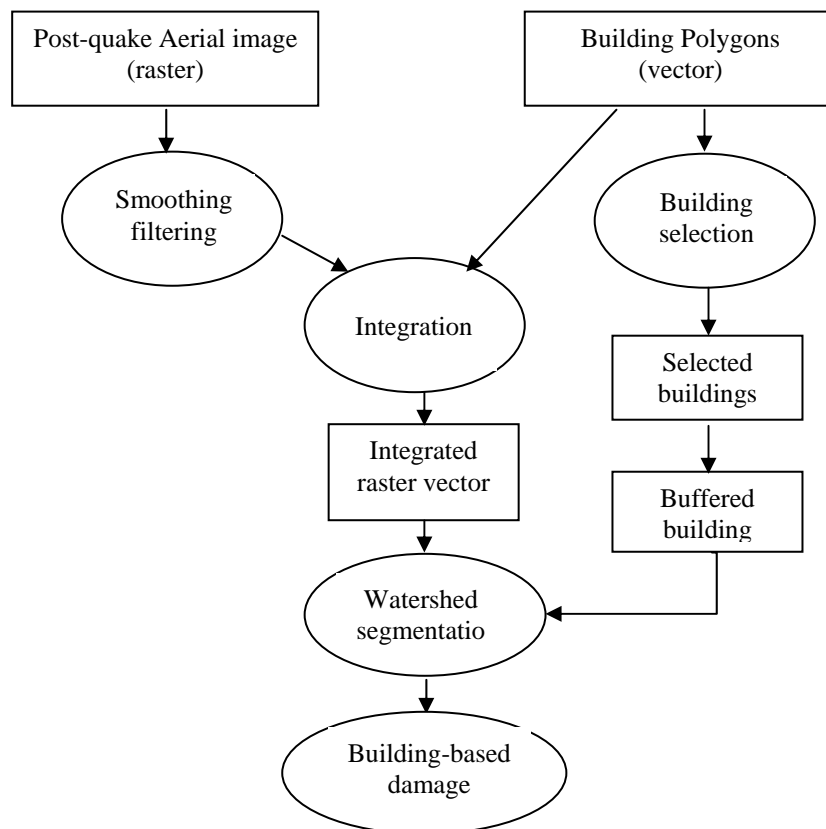


Figure 3.2. Procedural steps of building-based damage analysis (Source: Turker and Sumer, 2008)

Montoya (2003) explored the use of an off-the-shelf low-cost and rapid method of data collection for the development of a building inventory based on the combination of remote sensing, global positioning systems, digital video and geographic information systems. The method developed consists of a sequence of stages. The first stage involved the use of OBIA and GIS for stratification and mission planning purposes. The second stage consists of using GPS and digital video for the creation of spatially referenced images, and the third stage involved the use of GIS for display and analysis. The methodology developed was tested on the Costa Rican city of Cartago.

Marangoz et al. (2006) employed the object-oriented classification approach, which takes into account form, textures and spectral information. Its classification phase starts with the crucial initial step of grouping neighbouring pixels into meaningful areas, which can be handled in the later step of classification. Such segmentation and topology generation were set according to the resolution and the scale of the expected objects. This segmentation was done in multiple resolutions, thus allowing the differentiation of several levels of object categories. In this context, Taubenböck et al. (2006) summarized a number of related studies. A multi-resolution segmentation approach was presented by Baatz and Schäpe (2000). Segmentation concepts and their theoretical background for object-oriented approaches have been summarized by Schieve (2002). A recent segmentation procedure was applied by Esch et al. (2005) to analyze urban structures. Object-oriented classification methods have been presented by Herold et al. (2002). Classification approaches for highly-structured urban areas are applied by De Kok et al. (2003).

Automatic segmentation of common objects, e.g. buildings and houses from high-resolution images were investigated in several studies. The approaches can be grouped into three categories: point-based (e.g. grey-level thresholding), edge-based (e.g. edge detection techniques) and region-based (e.g. split and merge). In the region-based category, image objects are generated according to a certain homogeneity criteria (Darwish, 2003 in Marangoz et al. 2006). Marangoz et al. (2006), Hofmann (2001), Liu et al. (2005), Teo and Chen (2004), Vu et al. (2005) and Taubenböck et al. (2006)

concluded that object-oriented image analysis approaches can offer satisfying results for extracting the buildings using high resolution images. Hofmann (2001) and Teo and Chen (2004) incorporated LIDAR data in order to get accurate segmentation of building features in the urban area, while Liu et al. (2005), Vu et al. (2005) and Taubenböck et al. (2006) employed image transformation and filtering techniques without incorporating LIDAR data. Bitelli (2004) and Kouchi (2005) applied object-based image analysis in assessing macroseismic damage on urban areas.

3.5.3. OBIA Applications for Building Vulnerability Assessment

The vulnerability of buildings to geological hazards (including tsunamis) is dependent on a variety of form and functional parameters. A number of factors were identified through literature review and can be grouped as follows: (a) property type—nature, number of storeys, building type; (b) property age - indicator of foundation type, internal and external wall and roof construction, and the likely use of lime or cement in construction; (c) property design—extensions, bay windows, basements, listed building status; (d) openings—location, type and scale of windows, doors, air bricks; (e) state of repair—visible cracks, distortion, under-sailing; (f) context—conservation area status, trees/vegetation (where shrink–swell soils are present), site slope (Gwilliam et al., 2006).

Recent research conducted by Mueller et al. (2006) investigated the potential of high-resolution optical satellite imagery for the extractability of vulnerability-related building parameters in European countries. For an evaluation of large earthquake scenarios, the number of parameters in models for vulnerability was reduced to a minimum of relevant information such as:

- Building type, for example material, regularity and building shape in general, number of storeys, building height, year of construction
- Geology and soil conditions
- Context information e.g. the spatial position of a house in relation to other buildings.

Satellite image analysis was performed to directly extract the building shape, position and height as well as indirect assumptions about the house type based on the urban structure type that can be derived using additional knowledge about the roof type and context information. For a more precise assessment of vulnerability, the overview provided by satellite data allows the choice of suitable sample buildings for extrapolation. They concluded that remote sensing data does not offer the ultimate solution for a fast extraction of all necessary vulnerability parameters and it will not substitute existing, available, and up-to-date GIS data. However, this study presented the variety of information that can be extracted from high resolution satellite data, thus, making them a useful additional tool regarding the analysis and monitoring of urban areas.

A closely related study conducted by Münich et al. (2006) developed an interdisciplinary approach, combining remote sensing and civil engineering to assess vulnerability in urban areas. The strengths of civil engineering and the strengths of remote sensing lie within complementary areas. While remote sensing is capable of assessing situations rapidly and area-wide, civil engineering concentrates on local-scale, high detailed assessments of building vulnerability. The relevant building classes were defined through analysis of the thematic urban land cover classification by such parameters as roof type, building height and building density. These parameters serve as input to estimate the behaviour of structures affected by natural disasters. The damage functions were adjusted to the capabilities of remote sensing to simulate direct losses. Via remote sensing and civil engineering applications, the research showed first approaches of area-wide classification of the building stock.

Rashed and Weeks (2003) showed that the analysis of vulnerability can exploit the capabilities of remote sensing to obtain information that might not be measurable in other ways. This research has shown how the spectral characteristics of a Landsat TM image can provide detailed interpretation of urban form, moving beyond conventional, per-pixel classifications of imagery to the spectral unmixing approach.

CHAPTER 4

METHODOLOGY

4.1. Bottom-up Approach: Combining In-situ Survey and Remote Sensing Methods

The objective of this research is to develop a new bottom-up, remote sensing approach that combines in-situ survey and remote sensing techniques. The bottom-up approach used in remote sensing techniques starts with the collection of data and information in the field (in-situ survey) to form a basis for further remote sensing image analysis. This approach can also be regarded as an up-scaling approach, in which the information collected begins with a detailed scale in the field for use in a generalisation process on a broader scale later on. In this research, the detailed scale of information from the field comes in the form of building characteristics and their vulnerability classes, measured and assessed from the field survey. The broader scale of the information comes in the form of a building map derived from satellite image analysis.

In-situ survey is a process designed to assess building vulnerability by direct measurements in the field. To start, building samples were selected, using an appropriate sampling technique to ensure that the selected buildings represent the real condition of all buildings in the research area. Each building sample was measured and assessed to determine its class of vulnerability. In the process of determining building vulnerability from the field measurement, structural experts were referenced to ensure the validity of the methodology. Building vulnerability parameters were defined and listed in a questionnaire as a tool for building survey and measurement in the field.

Remote sensing technique algorithms were developed to determine a classification rule set based on spatial parameters of individual building samples, using object-based image analysis (OBIA). The OBIA approach allows us to set a desired rule based on

expert knowledge, and makes it possible for that rule to be transferred to other research areas. The general workflow of this hybrid approach is depicted in Figure 4.1 below

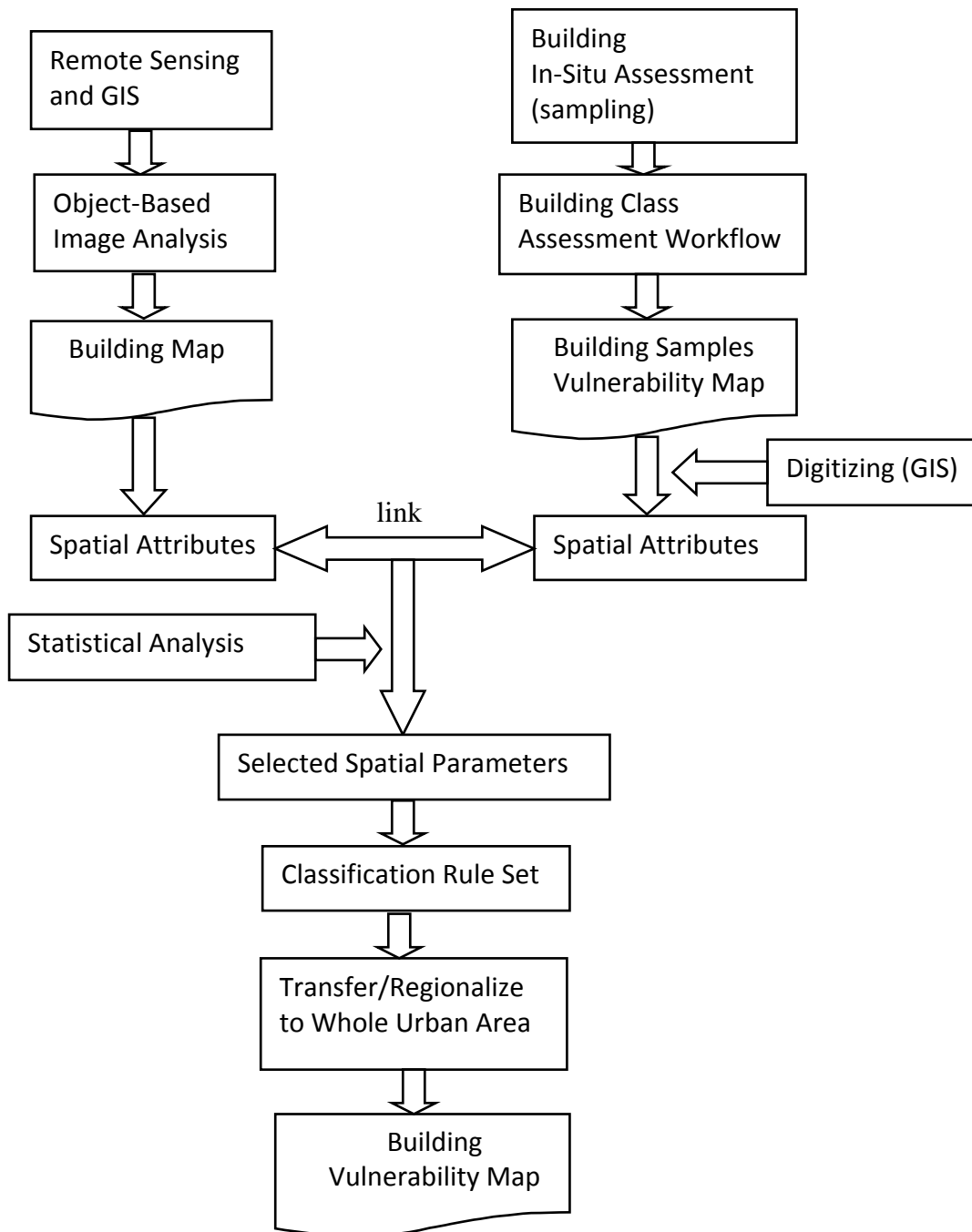


Figure 4.1. The general workflow of the combined in-situ survey and remote sensing approach

Figure 4.1 illustrates the combined approach of in-situ building survey and the remote sensing/GIS techniques. The information from the field measurement and sample building class were used for the development of a remote sensing rule set. This rule set is applied to perform the up-scaling process used to assess building vulnerability in all areas of research.

4.2. In-situ Survey

4.2.1. Sampling techniques

In-situ survey was conducted by performing direct measurements in the field. Buildings in the research area were selected based on the principles of representativeness of sampling and according to the following criteria:

1. The selected buildings should represent all types of buildings in terms of: dimension, height, shape, function, roof colour, location and accessibility.
2. The selected buildings should spread evenly throughout the area of research.

To meet the above criteria, the appropriate sampling technique known as “systematic stratified sampling” was used. In practice, sample selection was done by using very high resolution satellite imagery and the administrative boundary map. By using very high resolution satellite imagery, the types of buildings that meet the sample criteria can be clearly identified. An administrative boundary map was overlaid on the satellite imagery, making it easier to spread the samples on all villages in the area of research.

Survey teams, comprising structural engineering and remote sensing experts, were deployed in the field to conduct measurements according to pre-defined parameters. During the survey, the teams were equipped with the designed questionnaire (see Appendix). The questionnaire contains all information needed for building vulnerability assessment. All data and information from the field were compiled into a recapitulation table. This table then was regarded as raw data of in-situ building vulnerability assessment.

4.2.2. Building Vulnerability Parameters

In order to assess building vulnerability, adequate parameters were defined by using the expert judgement approach. We entered into intensive discussion with a number of experts in the field of building vulnerability to define appropriate parameters, weighting factors, scoring values and threshold values. In general, parameters required for in-situ building vulnerability classification can be grouped into 3 categories:

- building stability parameters,
- tsunami component parameters, and
- accessibility parameters

4.2.2.1. Building Stability Parameters

Building stability parameters were required to determine the level of building stability at the time an earthquake occurs. This consideration is very important because most tsunami events in Indonesia were preceded by a very strong earthquake. That is why building vulnerability to earthquake is the prerequisite requirement of building vulnerability to tsunami. Furthermore, building stability parameters are very important to ensuring that buildings are resistant against tsunami flow energy. Building stability parameters are listed in Table 4.1 below:

Table 4.1. Building stability parameters, thresholds and their weight factors

No.	Parameter	Threshold	Weight Factor
1	Height	15 m	4
2	Material of Concrete	Lab mix	8
3	Proportion of Mortar	1 : 4	8
4	Type of Foundation	Foot	4
5	Existance of Column	available	6
6	Ring Balk	available	4
7	Truss Beam	available	4
8	Column Anchored	available	4
9	Wall Anchored	available	4
10	Truss Anchored	available	4
11	Reinforcement	available	4
12	Truss Roof Brace	available	4

13	Hammer Test Value	15 – 20 MPa	10
14	Roof Material	Clay	0
15	The builder	Skilled Labour	4

Table 4.1 shows the list of building stability parameters with different weight factors. Because each parameter does not contribute equally in the calculation of vulnerability, the weight factor was applied. The parameters are weighted according to the importance of the respective parameters. Hammer test values have the largest weight factor, because this value reflects the strength of building columns as the main pillars of the building. The second rank in weight factor is material of concrete and proportion of mortar. Roof material is regarded as having no direct correlation to the building vulnerability, and is, therefore, weighted by zero. Parameters, threshold and weighting values available in Table 4.1 above were defined by expert judgement. This judgement was made after intensive discussion with civil engineers and architectural experts.

4.2.2.2. Tsunami Component Parameters

After being hit by earthquake, buildings face a second hit by the strength of a tsunami wave. Buildings that are expected to be still standing after the earthquake were taken into consideration during tsunami component analysis. Buildings that were judged as collapsed and or seriously damaged by the earthquake were not taken into account in this second step of assessment. Tsunami parameters consist of 2 main items as listed in Table 4.2 below.

Table 4.2. Tsunami component parameters

No.	Parameter	Threshold	Weighting
1	Building Geometry	Multipart (Complex)	16
2	Building Orientation	Diagonal to wave direction	25

Building geometry and building orientation are important parameters when looking at the tsunami run-up energy impact. The building geometries in the research area include simple geometry, multi-part and long span. Buildings with simple geometry

accumulate less run-up energy compared to buildings with long span geometry. Therefore, the best building in regard to this parameter is simple geometry, the worst building is long span.

Building orientation is regarded as a more important parameter than building geometry in the calculation of building vulnerability. This is evident when looking at the weight value of building orientation. Building orientation was weighted almost twice in comparison to building geometry weight. The importance of building orientation can be substantiated by the fact that long span buildings (the worst geometry) are not so vulnerable to tsunami run-up energy if their orientation is perpendicular to the wave direction. Building orientations in the research area are categorized into perpendicular, diagonal or parallel to the wave direction. After the 2004 tsunami, several field surveys made it clear that buildings with specific shapes (e.g. hexagonal, triangular, rounded, etc.) suffered lighter damage than long rectangular or “L” shaped buildings whose main walls were oriented perpendicularly to the direction of flow (Dominey-Howes and Papathoma, 2007).

4.2.2.3. Accessibility Parameters

Accessibility parameters were used to determine buildings that are potentially suited for vertical evacuation shelters. Accessibility parameters consist of 6 attributes, as listed in Table 4.3 below:

Table 4.3. Accessibility parameters

No.	Parameter	Threshold	Weighting
1	Width of main access	3-5 m	11
2	Accessibility to the building	2 direction	11
3	Tsunami evacuation plan	available	5
4	Space for tsunami evacuation	available	22
5	Floor level for tsunami evacuation	2	22
6	Access to evacuation floor	Stairs	22

4.2.3. The Concept of Building Vulnerability Classification

Building vulnerability classes were determined based on a decision tree algorithm illustrated in Figure 4.2 below:

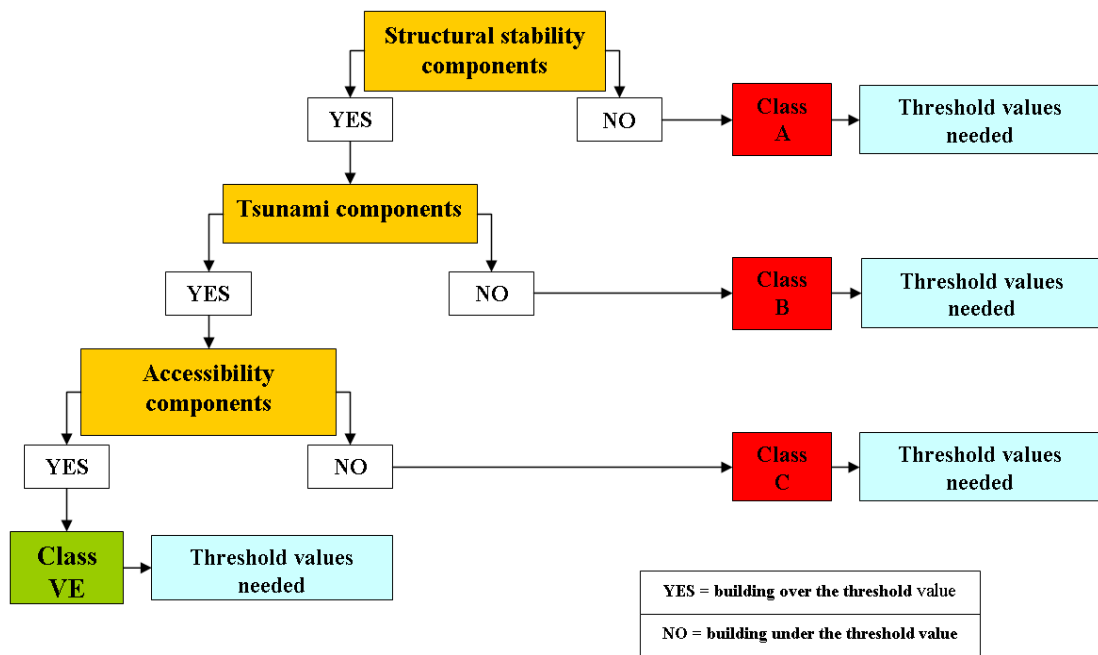


Figure 4.2. The decision tree approach of building vulnerability assessment

Figure 4.2 illustrates the four classes of building vulnerability, A, B, C and VE. Each class was determined using a scoring method with particular threshold values. The scoring method is described in section 4.2.4. Class A was determined in the first level of the decision tree by using the criteria of structural components. Buildings under the defined threshold value in the structural stability criteria were grouped into class A. Buildings over the threshold value in the structural stability criteria are further considered with tsunami component criteria. In this respect, buildings under the defined threshold value were grouped into class B, and the remaining buildings above the defined threshold value were further analysed by using accessibility components criteria to classify them into class C or class VE.

Class A is the most vulnerable building class. The probability level that Class A buildings will suffer damage is considered very severe. Such buildings will most likely collapse as a result of an earthquake and will be, therefore, no longer standing when a subsequent tsunami occurs. Class B buildings will most likely survive an earthquake hit, but most probably not withstand the strength of the tsunami waves that follow. Class C buildings have a low probability of being damaged by earthquakes and tsunamis, but they cannot be used for vertical evacuation. Class VE buildings share the low-risk attributes with Class C buildings, but these can be used as potential locations for vertical evacuation.

4.2.4. Scoring Method

A scoring method was employed by using a simple tabular operation and multiplying scores and weights. A score indicates the quality of a particular building property, while weight indicates the importance of this parameter.

As depicted in Figure 4.2 above, building vulnerability classification methods follow the multi-level decision tree analysis from the structural stability component, to the tsunami component and, finally, to the accessibility component. Each component was calculated by using parameters listed in subsection 4.2.2 above. Each parameter in each component was scored quantitatively by using relative scores. The value of 1 was regarded as the best score and the scores that follow were defined by using interval range scale. For example, if a particular parameter comprises 2 interval range scales (e.g. available and not available), the best score is 1 and the worst score is 2. This approach was then applied to every parameter in all level of components. Threshold values were defined by expert judgement, by considering the minimum requirement of buildings to survive the hazard.

After filling in all parameter scores and weights, the tabular operation follows the decision tree steps to calculate the total score of each sample building component. Buildings with scores under the structural component threshold were grouped into class A and not considered in the next step of calculation. Buildings with scores over

the structural component threshold were further calculated using the tsunami component threshold, and so on.

4.3. Remote Sensing and GIS Approach: Object-based Image Analysis

Remote sensing and GIS approaches were developed to classify building vulnerability using satellite image analysis. The goal of this approach is to develop a methodology for the building assessment for large areas and a large number of buildings.

This research employed QuickBird satellite images with very high spatial resolution. The panchromatic and the multi-spectral bands have a resolution of 0.6 m and 2.4 m, respectively. We used an object-based image analysis in this research. The procedural steps of this approach follow.

4.3.1. Pre-Processing

In the pre-processing stage, three main standard image processes were performed – geometric correction, pan-sharpening and filtering. The satellite image was geometrically corrected based on a topographical map created by Bakosurtanal (Indonesian National Coordinating Agency for Surveys and Mapping). Then, the pan-sharpening process was applied to fuse the lower spatial resolution multispectral satellite image (2.4 m) with the higher resolution co-registered panchromatic image (0.6 m), to get a composite high resolution multi-spectral image. This research employed UNB (University of New Brunswick) Sharpening algorithms (Zhang, 2002).

Image filtering was performed to provide better image pre-conditions for the purpose of the segmentation process, especially for edge detection. Because, in most cases, single buildings have heterogeneous spectral values and require distinctive object edges, appropriate filter algorithms needed to be selected. In this regard, we employed adaptive Local Sigma and Morphological Opening filter techniques to meet the required condition. The Local Sigma filter used the local standard deviation of pixels within a local box to determine valid pixels. This filter cleaned up noisy images by replacing the pixel value with the calculated mean, using only the valid pixels within

the filter box. The Morphological Opening filter smoothed the contours, broke narrow isthmuses and eliminated small islands and sharp peaks or capes in the analysed image. The opening of the image was defined as the erosion followed by subsequent dilation using the same structural element. The purpose of combining both filter algorithms was to get better edge detections.

4.3.2. Image Analysis

The basic step of object-based image analysis is the development of image objects as the basis of image classification. In this research, we used eCognition software developed by Definiens Imaging. The procedural steps of image analysis are as follows:

4.3.2.1. Segmentation

Image segmentation is the first step in object-oriented classification, for which each segment of image is regarded as an object to be classified in further processes. Instead of working with pixels, this method starts by segmenting the image into spectrally homogenous objects using region growing algorithms. In order to make the resulting objects more compact and smooth, at the expense of spectral homogeneity, some input parameters should be controlled, including segmentation algorithm, image layer (band) weighting, thematic layer usage, scale parameter, shape and compactness. The resulting objects become the most basic elements of the image, and each has its own "signature." A partial list would include the mean value and standard deviation of its constituent pixels, size, perimeter, primary orientation, compactness and texture, or the degree to which a pattern is present in each band. All of these measures are available to determine what feature the image object represents. In the segmentation concept, the semantic information necessary to interpret an image is not represented in single pixels, but in meaningful image objects and their mutual relationships (Baatz, 2000).

For better results in the process of image analysis, defining image objects of suitable size and shape is of the most importance. Good image objects are as large as possible, but small enough in representing the desired objects. In order to achieve this, multi-

level segmentation was performed to provide different object characteristics within image extent, on different levels. Each level of segmentation contains different input parameters that were designed to get better, more meaningful image objects. Input parameters have to be controlled properly on each level, based on classification requirements. On the lowest level (the finest segment), segment optimization was more urgently done in order to fit the segment with buildings edges.

A scale parameter was defined to determine the maximum heterogeneity allowed within desired objects. The size of produced image objects was varied by giving different scale parameter values. The larger scale parameter resulted in larger image objects. Shape and compactness criteria were defined to determine object homogeneity. Shape and compactness are regarded as the optimisation variables for the object's spectral homogeneity and spatial complexity. We created multiple image object levels comprising seven image object levels and layered them above the basic pixel level, from fine resolution on the lowest level to coarse resolution on the highest level. By default, eCognition software organised all image objects into a hierarchical network of image objects. Image objects within an image object level were linked horizontally and image objects in different level were linked vertically as illustrated in Figure 4.3.

Figure 4.3 illustrates the fact that image objects were networked in such a way that each image object represents its context as neighbour, super-object and sub-objects. There is no image object with more than one super-object but image objects can have more than one sub-object.

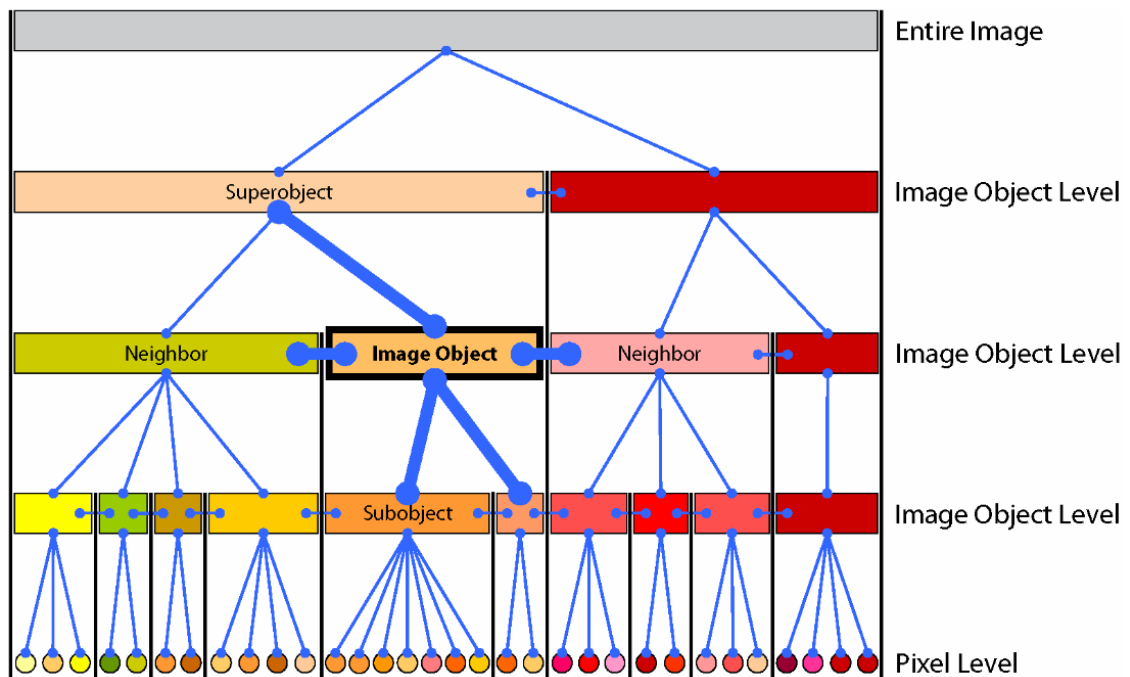


Figure 4.3. Multiple objects level of segmentation algorithm (Source : Definiens, 2007)

4.3.2.2. Image Classification

Image classification was performed by grouping resulting objects into desired classes. A single object is assigned by its feature characteristics calculated in the segmentation process. The characteristic features of an object were grouped into spectral signature, shape, size, texture and neighbouring relations to other objects. These representative features were analysed, selected and semantically modelled to classify objects into defined object classes.

The semantic model of image classification was developed as a rule-based semantic network. By using such a semantic network, we arranged a hierarchical classification procedure and interlinked all appropriate information on the objects in a so-called classification rule set. In the classification rule set, we developed appropriate conditions as the basis of classifying objects into the same classes. In order to define whether or not an object belongs to a certain object class, we employed a fuzzy logic algorithm. In this fuzzy logic algorithm, we defined confidence level (membership

function) of whether or not an object belongs to a certain class. Several conditions possibly characterise an object class by using Boolean operators such as “and, or, not”.

A fuzzy logic algorithm was employed to get membership values of objects that were grouped into particular classes. In the OBIA approach, each object in every level of segmentation contains specific features. These form the basis for object grouping into particular classes. The process of image classification – analysing, finding and customising appropriate object features for grouping similar objects – is the critical and core step, and it is very much influenced by the quality of the segmentation process. The better the image segmentation process is, the better it will provide superior image features for the classification process. The reason for this is that membership of a class varies depending on the feature intensity, thus an object may belong to more than one object class. Finally, the object is assigned to an object class in which it will have the highest value.

In addition, object feature separation analysis was used in combination with fuzzy logic. Fuzzy logic analysis was performed mainly for classifying such large objects as bodies of water (seas and rivers), vegetation and ground. Feature separation analysis was conducted, particularly in building extraction. Feature separation analysis was based on Bhattacharyya distance. According to Nussbaum et al. (2007), the Bhattacharyya distance can be used as a suitable separability measure where this distance value is justified as a measure of separability from the Bayesian decision rule for misclassification probability. For two classes (C1, C2) normally distributed with size mean values m_1, m_2 and standard deviation, σ_1, σ_2

$$B = \frac{1}{8}(m_1 - m_2)^2 \frac{2}{\sigma_1^2 + \sigma_2^2} + \frac{1}{2} \ln \left[\frac{\sigma_1^2 + \sigma_2^2}{2\sigma_1\sigma_2} \right]$$

the range value of the Bhattacharyya distance B will be in half-closed interval $[0, \infty)$. This range is transformed into the closed interval $[0, 2]$ by using a simple transformation namely Jeffries – Matusita distance measure (J)

$$J = 2(1.e^{-B})$$

$J = 0$ indicates that the two distributions are completely correlated (unseparated) and $J = 2$ indicates that the distributions are completely uncorrelated (well separated).

The feature analysing tool SEaTH (Separability and Threshold) was used to identify object feature characteristics with a statistical approach based on training objects. The statistical measure for determining the representative features for each object class is the pairwise separability of the object classes among each other. Subsequently, SEaTH calculates the thresholds which allow the *maximum* separability in the chosen features (Nussbaum et al., 2007).

Image classification was performed using the top-down approach. In this approach, we started classifying the image from the higher to the lower level of image objects. In the higher level, we classified large-size objects into particular classes such as water body (sea water), and in the lower level we classified small-size objects such as buildings. In the classification process, we analysed a large number of predefined features describing object properties. Furthermore, we developed user-defined features for the purpose of object grouping enhancement. The selected features utilised during object classification are listed in Table 4.4.

Table 4.4. Selected features for object classification

Object Features	Layer values	Mean	Brightness
			Blue
			Green
			Red
			Near infra red
	Shape	Generic	Area
			Length
			Width
			Length/Width
			Elliptic Fit
			Main direction

	Texure	After Haralick	GLCM (Gray Level Co-occurrence Matrix) Mean	Green (direction 45°)	
			GLDV (Gray-Level Diff. Vector) Contrast	All directions.	
	Customized	Arithmetic	NDVI	$(B4-B3)/(B4+B3)$	
			NDWI	$(B2-B4)/(B2+B4)$	
			Band Ratio 1	$B2/B3$	
			Band Ratio 2	$B3/B4$	
			Band Ratio 3	$B3/B2$	
			Band Ratio 4	$B4/B1$	
			Band Ratio 5	$B4/B3$	
			Band Ratio 6	$(B3/B4)/(B3/B2)$	
			Band Ratio 7	$B2/(B1+B2+B3+B4)$	
			Band Ratio 8	$(B3-B1)/(B3+B1)$	
			Band Ratio9	$(B4/B3)/(B1+B2+B3+B4)$	
			Band Ratio 10	Brightness($B1/B3$)	
			Band Ratio 11	Brightness($B1/B2$)	
			Band Ratio 12	$(B3-B2)/(B3+B2)$	
		Thematic Attributes	Thematic object ID	Road network	
	Class-Related features	Relations to neighbor object	Related Border to	Neighbour buildings	
Distance to			road		
	Relations to super objects	Existence of Available class	Water, Vegetation, Teracotta roof, White roof		
Mathematic Logical operators	and				
	or				

The main purpose of the image analysis procedure is to extract building objects. We classified non-building objects before classifying buildings. A multi-level classification algorithm was performed to extract non-building objects such as water, vegetation types, shadow and ground. After classifying non-building objects, the remaining objects were regarded as building objects. In order to get individual building attributes, buildings were classified based on roof colour. The algorithm of building extraction is illustrated in the following flow chart (see Fig. 4.4 below)

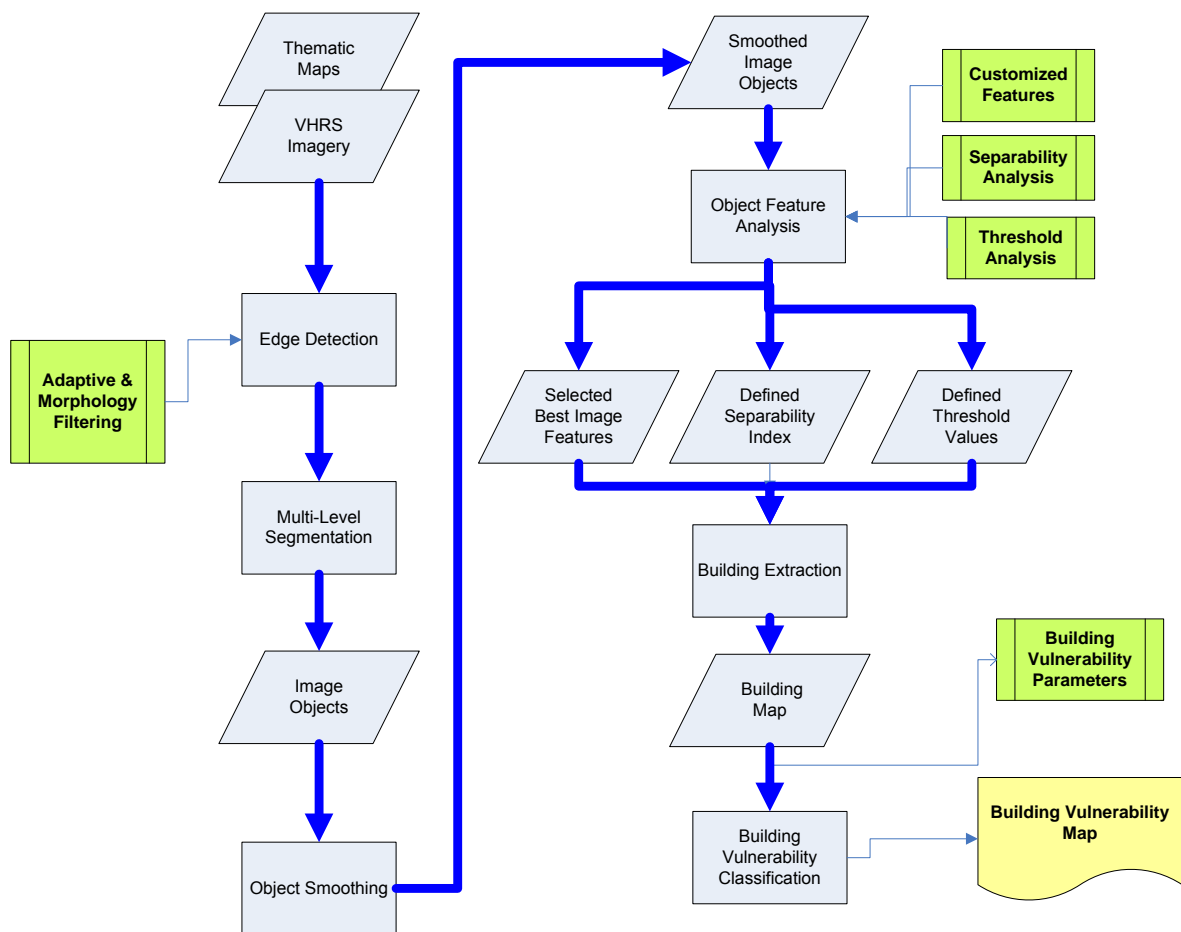


Figure 4.4. Flow chart of the building extraction algorithm

Image classification started with the classification of non-building objects such as water, vegetation, and ground, using a higher segmentation level. Water was classified in level 6 using the customized feature Band Ratio 7 (see Table 4.5). Band Ratio 7 (BR

7) was customized by the author, who developed a ratio of all available bands in the following formula:

$$(BR\ 7) = \text{Mean Band 2} / (\text{Mean Band 1} + \text{Mean Band 2} + \text{Mean Band 3} + \text{Mean B 4})$$

The threshold of BR 7 was identified using feature range updaters and was applied in membership function, as demonstrated in Figure 4.5.

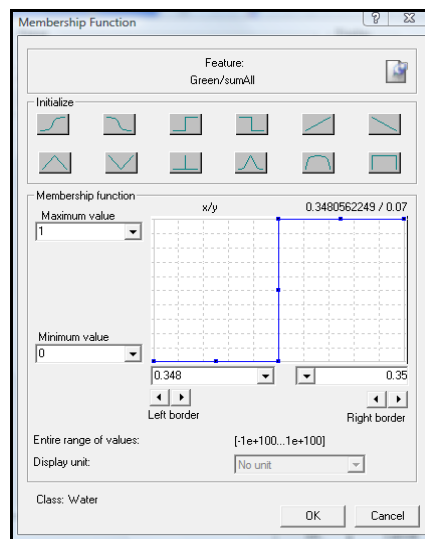


Figure 4.5. Membership function of customized feature BR 7 for water classification

Band Ratio 7 very effectively detected a water body under normal conditions (without waves). The very bright water wave near the shoreline was classified by using neighbourhood parameters that combined brightness and distance to other object features (in this case: distance to water). The brightness and distance threshold values were identified using feature range updaters and were applied in the membership function

After water, vegetation was the next object that needed to be masked in the higher segmentation level. Level 4 was the best level in which to detect vegetation objects. Because the main goal of this research is building detection, vegetation was classified only to produce a non-building object mask to facilitate easier building classification in the lower segmentation level. Two classes of vegetation were enough to block any

type of vegetation in this segmentation level, namely vegetation1 and vegetation2. Vegetation1 represented trees and dense vegetation, and vegetation2 represented shrub, grass and coarse vegetation. Vegetation1 and vegetation2 were separated based on spectral analysis, using a customized feature. Ratio of Mean Band 4/Mean Band 3 effectively detected these vegetation objects. Vegetation1 and vegetation2 threshold values were identified using feature range updaters and were applied in membership function.

Open land and sand (ground) were also classified in level 4, using texture feature analysis. We used a GLDV Contrast feature which is one of texture after Haralick type calculated by the gray level co-occurrence matrix (GLCM), a tabulation that reveals how often different combinations of pixel gray levels occur within an image. GLDV is the sum of the diagonals of the GLCM calculating the occurrence of references to the neighbour pixels' absolute differences (Definiens, 2007). Ground object threshold values were also identified by using feature range updater and applied in membership function

Building objects could be detected beginning from Level 3 of the segmentation level, especially white-roof buildings. Still, other types of buildings were difficult to detect in this level, owing to lower segmentation accuracy when detecting the building edges. White-roof buildings appear in much greater contrast to the surrounding objects, something that provided good conditions for an accurate segmentation. White-roof building edges were well segmented in this level. White-roof buildings are ready to classify in this level while non-white building objects need a finer segmentation resolution. White-roof buildings were classified by using a customized feature the author developed and named Band Ratio 10. Band Ratio 10 (BR 10) was customized by the author by developing a ratio of brightness and mean values of band 1 and band 3 formulated as:

$$(BR\ 10) = \text{Brightness} * (\text{Mean Band 1} / \text{Mean Band 3})$$

The threshold of BR 7 was identified by using feature range updaters and was applied in the membership function.

Terracotta-bright-roof (TBR) buildings were well-segmented in Level 2 and were classified by using a customized feature the author developed and named Band Ratio 3. Band Ratio 3 (BR 3) was customized by the author by developing a ratio of mean value of Band 3 and mean values of band 2 formulated as:

$$(BR\ 3) = \text{Mean Band 3} / \text{Mean Band 2}$$

The threshold of BR 3 was identified using feature range updaters and was applied in the membership function.

The remaining objects that needed to be classified were gray-roof buildings, brown-dark-roof buildings, and shadows. All of these objects were classified in the same segmentation level, level 1. The classification of three class types within the same segmentation level requires more effort when selecting the appropriate object features. One feature object is not enough to separate three objects. Two or more feature objects are needed to solve the problem. In this case, object feature separability and threshold analysis are needed to define the optimum parameters as object detectors. Bhattacharyya distance algorithm provides a good solution to analyze the separability and to define the thresholds, which allow the maximum separability in the selected features (Theodoridis and Koutroumbas, 2006). In this research, we employed a tool SEaTH (Marpu et al., 2008) to analyse the feature separability based on Bhattacharyya distance and Jeffries – Matusita distance algorithms. The result of the separability analysis is listed in Table 4.5 below.

Table 4.5. Results of the Feature Separability analysis

Class Comparison	Separability	Feature	Arithmetical membership	Threshold
Brown dark-Gray	1.45	Band Ratio 11	Smaller	224.07
	1.45	Band Ratio 10	Smaller	224.07
Brown dark-Shadow	1.65	Brightness	Greater	149.84
	1.59	Mean Red	Greater	162.09
Gray - Shadow	1.87	Brightness	Greater	156.21
	1.84	Mean Green	Greater	262.59

Table 4.5 describes the separability level between the investigated classes using defined appropriate features and their membership thresholds. For example, dark, brown-roof buildings can be separated from gray-roof buildings by using Band Ratio 11 and Band Ratio 10 with the threshold values of 224.07. Using the feature properties, the separability of brown dark-roof buildings and gray-roof building is 1.45. Since the maximum value of separability value is 2 (well separated), both objects are not completely separated. There is a spectral space where both object spectrals are confused. In the case of gray-roof buildings and shadows,, the separability value is 1.87 when using the brightness object feature. This separability value indicates that both objects almost completely separated with a threshold value greater than 156.21.

4.3.2.3. Accuracy Assessment of the Building Detection

To evaluate the quality of the building detection analysis, an accuracy assessment using an error matrix was performed. An error matrix is a matrix formulated in a tabular form and is used to compare two thematic maps i.e. a reference map and a map derived from automated building detection (Congalton, 1991). A reference map was generated by the manual digitising of building samples. Building samples were selected by random selection. The accuracy assessment was carried out by overlaying both the digitised building map and the automatically derived building map in a GIS environment. The accuracy was calculated based on the difference of the areas between the two overlaid maps.

4.3.2.4. Statistical Analysis

Statistical analysis was carried out to investigate key spatial parameters of in-situ building vulnerability assessment that are applicable for the remote sensing assessment. These parameters can be regarded as connectors of in-situ assessment and remote sensing assessment (see Figure 4.1). The selected parameters are integrated in the remote sensing classification rule set designed to regionalize building vulnerability assessment to the whole area of study.

Descriptive statistics analysis was carried out to recognize the pattern of data distribution. Descriptive statistics are used to describe the main features of a collection of data quantitatively (Mann, 1995). In this regard, the main features of building classes related to their spatial attributes – such as area, height, shape, etc. - were analyzed. Boxplot diagrams were depicted to demonstrate groups of numerical data graphically through their five-number summaries: the sample minimum, lower quartile (Q1), median (Q2), upper quartile (Q3), and sample maximum. In boxplot diagrams, extreme values will be considered as outliers. By using descriptive statistics and boxplot diagram analysis, threshold values of selected spatial parameters were defined.

4.3.2.5. Building Vulnerability Classification

Building vulnerability classification was conducted based on the spatial parameters of extracted individual buildings from the previous steps. The spatial parameters were taken from surveyed buildings that were classified based on their vulnerability.

The algorithm of building vulnerability classification is illustrated in the form of a decision tree flow chart, as depicted in Figure 4.6.

Figure 4.6 illustrates the procedural steps of building vulnerability classification using spatial parameters, executable in object-based image analysis comprising size, shape, orientation, height and accessibility. The spatial parameters were derived from spatial characteristics of in-situ building classes as described below:

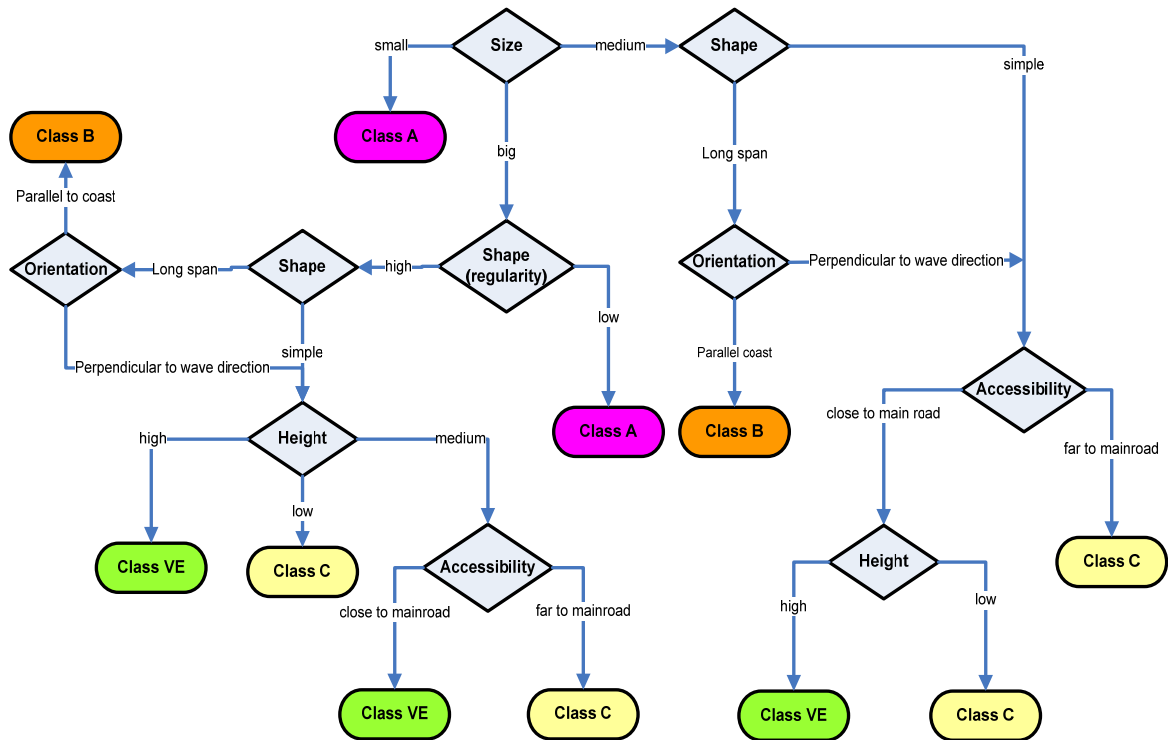


Figure 4.6. Decision tree analysis for building vulnerability classification using object-based image analysis

a. Building Size

During field survey and data analysis, we found that most small building samples were regarded as unstable buildings. Only a few of the larger buildings were regarded as unstable buildings. These large, weak buildings were identified as very old buildings or non-permanent buildings. In normal conditions, larger buildings were mostly found to be stable. To determine the relationship between building size and building stability, we used box plot statistical analysis: Using this statistical analysis, data distribution can be determined. In the decision tree analysis, building size was regarded as the indicator of building stability – small buildings were classified as class A (very vulnerable buildings).

b. Building Shape

The building shape parameter was defined to regard building geometry as one of the tsunami component parameters. This parameter was defined to differentiate between simple buildings and long-span (long rectangular) buildings. The building shape was calculated by using length/width ratio value of an object feature.

c. Building Orientation

Building orientation is the orientation of the main wall of buildings relative to the direction of the tsunami flow. In this research, we categorized building orientation into 3 possible orientations – perpendicular, diagonal and parallel. Building orientation was calculated by using the main direction value of the object feature.

d. Building Regularity

The building regularity parameter was derived from the elliptic fit feature object. The creation of an ellipse with the same area as the considered object is a first step in the calculation of the elliptic fit. In the calculation of the ellipse, the proportion of the length to the width of the object is regarded. After this step, the area of the object outside the ellipse is compared with the area inside the ellipse not filled out with the object. While 0 means no fit, 1 stands for a completely fitting object.

e. Building Accessibility

Building accessibility was measured using the distance of a building from the road. This parameter was applied specifically to identify buildings with the potential for use in vertical evacuation. Vertical evacuation buildings are ones close to the road so that they can be easily accessed by evacuees.

f. Building Height

Building height is considered the height of buildings from the ground to the top of the roof. This parameter was used to identify buildings with more than one storey. This information was specifically used to identify buildings with the potential for use in

vertical evacuation. Building height information was provided by elevation data derived from airborne radar covering the Cilacap area.

4.3.2.6. Accuracy Assessment of the Building Vulnerability Classification

To evaluate the quality of the building vulnerability classification, an accuracy assessment using a confusion matrix was performed. Much like the error matrix, the confusion matrix is a matrix formulated in a tabular form for the purposes of comparing two thematic maps – a reference map and a map derived from automated building detection. A reference map was created using the results of in-situ building assessment: Building classes were plotted into their actual positions on the map. To get the independency of the accuracy assessment, building samples taken in the accuracy assessment were separated from the building samples that were used in the spatial parameter analysis. The accuracy assessment was carried out by comparing the classification results of the in-situ assessment and the classification result of the remote sensing techniques. Table 4.6 illustrates the calculation of the error matrix by using a tabular operation.

Table 4.6. Confusion matrix for accuracy assessment of building vulnerability classification

Classified \ Reference	Classified					
	Class A	Class B	Class C	Class VE	Row Total	Omission
Class A	Σ Matched A-A	Σ Misclass A-B	Σ Misclass A-C	Σ Misclass A-VE	Σ Row Class A	Σ Misclass/ Σ Row Class A
Class B	Σ Misclass B-A	Σ Matched B-B	Σ Misclass B-C	Σ Misclass B-VE	Σ Row Class B	Σ Misclass/ Σ Row Class A
Class C	Σ Misclass C-A	Σ Misclass C-B	Σ Matched C-C	Σ Misclass C-VE	Σ Row Class C	Σ Misclass/ Σ Row Class A
Class VE	Σ Misclass VE-A	Σ Misclass VE-B	Σ Misclass VE-C	Σ Matched VE-VE	Σ Row Class VE	Σ Misclass/ Σ Row Class A
Column Total	Σ Column Class A	Σ Column Class B	Σ Column Class C	Σ Column Class VE	Σ Total	
Commission	Σ Misclass/ Σ Column Class A	Σ Misclass/ Σ Column Class B	Σ Misclass/ Σ Column Class C	Σ Misclass/ Σ Column Class VE	Overall Accuracy	Σ Matched In diagonal/ Σ Total

4.3.3. Transferability Analysis

Transferability analysis was carried out by applying the resulted OBIA rule-set of building vulnerability assessment of Cilacap city area to another area. Padang city was selected to be a test area, because Padang is one of pilot areas of GITEWS project. In Padang area, data available for transferability analysis consists of:

- IKONOS satellite image with 4 multi-spectral bands (blue, green, red and near infra red) and one panchromatic band. The spatial resolution is 4 m for multi-spectral bands and 1 m for panchromatic.
- Elevation dataset which is derived from 5 m spatial resolution SAR data
- Street network

For the first step, pre-processing was applied to IKONOS data before inputting it into the OBIA rule-set. The pre-processing procedures were the same as procedures applied for Cilacap satellite image dataset: geometric correction, pan-sharpening and filtering. In the process of transferability analysis, all available datasets of Padang area were inputted in the OBIA rule-set replacing datasets of Cilacap area. Finally, the OBIA rule-set developed for Cilacap was applied to Padang in order to evaluate the transferability of the developed approach.

CHAPTER 5

RESULTS OF THE RESEARCH

5.1. In-Situ Survey

5.1.1. Building Sample Selection

Figure 5.1 depicts the distribution of building samples in the research area. The building samples are shown as black dots with the Quickbird image as background. The total number of building samples numbers around 500 samples. All of the samples are well distributed within the research area, and represent all of the types of buildings available.



Figure 5.1. The distribution of building samples for in-situ assessment

5.1.2. Building Samples Classification using Direct Field Measurements

Based on the scoring and weighting method described in section 4.2, the building samples were classified into the vulnerability classes A, B, C, and VE. Figure 5.2 depicts the map of building vulnerability by using in-situ assessment.

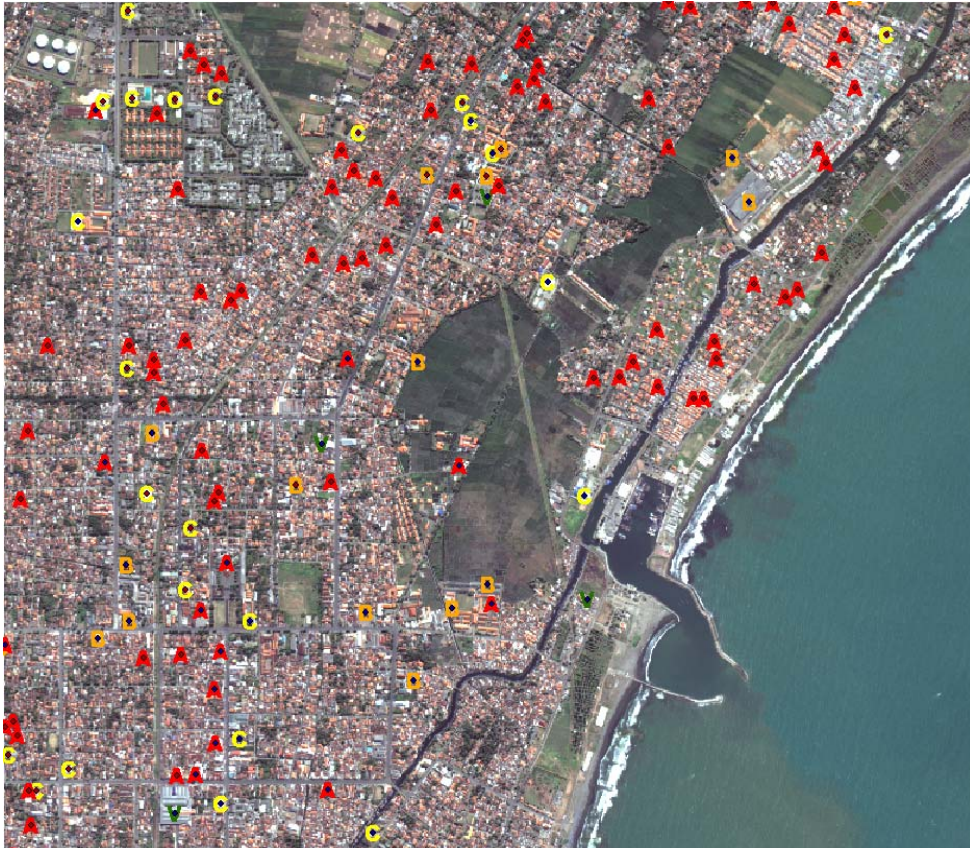


Figure 5.2. Building vulnerability classification using in-situ assessment

Figure 5.2 demonstrates the distribution of building samples and their classes of vulnerability. This vulnerability map is regarded as the reference in order to assess the accuracy of the remote sensing approach.

5.1.3. Statistical Analysis

To get the basis of the up-scaling process from field measurement data to the remote sensing approach, we performed statistical analysis. The results of this analysis are used to derive thresholds for the decision tree analysis in the subsequent remote

sensing approach. Two examples of this analysis are shown in the following sub-chapters.

5.1.3.1. Boxplot Analysis of Building Size

Figure 5.3 depicts the results of a boxplot analysis of building size and the building vulnerability classes.

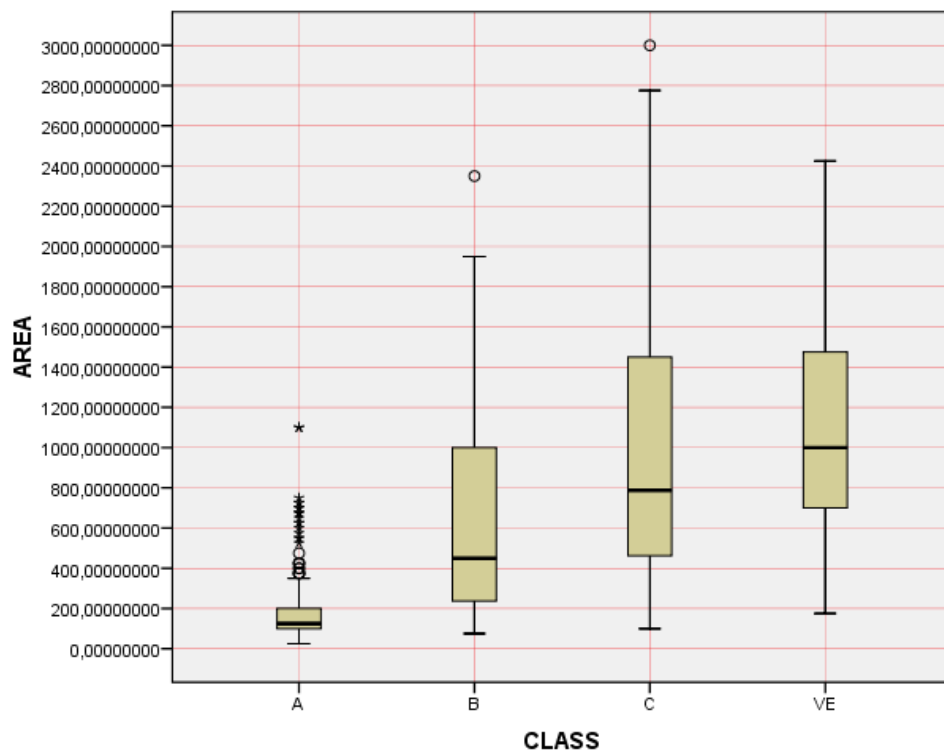


Figure 5.3. Boxplot analysis of building size (area) and building vulnerability classes

Figure 5.3 shows that most small buildings were classified as class A, while with respect to the classes B, C and VE there is no clear correlation with the building size. In this case, building size can be regarded as an important parameter for classifying class A buildings.

5.1.3.2. Boxplot Analysis of Building Height

Figure 5.4. depicts the results of a boxplot analysis of building heights and building vulnerability classes.

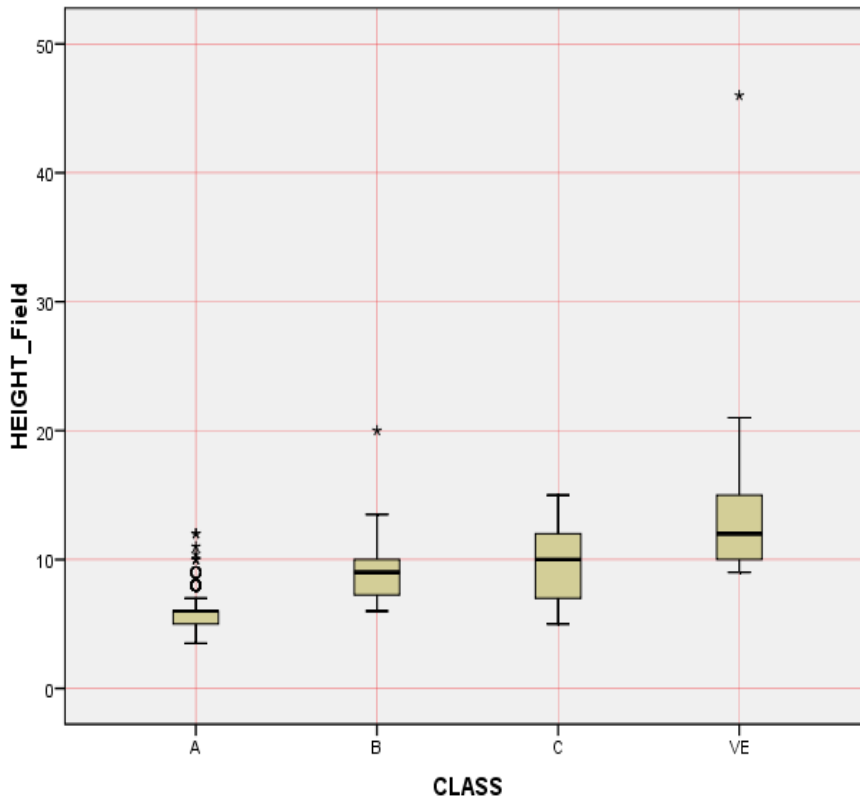


Figure 5.4. Boxplot analysis of building height and building vulnerability classes

Figure 5.4 demonstrates that most of class VE buildings are higher than class A, B or C although some of the samples have equal height. The diagram does not show a clear pattern of data distribution of class B and class C buildings. In this case, building height can be regarded as an important parameter for classifying class VE buildings.

5.2. Remote Sensing Approach

5.2.1. Pan-Sharpener

Figure 5.5 depicts the results of the image pan-sharpening process. From this figure we can see that the pan-sharpened image clearly reflects the high resolution of the

panchromatic image in combination with the multi-spectral information. This result is used as input for the next processing step, i.e. the filtering and segmentation process.

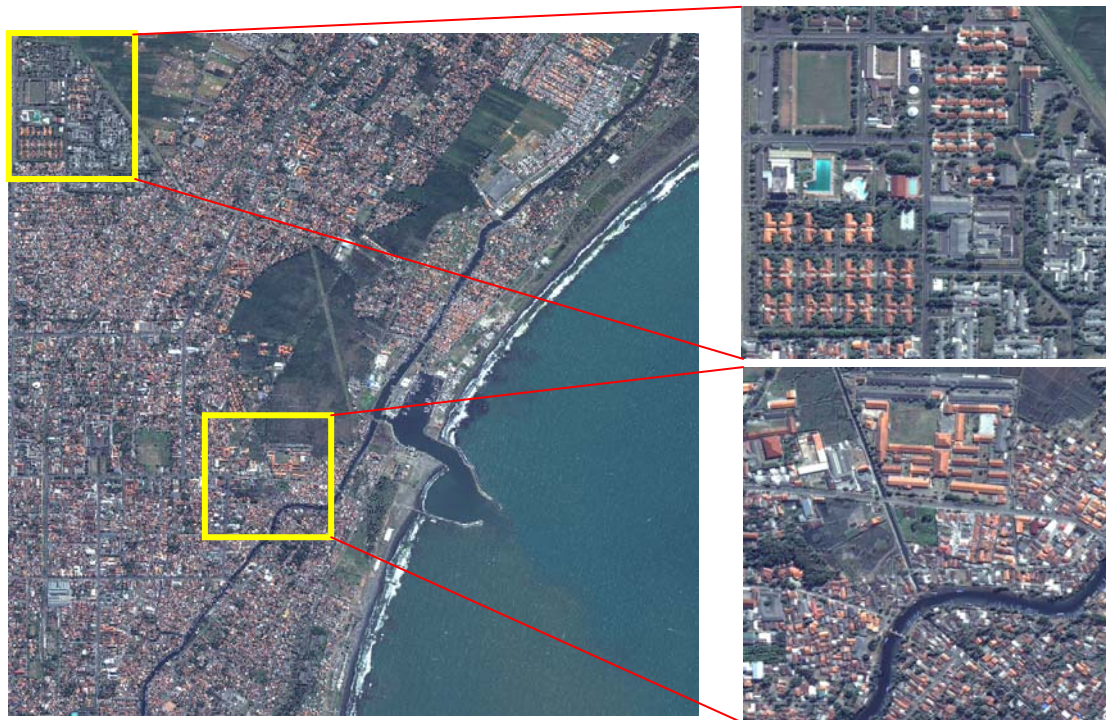
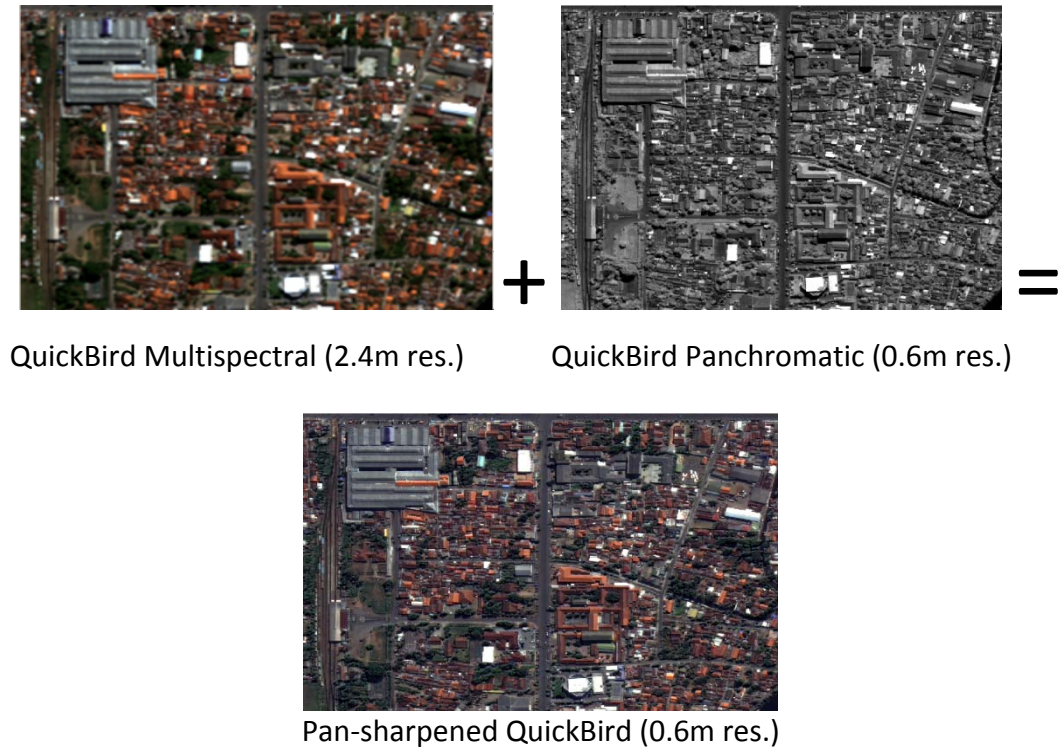


Figure 5.5. The results of the image pan-sharpening process

5.2.2. Image Filtering

Image filtering was performed to provide a better image input for the edge detection process. Better edge detection resulted in better segmentation and classification results. The combination of two image filtering techniques – namely adaptive local sigma and morphological opening algorithms – demonstrated good results in edge detection by means of edge sharpening. Adaptive box-filtering algorithms were applied to remove random bit errors and to smooth noisy data (Eliaison et al., 1990). In the adaptive filtering procedure, the standard deviation of those pixels within a local box surrounding each pixel was used. A series of two or three filters with decreasing box sizes was applied to clean up extremely noisy images and to remove bit errors near sharp edges. Morphological opening filters smoothed the contours, broke narrow isthmuses and eliminated small islands and sharpened peaks or capes in the image. The opening of the image was defined as the erosion of the image followed by subsequent dilation using the same structural element (Haralick et al. 1987). Figure 5.6 depicts the result of filtering techniques using adaptive local sigma and morphological opening algorithms.

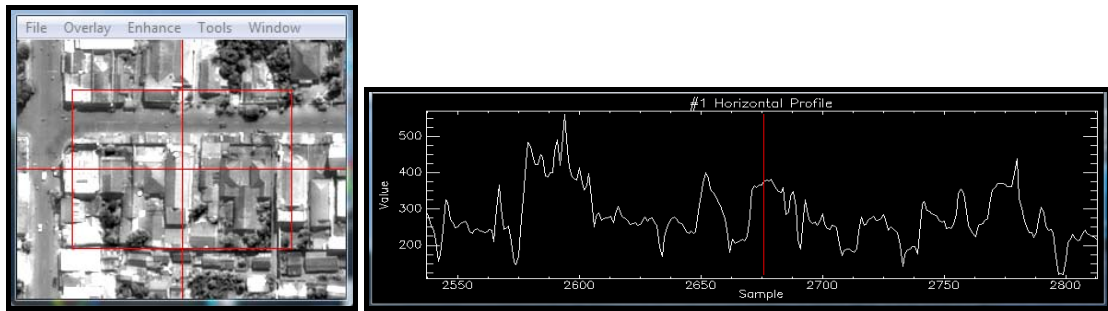


(a) Before filtering

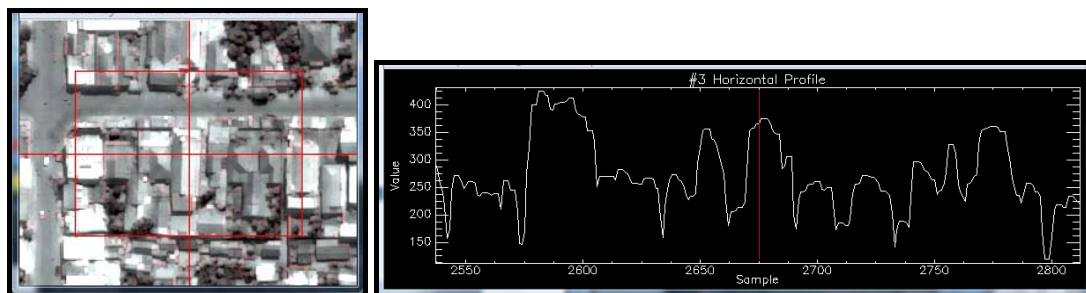
(b) After filtering

Figure 5.6. Image filtering results using adaptive local sigma and morphological opening algorithms.

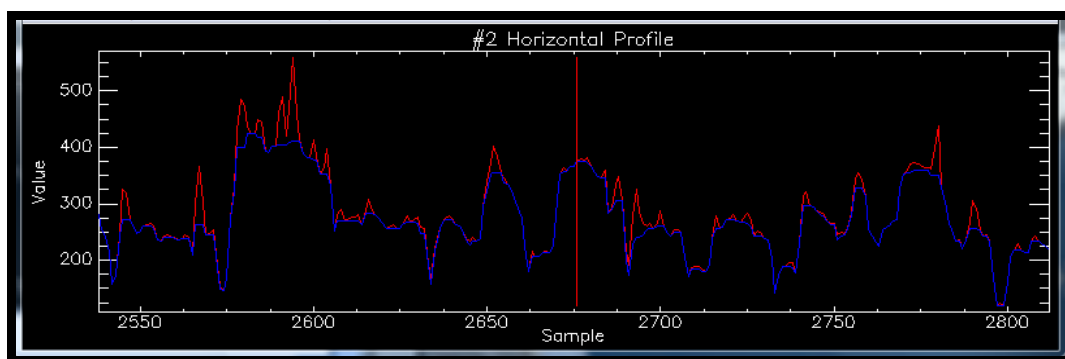
Figure 5.6 demonstrates the image before the filtering process (a) and after the filtering process (b). Figure (b) appears with smoother building objects, and sharper edges contrast with the surrounding objects. Figure 5.7 depicts a horizontal pixel profile in a subset of the images before and after the filtering process, which shows the effect of this processing step..



(a)



(b)



(c)

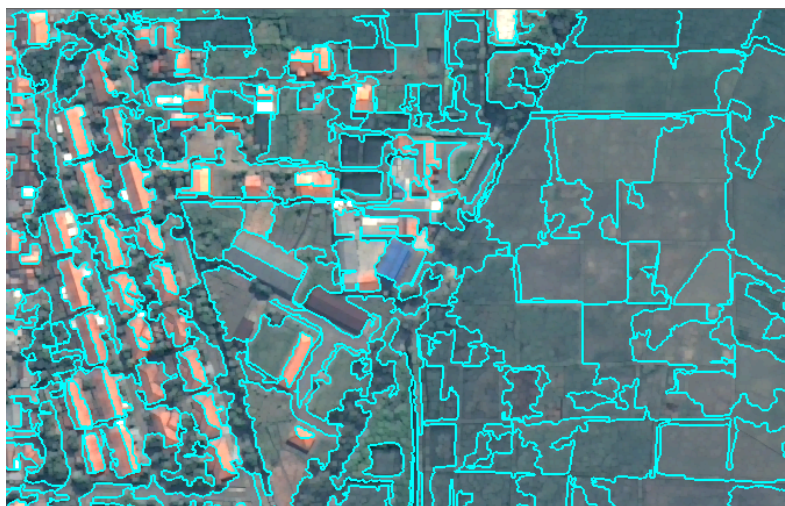
Figure 5.7. Horizontal pixel profile of the red band of the Quickbird image: (a) before filtering process, (b) after filtering process and (c) comparison before (red line) and after filtering (blue line).

5.2.3. Image Segmentation

As described in chapter 4.3, a hierarchical image segmentation was performed. Figure 5.8 illustrates the results of the multi-level segmentation process. Features in the entire image were segmented into smaller objects. The size and shape of the objects varies in different levels. The same feature in the image was segmented differently in another image object level because of the different input parameters used in the segmentation process. The definition of the scale parameter is the key to performing different segmentation results in different image object levels.



Level 6



Level 4

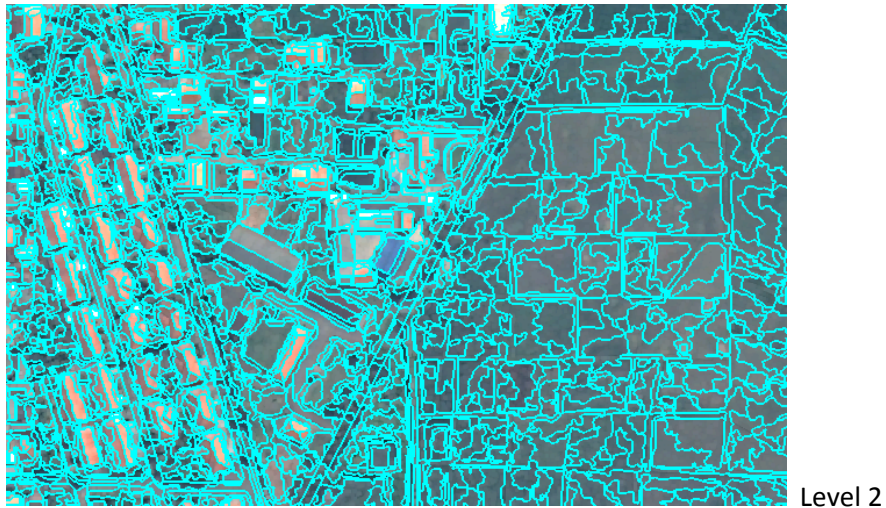


Figure 5.8. The results of multi-level image segmentation

The objects shown in level 6 were segmented more generally (with larger object size) than in level 5, level 4 and other lower levels. From the top level to the bottom level, objects were segmented gradually into finer objects. Accordingly, objects in level 1 are the finest objects amongst different levels. Each level provided different image object characteristics suited for detecting particular objects. In level 4, the building edges have not been well detected, but in level 2, terracotta-bright-roof building edges have been well detected. Figure 5.9 below demonstrates the suitability of level 4 for vegetation detection.

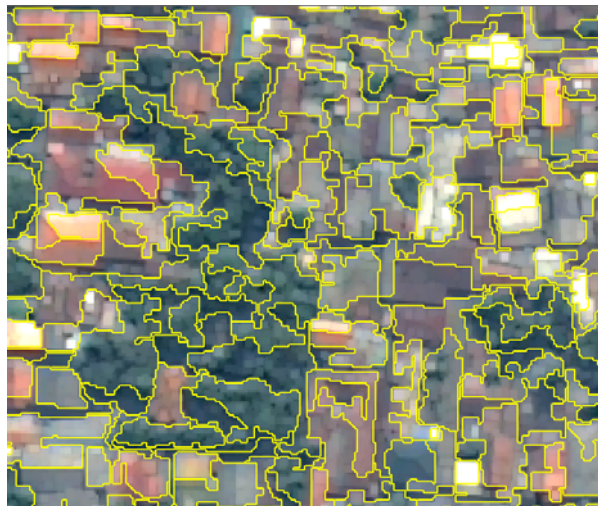


Figure 5.9. Segmentation level 4 is suitable for vegetation detection.

Furthermore, in the same image object level, different features were segmented differently owing to different statistical values of pixel group aggregates. Large, bright-roof buildings were segmented separately from darker features in their immediate vicinity. The homogeneity of pixel values in a particular area is the main consideration in identifying different image objects. In this case, composition of homogeneity criterion (shape and compactness) is the key input parameter in identifying image objects. A good segmentation result must be one in which a particular feature in an image is segmented separately from other features. In other words, different features in an image should be segmented in different image objects. The ideal segmentation is achieved when each feature in an image is segmented so individually and precisely that it becomes a single object. This will define the quality of the segmentation process. Figure 5.10 shows good segmenting of contrast features, such as white-roof buildings and bright terracotta-roof buildings. The best segmentation result for each feature is shown in different image object levels. For example, water image objects are segmented best in level 7 or level 6, vegetation in level 4, etc. The best segmentation level for building classification is mostly in the finer segmentation levels 1, 2 or 3, depending on the building type.

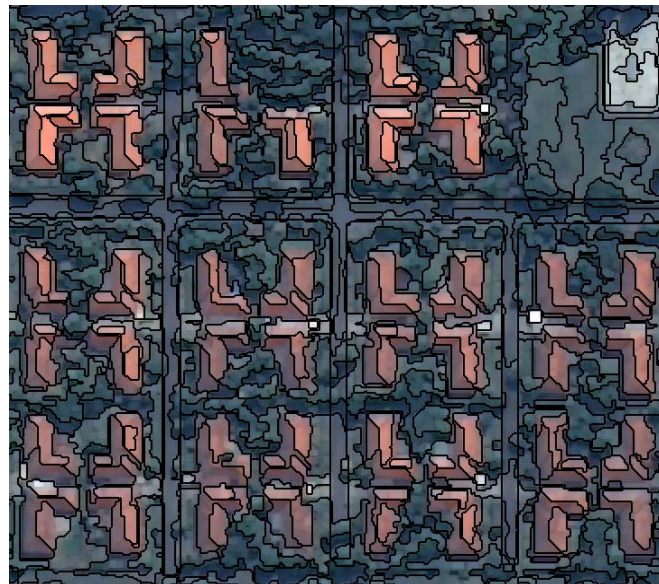


Figure 5.10. Level 2 is suitable for buildings segmentation

5.2.4. Building Detection Analysis

5.2.4.1. Object Feature Selection

Object features play important roles as the central parameters of object classification. We have investigated a number of features to get the most appropriate features for object classification. Table 4.5 shows the list of selected features as the key parameters to object classification. The selected features were investigated by using feature range analysis and separability analysis. Building detection was performed using these selected features.

5.2.4.2. Building Detection

We performed the building detection process to classify individual buildings as the basis of building vulnerability classification. Figure 5.11 displays the result of the building detection process. Most of building objects were classified based on their roof colour. Nevertheless, some remaining building blocks could not be classified individually because there was no segment separating each building during the segmentation process. This occurred in the building blocks, where the edges of the buildings were not defined sharply enough to be regarded as a boundary of separated objects. Even the human eye hardly delineates the building edges. Buildings surrounded by sharp edges allowed the building detection algorithm to easily classify buildings individually. Figure 5.12 depicts the building map as the result of building detection analysis.

5. Results of the Research

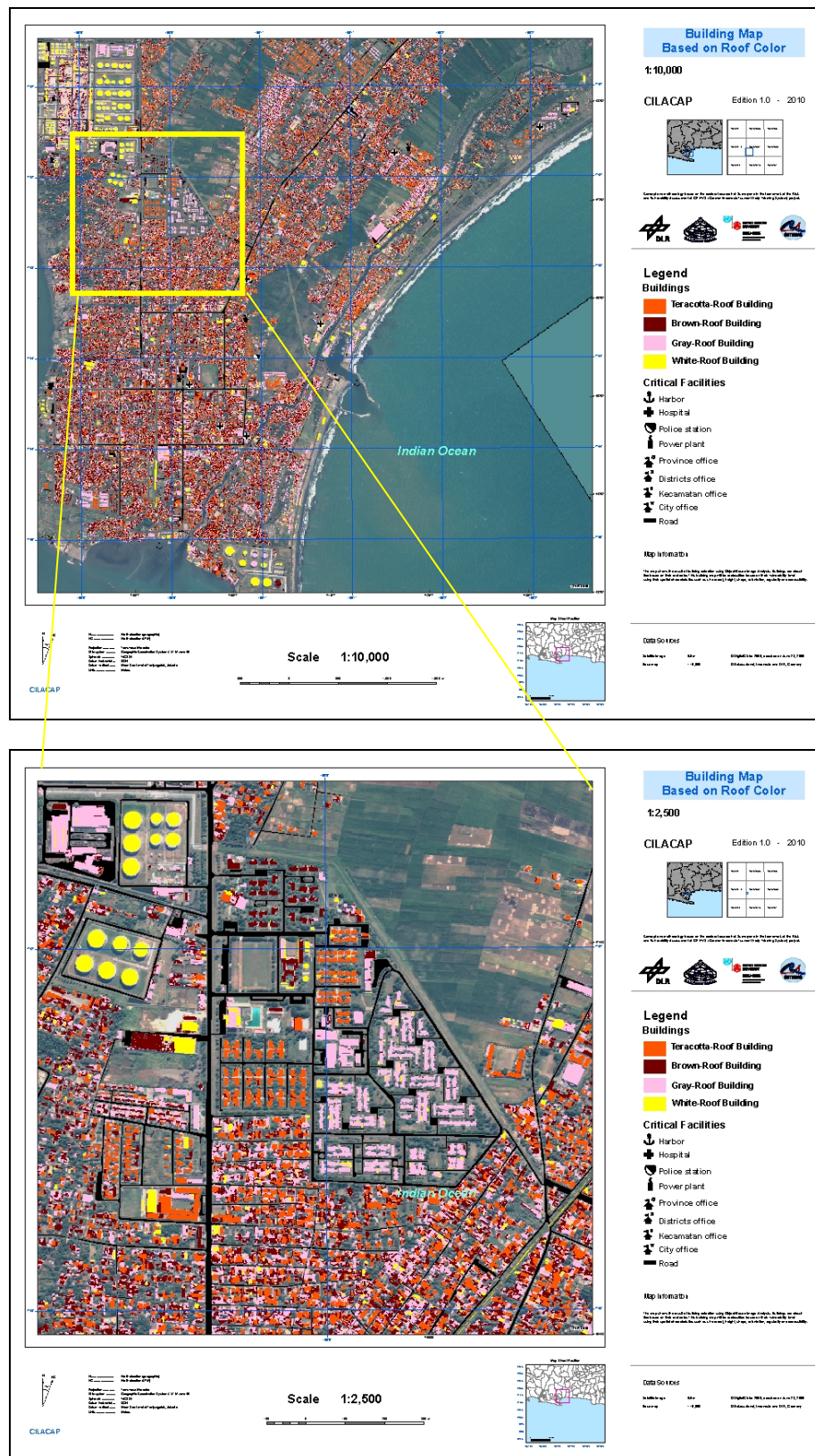


Figure 5.11. The result of building detection process based on roof colour

5. Results of the Research

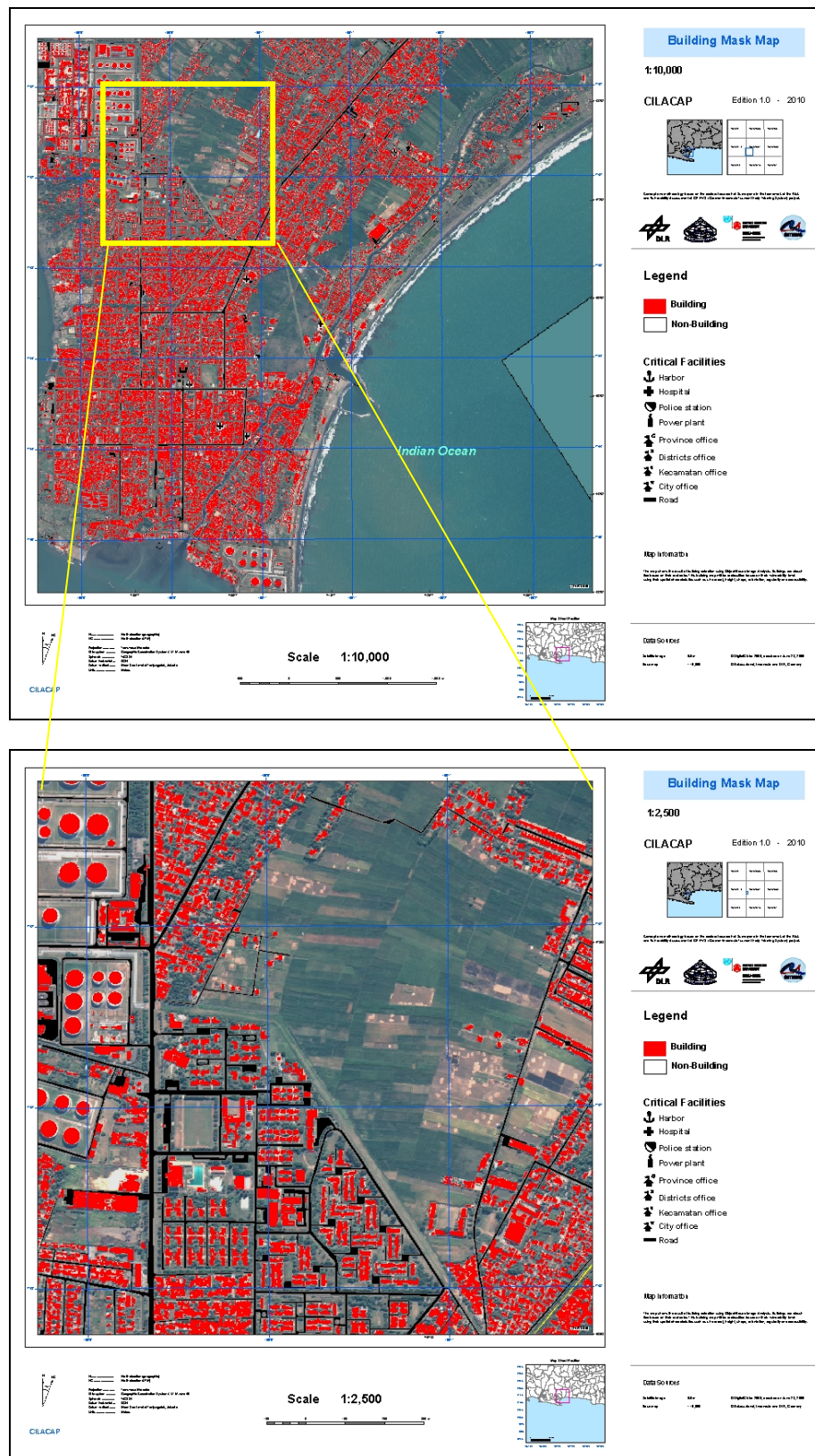


Figure 5.12. The result of building detection analysis

5.2.5. Remote Sensing Techniques for Building Vulnerability Classification

Building vulnerability classification was performed according to the approach shown in Figure 4.6. The building vulnerability map was created using that model. The results are shown in Figure 5.13. Building vulnerability classes are depicted in red (class A), orange (class B), yellow (class C) and green (class VE). Class A is for buildings classified as the most vulnerable and class VE is for buildings classified as less vulnerable and potentially suited for use as vertical evacuation sites.

5.2.6. Accuracy Assessment

Accuracy assessment was performed to evaluate the accuracy of the building detection and the accuracy of the vulnerability categorization.

5.2.6.1 Accuracy of building detection

For the purpose of this accuracy assessment, a reference map was generated by manually digitising building samples, which were selected by random selection. A total number of 520 building samples were selected and digitised, as depicted in Figure 5.14, and this map is regarded as a reference map for accuracy assessment.

5. Results of the Research

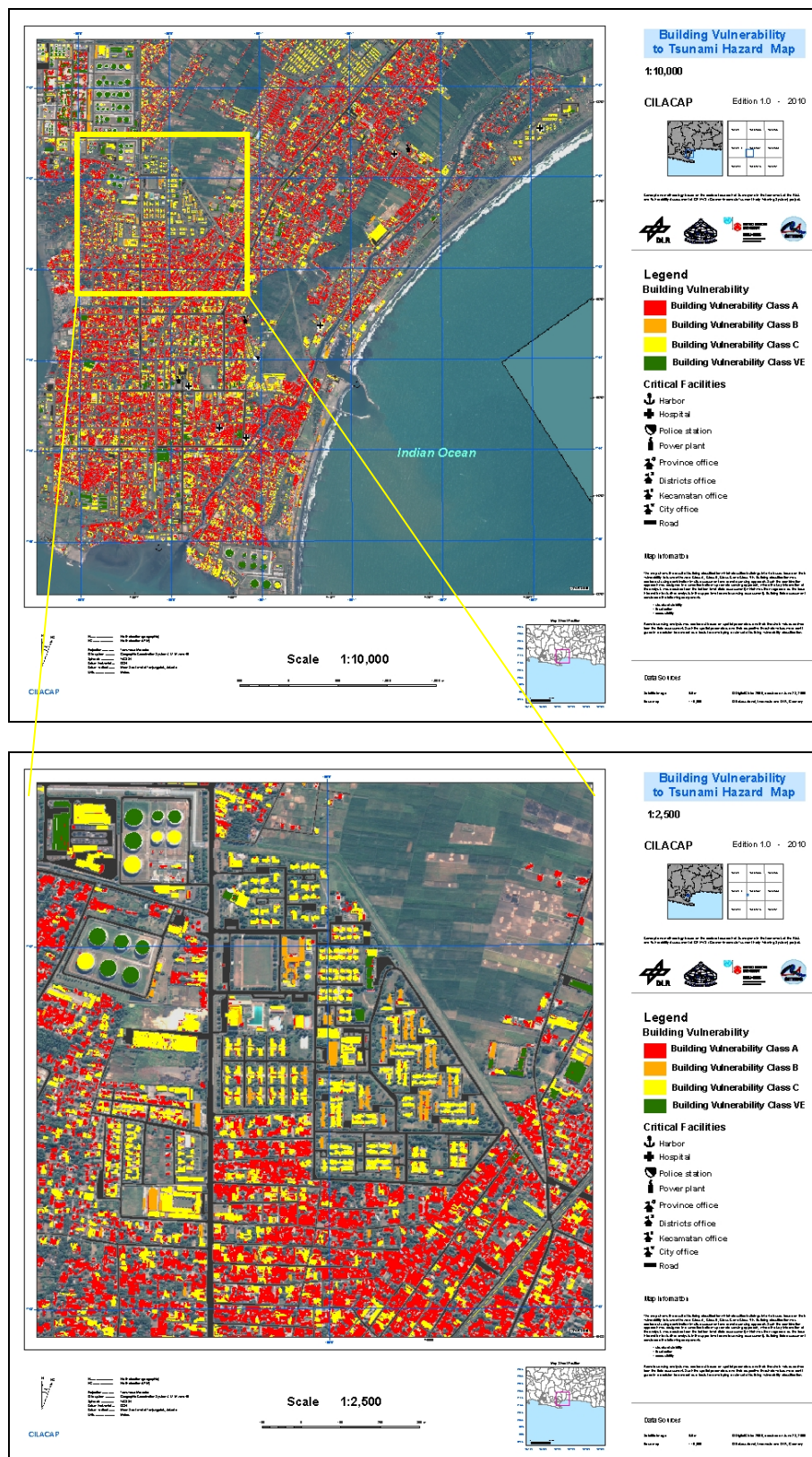


Figure 5.13. Building vulnerability classification results

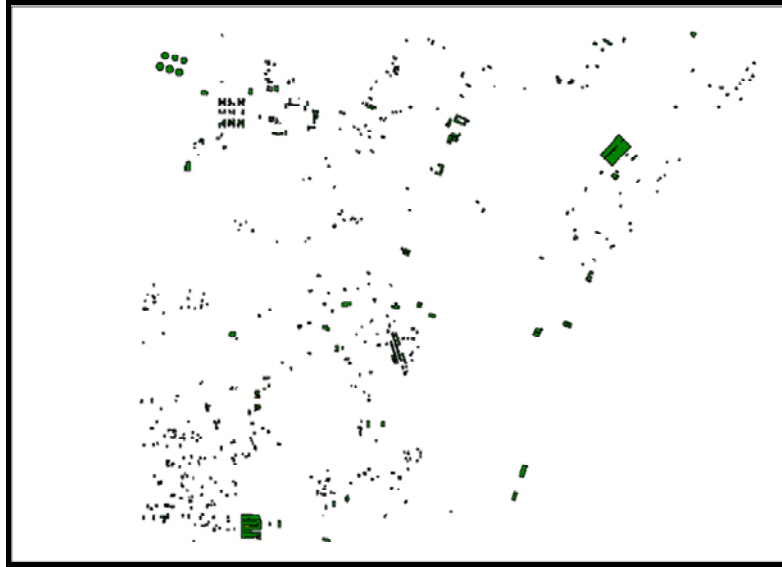


Figure 5.14. Manually digitized buildings for a reference map of accuracy assessment

The accuracy of building detection based on the comparison with these reference buildings resulted in an overall accuracy of the remote sensing based building detection 84 percent.

5.2.6.2 Accuracy of building vulnerability classification

The accuracy assessment was conducted by comparing the classification result of the in-situ assessment and the classification result of the remote sensing technique. Table 5.1 illustrates the calculation of the error matrix resulting in an overall accuracy of about 81 percent. Additionally the table shows various values of commission and omission errors in each class.

Table 5.1. Error Matrix of building vulnerability classification in Cilacap Area

Classified \ Reference	Class A	Class B	Class C	Class VE	Row Total	Omission
Class A	61	0	6	1	68	10.29
Class B	1	6	1	1	9	33.33
Class C	4	1	24	7	36	33.33
Class VE	0	0	2	14	16	12.50
Column Total	66	7	33	23	129	
Commission	7.56	14.29	27.27	39.13	Overall Accuracy	81.39

5.2.7. Transferability Analysis

The transferability analysis indicated that the OBIA rule-set developed for Cilacap datasets was transferable for Padang datasets. However, adaptations in the selection of the threshold values and the object feature values for the building extraction and in the rule-set for the vulnerability classification are necessary. Figure 5.15 depicts the result of building extraction analysis of Padang city. The accuracy assessment of the building extraction was done using the same method as described in section 4.3.2.3. The accuracy of building extraction in Padang area is about 82 percent.

It is clear that buildings in Padang city area are well classified by using the OBIA rule-set. Buildings were classified based on their roof colour. Based on this building map, building vulnerability classification was carried out and the result of this process is figured out in Figure 5.16.

5. Results of the Research

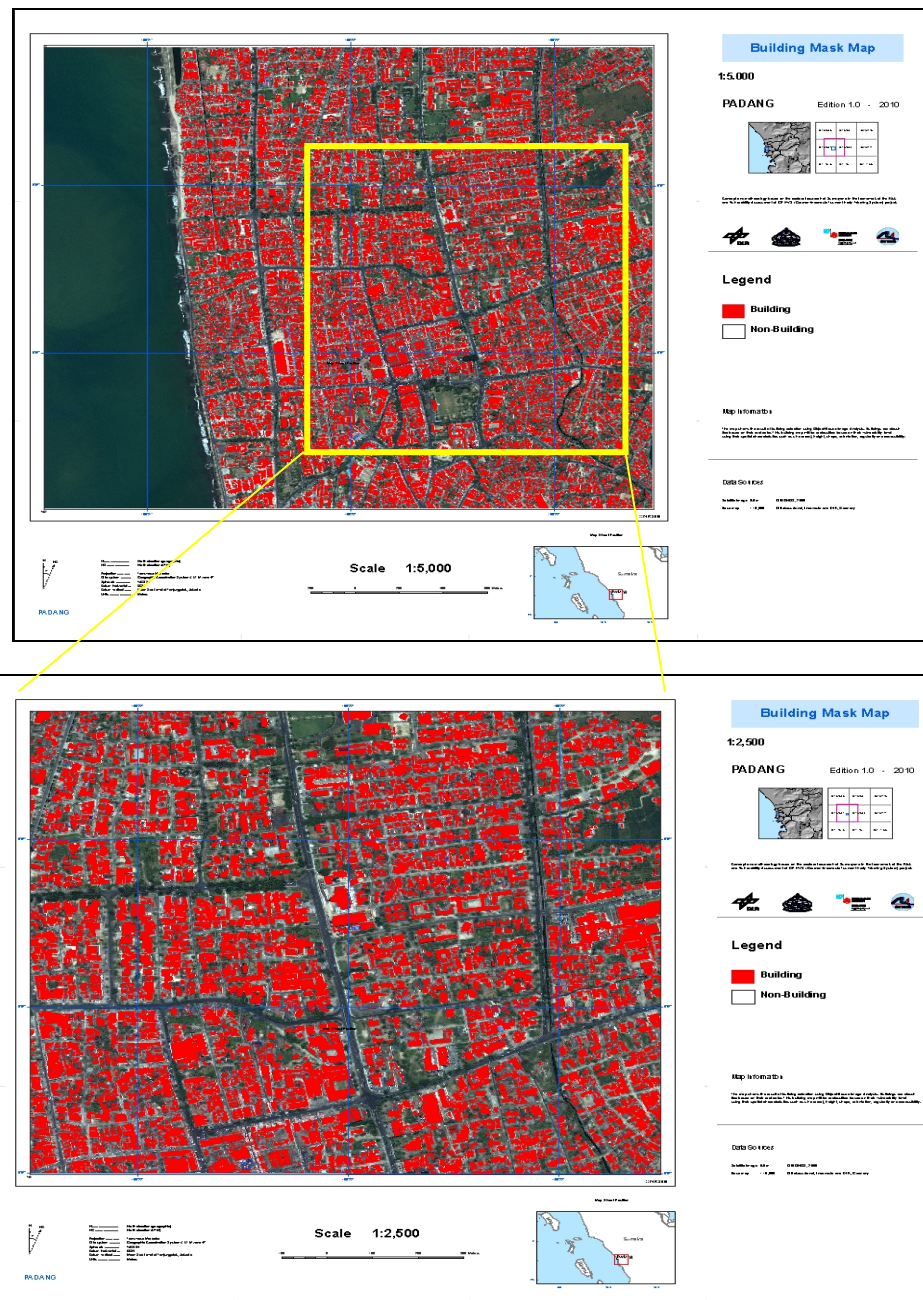


Figure 5.15. The result of building extraction analysis of Padang city area using IKONOS

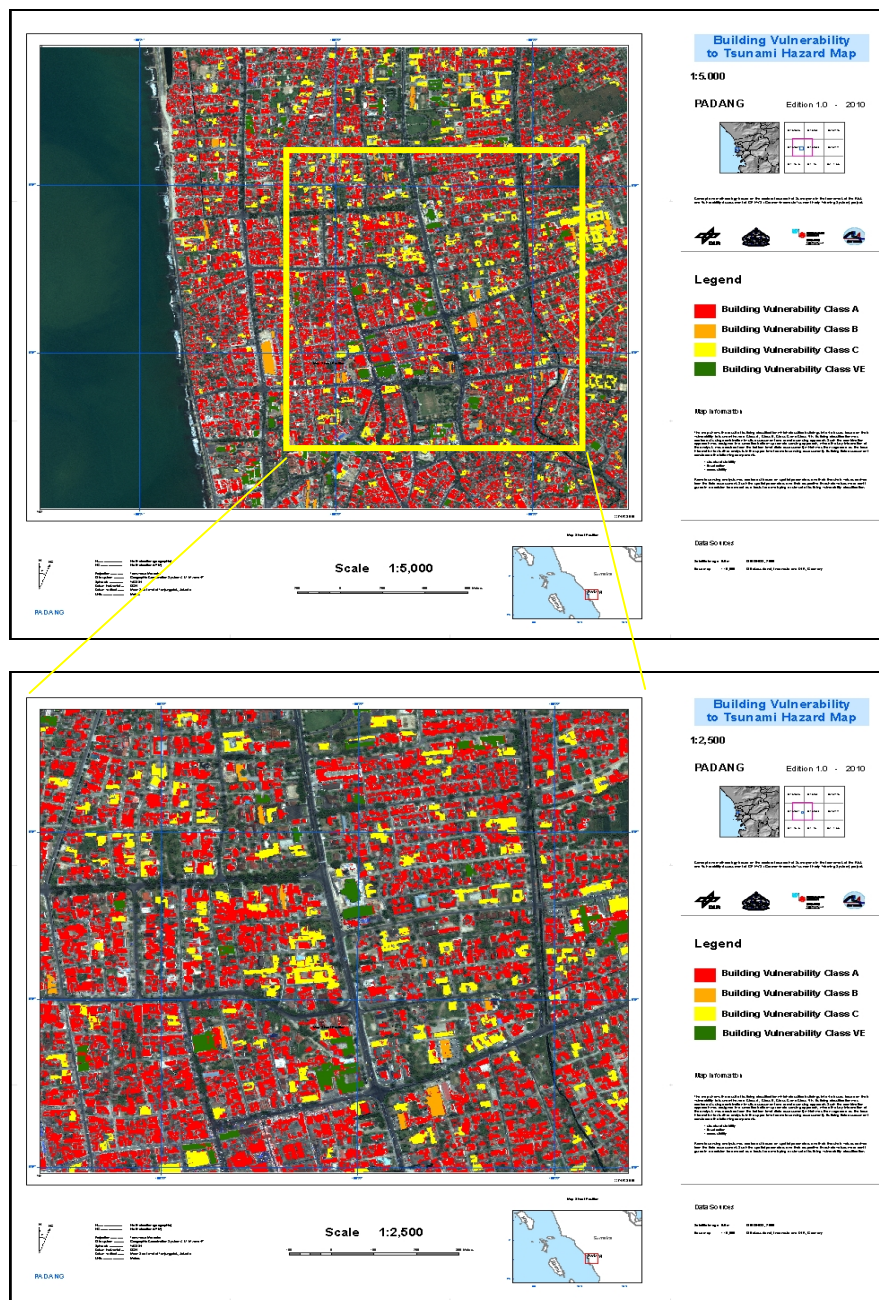


Figure 5.16. The result of transferability analysis of building vulnerability classification in Padang

The accuracy assessment of the building vulnerability classification was done using the same method as described in section 4.3.2.6. Table 5.2 shows the total accuracy of the building vulnerability classification is about 81 percent.

Table 5.2. Error Matrix of building vulnerability classification in Padang Area

Classified Reference	Class A	Class B	Class C	Class VE	Row Total	Omission
Class A	73	7	1	0	81	8.64
Class B	10	20	2	1	33	15.15
Class C	1	0	6	1	8	25.00
Class VE	0	0	1	3	4	25.00
Column Total	84	27	10	5	126	
Commission	13.09	25.92	40.00	40.00	Overall Accuracy	80.95

CHAPTER 6

APPLICATION OF THE RESEARCH: Tsunami Evacuation Modelling

6.1. Introduction

The main products of the building vulnerability assessment research previously described here are maps of building vulnerability classes and potential candidates for vertical evacuation buildings. Because of the geographical layout of the city, it is imperative to map vertical evacuation buildings in Cilacap. Cilacap city is a flat area, and horizontal evacuation shelters are far away from its centre. Therefore, in the case of a tsunami event vertical evacuation is of high importance. This chapter describes the application of the previous research results for generating a tsunami vertical evacuation map. In the context of disaster management, a tsunami evacuation map is an important issue in the disaster management cycle, especially in the preparedness stage.

Risk assessment forms an important input in disaster management, especially in the formulation of main emergency response planning. Risk assessment is also regarded as the starting point for evacuation planning.

The objective of this application is to develop a GIS-based model of tsunami evacuation routes in Cilacap city, based on information derived from the research of the building vulnerability assessment and other related data. A series of evaluative workflows were developed to achieve the research objective, as depicted in Figure 6.1. Figure 6.1 features the fact that a building vulnerability map is one of important inputs in the tsunami evacuation modelling. The following sub-chapters describe the procedural steps of the modelling methodology.

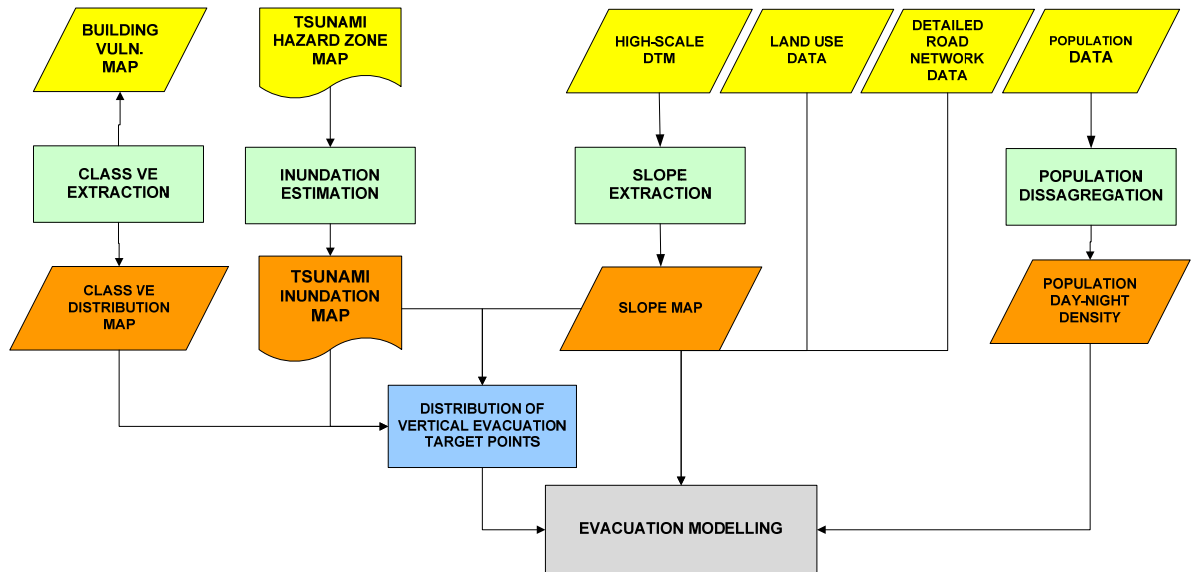


Figure 6.1. Tsunami evacuation modelling concept

6.2. Distribution of Vertical Evacuation Target Points

To determine vertical evacuation target points, a tsunami inundation map was generated and superimposed on the building vulnerability map. The most important information extracted from the building vulnerability map was the class VE building distribution map. Class VE buildings situated in the inundated area were regarded as vertical evacuation target points. The inundation map was derived from a tsunami hazard zone map created by the Alfred Wegener Institute for Polar and Marine Research (AWI) within the GITEWS project framework. Figure 6.2 depicts the methodological flow of hazard zone map modelling.

The tsunami hazard zone was presented in two levels, warning and major warning levels, which statistically modelled with a multi-scenario approach. In this application research, the major warning level was applied with a minimum wave height higher than 3 meters. Figure 6.3 shows the hazard zone map of the study area. The red area represents the inundated area and is regarded as the hazard zone. Class VE buildings located in this area are regarded as safe areas for vertical evacuation.

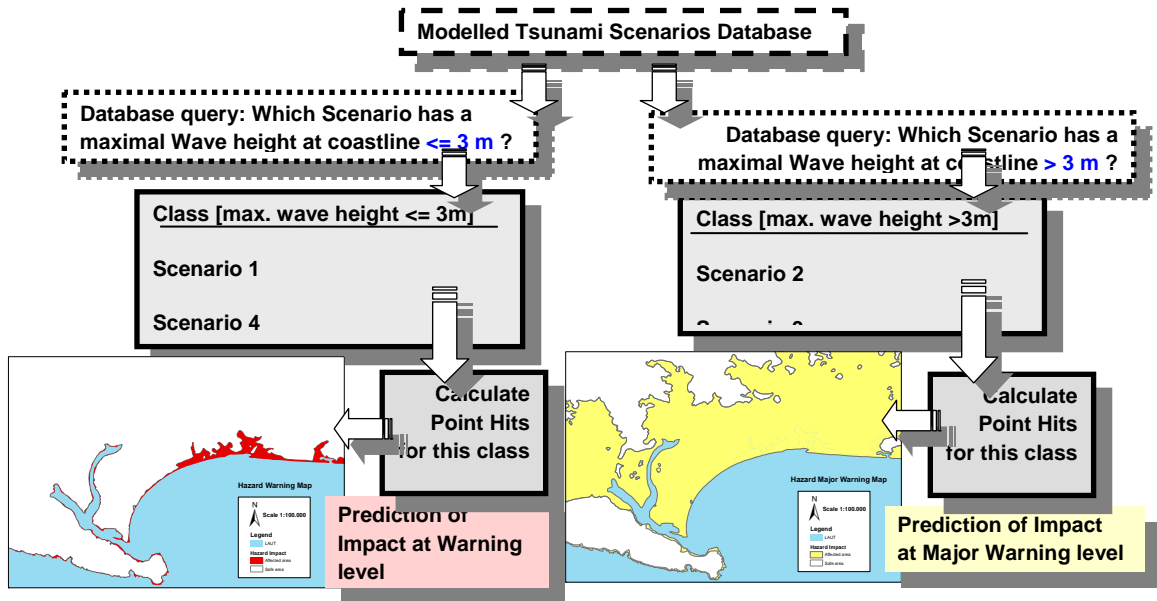


Figure 6.2. Hazard zone map modelling using pre-calculated scenarios

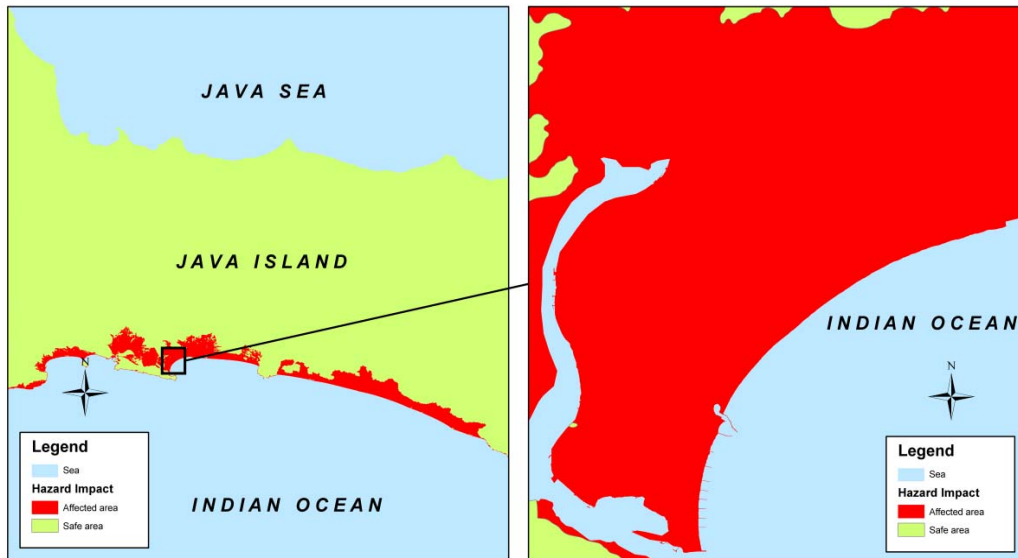
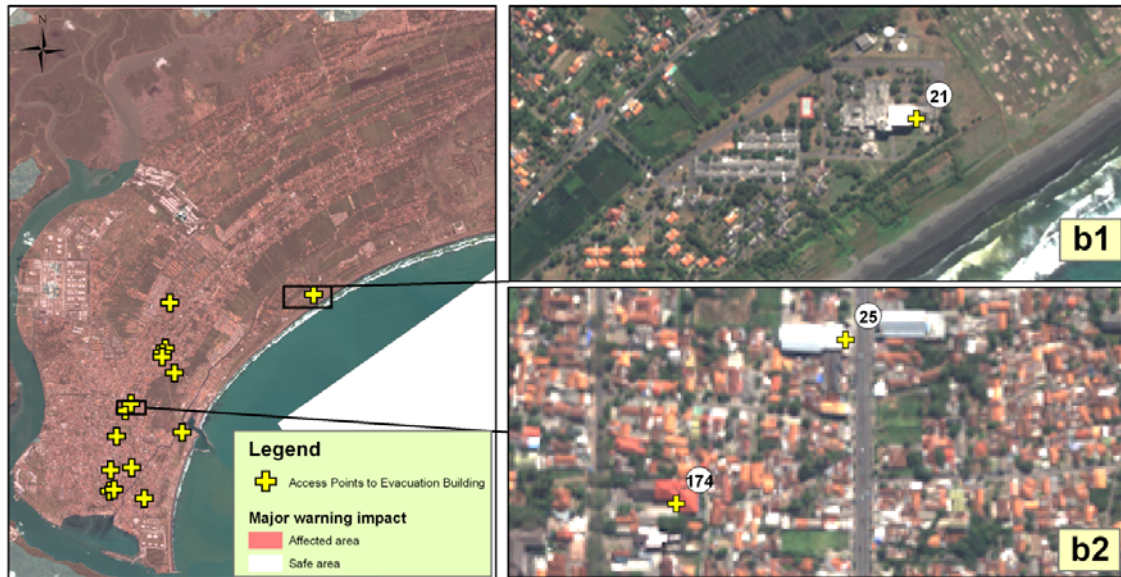


Figure 6.3. Hazard zone map for tsunami major warning level

Based on the results given in chapter 5, the evacuation target points for vertical evacuation shelters were determined. The Tsunami Evacuation Building Capacity (TEBC) was then calculated by using the following equation:

$$TEBC = \{(Capacity\ Score * Building\ Area * Amount\ of\ floor) / Space\ needed\ for\ 1\ person\}$$

Figure 6.4 depicts the map of vertical evacuation target points.



a. Distribution of vertical evacuation buildings in the study area

b1 and b2. Vertical evacuation access points

Figure 6.4. Vertical evacuation building distribution

6.3. Accessibility Modelling

Accessibility modelling in this research was defined as the process used to calculate the cost surface for the evacuees. A cost surface consists of a regular two-dimensional grid, in which each cell in the grid represents either a route or a network such as roads, railway lines, tracks, or relatively inaccessible land and water bodies. Figure 6.5 shows the methodological flow of the accessibility modelling.

Figure 6.5 demonstrates that a building mask is one of the most important pieces of information in accessibility modelling. The building mask map was derived as the result of the building detection.

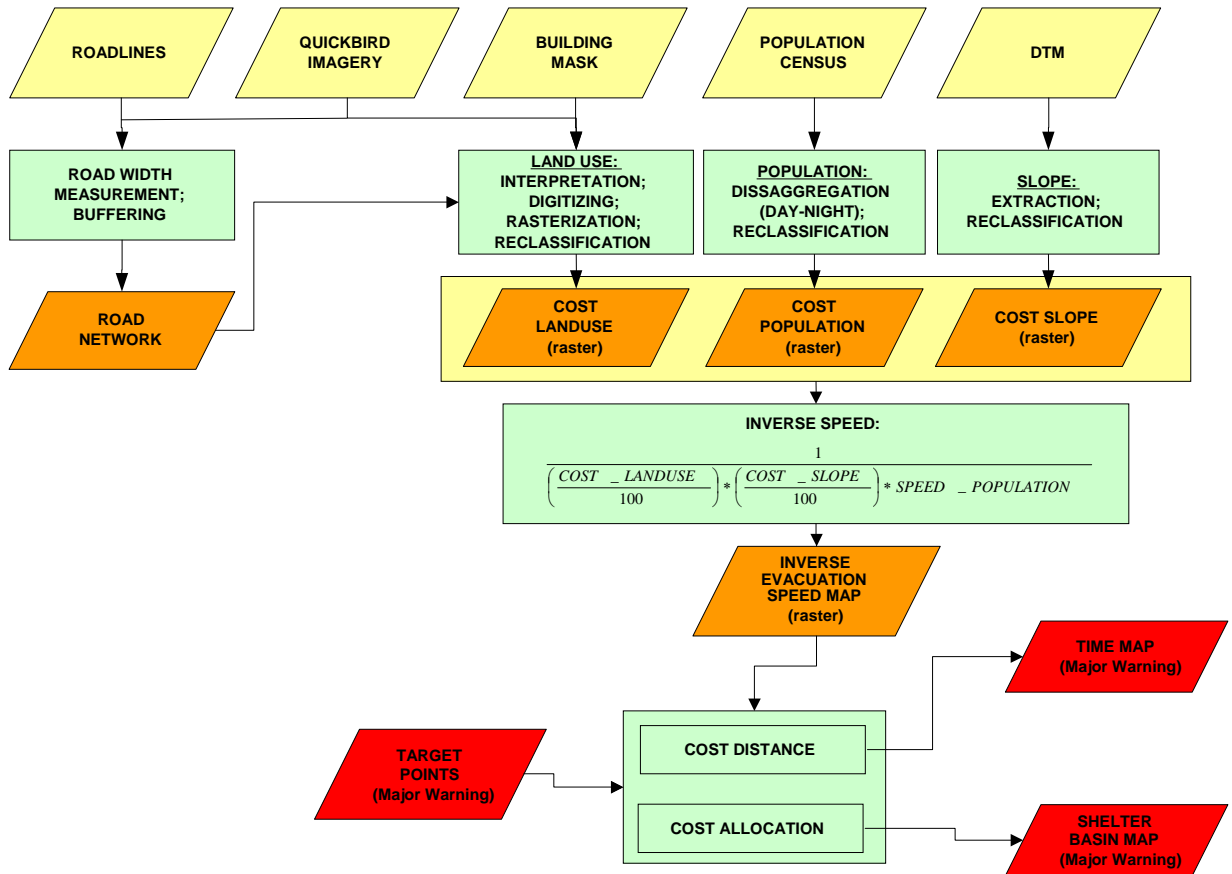


Figure 6.5. Workflow of accessibility modelling

6.4. Evacuation Modelling

Evacuation modelling was calculated based on the accessibility and capacity of the shelter area. The first evacuation modelling step was to calculate the number of people in each catchment area able to reach the evacuation target point within a given time. Referring to the Tsunami Hazard map produced within the GITEWS project, the estimated time arrival (ETA) of the study area is about 40 minutes. Furthermore, it was assumed that it will take 5 minutes to issue an official warning to the exposed area and it will take another 5 minutes for people to react and respond to the warning message (GTZ-IS, 2007). Therefore, 30 minutes was set as evacuation time in this research, which means people in the study area have about 30 minutes to go to the evacuation shelter and escape tsunami waves.

6.4.1. Evacuation Shelter Capacity and Time Area

To have a better understanding of the evacuation shelter capacity and time area approach, this research used the terms L1 and L2 explained as follows (see Figure 6.6):

- L1 (*Evacuation Time Area*) defines the total number of people in a certain area able to reach the evacuation building in a given time. This was derived from the evacuation time map.
- L2 (*Evacuation Shelter Capacity Area*) defines the number of people in a certain area who can be sheltered in the evacuation building at a given time, taking into consideration the capacity of this building. This information was derived from the tsunami evacuation building capacity calculation (TEBC formula), as previously explained.

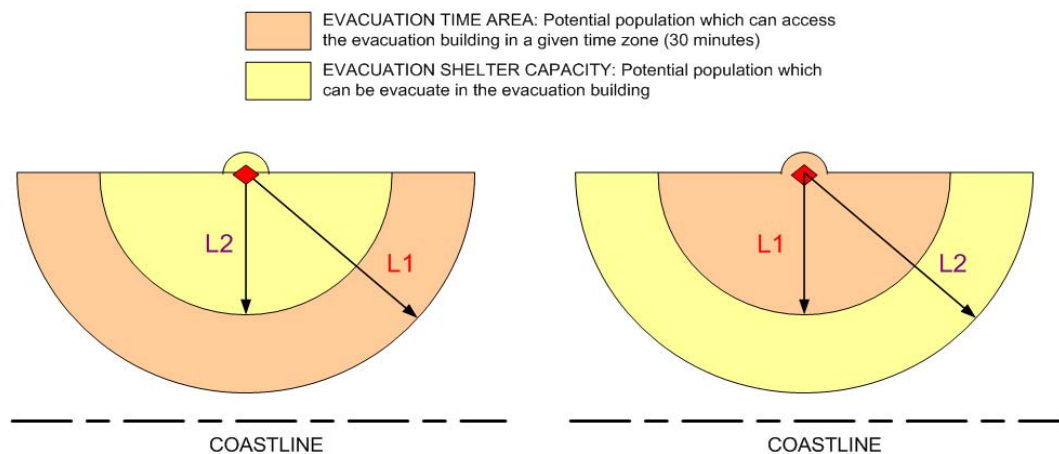


Figure 6.6. Evacuation shelter capacity and time area approach (Source: Cabinet Office, 2005)

For the modelling it was assumed that the evacuation building could only be accessed by people who come from the coastline direction, unless their distance is close enough (3 minutes) to reach the building. The procedural workflow of defining shelter capacity and time area is shown in Figure 6.7. Figure 6.8 depicts the map of evacuation shelter capacity and time area.

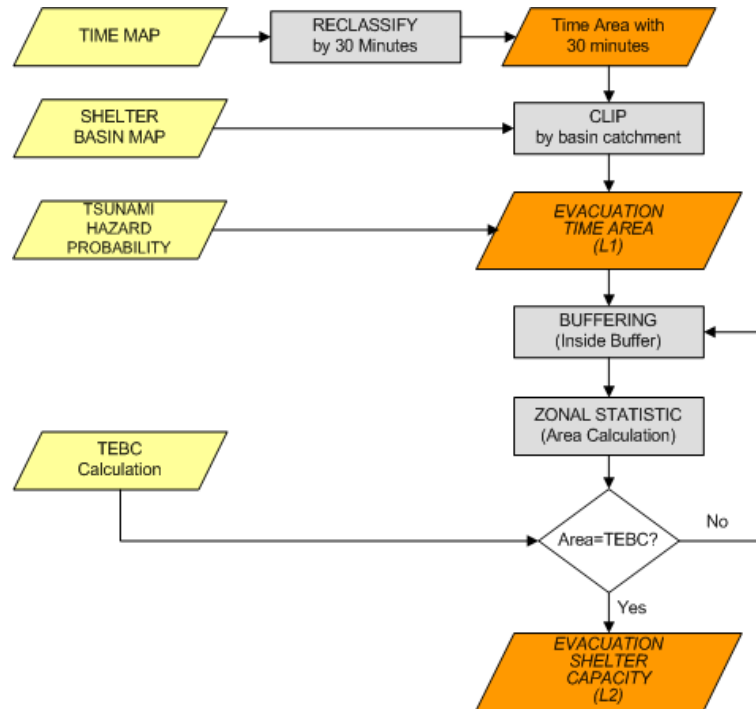


Figure 6.7. Workflow of evacuation shelter capacity and time area

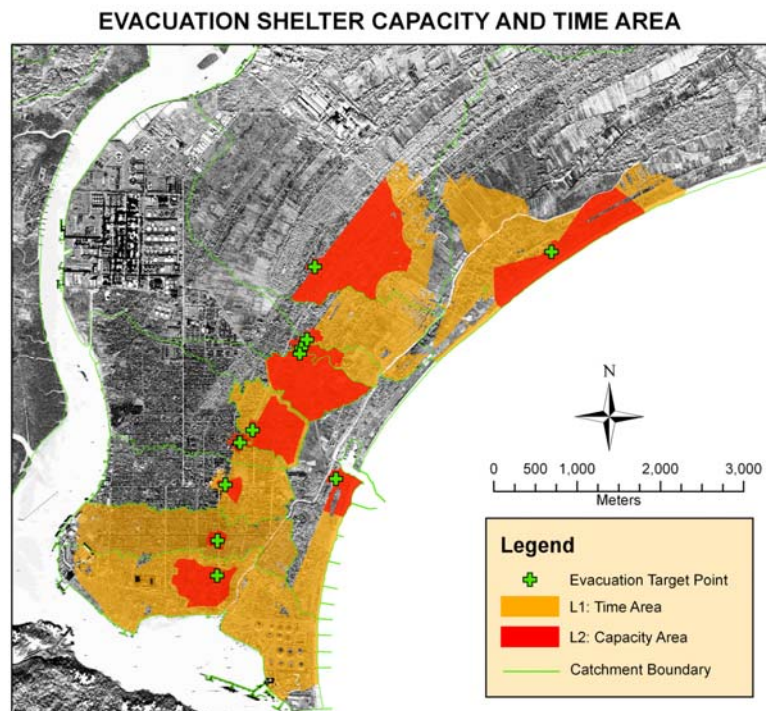


Figure 6.8. Evacuation shelter capacity and time area in Cilacap city

Figure 6.8 shows that each evacuation building has its own shelter capacity and time area, based on its basin area and building capacity. This research shows that only

people coming from the coastline direction, as well as people from the opposite direction who are within visible range of the shelter buildings, can be evacuated to the shelter buildings. Thus, the shape of each evacuation capacity area (L2) is different owing to its location and coastline orientation.

As seen in Figure 6.8 above, the evacuation time area (in orange) for some buildings is larger than the evacuation shelter capacity area (in red). That means that a lot of people in the surrounding evacuation building areas can reach the evacuation buildings within 30 minutes, but not all of the evacuees can be sheltered in the buildings because of capacity limitations.

6.4.2 Evacuation Routes

The first step in generating the fastest evacuation route was to create flow direction and flow accumulation using the ArcGIS-Hydrology Modelling module and to set the evacuation time map as an input.

a) Flow Direction

To calculate the network, a grid coded for the direction in which each cell in a surface drains had to be created. In generating the evacuation route, flow direction was used as an important input to determine the direction of route flows for each cell in the surface area. For every cell in the surface grid, the ArcGIS grid processor finds the direction of the steepest downward descent.

b) Flow Accumulation

Flow accumulation was used to generate a network by determining the ultimate flow path of every cell on the landscape grid, based on the flow direction of each cell. By selecting cells with the greatest accumulated flow, a network of high-flow cells was created. For evacuation modelling, once flow accumulation is calculated, cells with higher cost will flow into cells with lower speed cost.

As soon as the hydrology modelling tool is activated, the interactive evacuation routes and the fastest path from any point to the shelter access point in the study area can be visualized (see Figure 6.9).

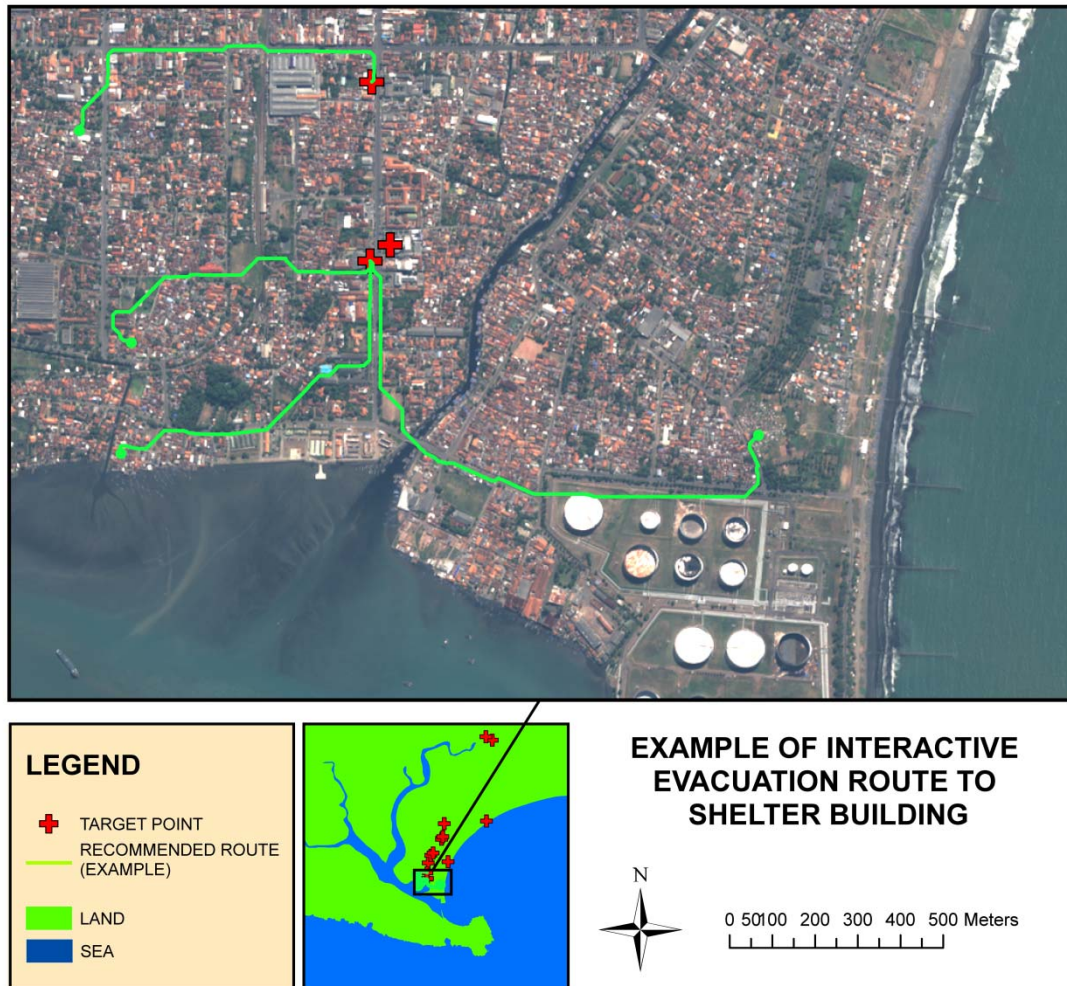


Figure 6.9. Interactive evacuation routes

CHAPTER 7

DISCUSSION

7.1. Building Vulnerability Assessment Using Bottom up Approach

The results of this research show that building vulnerability to tsunami hazard assessment can be carried out by using combined in-situ assessment and remote sensing approach with the total classification accuracy of about 82 %. The results for the different categories are discussed as follows.

- **Building Vulnerability Class A**

Class A is regarded as the most vulnerable building to tsunami hazard. Most of class A building samples consist of small buildings. Figure 5.3 illustrates the data distribution of class A building samples related to their size (area). This boxplot diagram confirms that most of data samples of class A are distributed under the value of 200 m² with only few data in the range of 200 m² to 1,200 m². Class B, C and VE data are distributed above the value of 200 m² with the median value more than 400 m². In that case, the threshold value of building size for class A is defined based on the value of upper quartile (Q3) of the data distribution of class A. The definition of Q3 as the threshold value of class A refers to the comparative analysis of the data distribution where Q3 value of class A demonstrates the best separation of class A from other classes. Descriptive statistics of class A confirms that the upper quartile value of class A is 200 m². The definition of threshold value for class A by 200 m² in remote sensing analysis implies the confusion of classification related to the inclusion of small part of class B, C and VE with area distributed below the value of 200 m². Table 5.1 confirms the confusion of building vulnerability classification in Class A with the commission value of 7.56 percent. This means that in the remote sensing analysis, 7.56 percent of buildings from other classes are classified as class A.

Based on the information acquired from the in-situ building assessment during the field survey in Cilacap, most small buildings were dominated by structurally unstable buildings. The source of structural instabilities varied from building to building. Some buildings were instable owing to concrete problems, while the other buildings were instable in column, wall, reinforcement or a combination of those instabilities. Figure 7.1 depicts some of the photographs of class A buildings taken during the field assessment.



Figure 7.1. Buildings classified as class A

Most of the small buildings situated in a slum area of the city were built using poor materials and bad structural engineering. Figure 7.2 confirms that such buildings are very vulnerable to earthquake and tsunami hazards due to the lack of structural stability. These photographs were taken from previous Aceh and Pangandaran (near Cilacap) tsunami events.



Figure 7.2. Typical small buildings which are vulnerable to tsunami hazard

In the slum area of the city, building density is very high and there is almost no space between one building and other buildings. The poor quality of building roofs – such heterogeneous materials as rusty zinc and asbestos can be found in a single building – triggered the difficulty of building detection analysis on an individual basis. These buildings tend to be classified in remote sensing analysis as a group of buildings, not individual buildings. In many cases, such building group polygons have a big dimension. If the size parameter as a proxy of building stability is applied in such the group building polygon, it will trigger to a misleading classification. Due to its large size, such a polygon will not be classified as class A. A large polygon tends to be classified as class B or C, depending on building orientation. In order to avoid such a misleading classification, we added an additional parameter to solve the problem. A building regularity parameter was applied to classify typically large polygons. The building regularity algorithm was described in the chapter on methodology (see section 4.3.2.5). It was derived from an elliptic fit feature object in an OBIA environment. This means that individual building polygons tend to be more regular than grouped building polygons. The regular shape of a building tends to have a big impact on elliptic value, as illustrated in Figure 7.3a.

Figure 7.3 demonstrates the applicability of regularity parameters to classify the grouped buildings in a slum area. The elliptic fit value algorithm is conducted by overlaying an ellipse object over the building polygon. After this step, the area of the object outside the ellipse is compared with the area inside the ellipse that is not filled

out with the object. The elliptic fit value ranges from 0 to 1: 0 means no fit and 1 stands for a complete fitting object. Figure 7.3b shows the result of the elliptic fit value calculation. It shows the gray scale map of the area, in which brighter objects indicate the higher value of elliptic fit and duller objects have the lower. Individual buildings appear brighter than grouped buildings. The elliptic value of the highlighted individual buildings in Figure 7.3a is 0.773, and the highlighted grouped buildings appear completely dark where its elliptic value is zero.



a. Individual building segmentation with elliptic value = 0.773



b. Grouped building segmentation with elliptic value = 0

Figure 7.3. Detecting irregular buildings using elliptic fit value object feature

In regard to the confusion matrix (see Table 5.1), the commission and omission error of class A was very low. Most class A buildings in the reference data (in-situ assessment) were put into class A using the remote-sensing technique. In the commission error, some class B and class C buildings were confusedly classified into class A. This kind of

error was caused by building regularity. Large buildings with low regularity (low elliptic fit value) are classified into class A. In the omission error of class A, some class A buildings were misclassified into class C. This kind of error was caused by the grouped building detection effect.

- **Building Vulnerability Class B**

In the decision tree analysis of building vulnerability assessment, class B was defined by evaluating all buildings not classified as class A using tsunami components. Tsunami components are made up of two parameters – building geometry (shape) and building orientation. For the purpose of in-situ measurement, building shape in this research was put into 3 categories: simple, multi-part (complex) and long-rectangular, each of which was weighted by different value. The threshold value is the multi-part-shaped building value. Simple and multi-part-shaped buildings were regarded as safer buildings than the long-rectangular ones. This rule is in line with the rule established in the work of Dominey Howes and Papathoma (2007) stating that buildings with specific shapes (e.g., hexagonal, triangular, rounded, etc.) suffered lighter damage than long, rectangular-shaped buildings whose main wall was orientated perpendicular to the direction of flow. In this case, not all of the long-rectangular buildings were classified into class B. We took into account the main-wall orientation of the buildings to the direction of wave flow when seeking to classify them. Building orientation was put into 3 categories: parallel, diagonal and perpendicular, each of which was weighted differently. The diagonally-shaped building value was regarded as the threshold. Using this algorithm, a building was classified as class B if the building shape was simple or long-rectangular and oriented perpendicularly to the direction of flow. In this research, flow direction was assumed to be perpendicular to coast line. Figure 7.4 features photographs of class B buildings taken during the field assessment.

Using the remote-sensing technique, both building shape and building orientation can be detected using object-based image analysis. This is one of the advantages of using object-based analysis compared to pixel-based analysis.



Figure 7.4. Buildings classified as class B

Pixel-based analysis offers nothing in the way of detecting object shape and orientation. Using object-based image analysis, building shape was categorized into 2 categories: long-rectangular and non-long-rectangular. There is no algorithm in object-based tools to detect multi-part shape. Because a multi-part-shaped building was regarded as a safe building, this simplification is still acceptable. Feature analysis was employed to detect object shape and object orientation. Object shape was detected using simple feature arithmetic calculation: length/width. Long-rectangular buildings were detected by applying a formula of “feature length/width > 2” in the class description and, accordingly, non-long rectangular buildings were detected by applying a formula of “feature length/width ≤ 2”. Building orientation was detected by using main direction value of the object feature.

In the analysis of the building orientation it was assumed that the tsunami flow direction is always perpendicular to the coastline. Due to hydrodynamics this is of course generally not true. If tsunami flow direction data is available, this approximate assumption can be ruled out and the presented methodology could be easily improved by using tsunami flow direction information. However, this data was not available during the time of the research work.

In regard to the confusion matrix of class B (see Table 5.1), the commission error was low but the omission error was high. The omission error indicated that a number of class B buildings classified using in-situ assessment were classified as other classes, i.e.

classes A, C and VE. The source of this inaccuracy is the building shape detected by remote sensing. When the shape of the building was not properly detected, the classification result changed accordingly.

- **Building Vulnerability Classes C and VE**

Buildings that are neither classified as class A nor as class B will be classified as class C or class VE. To define to which of these 2 classes the buildings will be assigned, additional parameters were applied. Refer to Figure 4.3: Accessibility components were applied to classify buildings into class VE. Buildings that did not fulfil the accessibility component requirements were classified as class C.

Refer to Table 4.3: It is clear that accessibility components do not deal with a building's structural performance. Class C and class VE structurally are equal. Both classes were regarded as buildings with low vulnerability to tsunami hazard, as relatively large in size and as non-long-rectangular, situated perpendicularly to flow direction. Among all accessibility parameters, the floor position parameter is the most important used to differentiate between class C and class VE. Figure 7.5 and Figure 7.6 feature photographs of class C and class VE buildings taken during the field assessment.



Figure 7.5. Buildings classified as class C

For the purpose of tsunami evacuation, the floor position should be in the second floor or higher (this means that the building should have minimum 2 storeys). The number

of floors parameter ensures that there is a space for vertical evacuation that will not be inundated by the run-up wave of a tsunami.



Figure 7.6. Buildings classified as class VE

Unfortunately, the number of floors parameter is very difficult to be assessed using a remote-sensing technique. In this case, a proxy parameter was needed to predict the information. In the remote-sensing approach, the building height was applied as a proxy parameter of number of floors. Buildings with more than one storey are usually higher than single storey buildings. Elevation data was incorporated in the remote-sensing analysis of building vulnerability, especially to classify buildings into class VE. The elevation data used in this research was derived from SAR data with a spatial resolution of 5m. The threshold of the building height parameter was defined using statistical analysis of empirical data from the field survey. Figure 5.4 demonstrates boxplot analysis of building height related to the vulnerability class. This boxplot diagram indicates that the first quartile (Q1) value of class VE building height can be regarded as the height threshold. The descriptive statistics indicates that Q1 value of class VE is 10 m. This threshold value demonstrates a good separability of class VE from other classes. Nevertheless, this threshold still includes parts of other building classes in class VE due to their overlapped thresholds. Class C has the biggest overlapping threshold with class VE.

Another accessibility parameter incorporated in the remote-sensing technique was information about distance to the road. This parameter ensures that class VE buildings

are accessible by a large number of people. The threshold of the distance to the road parameter was defined using empirical data from the field survey.

Refer to the accuracy assessment table (Table 5.1): There were confusions in classifying class C and class VE, as indicated in the commission and omission errors. The confusion of classifying class C and class VE can be explained by the following:

- a. The difference of spatial resolution between QuickBird data and elevation data: As previously mentioned, the spatial resolution of QuickBird data is 2.4m (multi-spectral), while the spatial resolution of the elevation data is 5m. In some cases, such a spatial resolution difference influences the accuracy of height information and, finally, influences the accuracy of classification accordingly.
- b. In some cases, there were tall, single-storey buildings, such as factories or warehouses. Such buildings should be classified as class C but tend to be classified as class VE due to the height information.

In general, buildings in Cilacap city were mostly classified as class A, meaning very vulnerable to earthquakes as well as tsunami hazards. A large number of buildings (class A) are assumed to probably collapse should a big earthquake occur in Cilacap. Any quake then has the potential to trigger even worse casualties if tsunami results and hits this area. In order to reduce the disaster risk, building code needs to be applied to standardize the quality of buildings. People's awareness of building vulnerability needs to be improved and regulations about a better way to develop buildings need to be legalized.

7.2. Image Segmentation

The multi-resolution segmentation algorithm was developed to allow the use of multi-spectral inputs as a basis of segmenting the image coverage. Pan-sharpened Quickbird images allowed the utilization of four different bands – blue, green, red and near-infrared – with higher resolution provided by the panchromatic band. The panchromatic band provided sharp details of the image features, whilst multi-spectral

bands provided various sensitivities of different bands. The combination of all of the bands led to more precise and better segmentation results

The main goal of this segmentation process is to get accurate edge delineation of individual buildings in the research area to ensure proper individual building extraction from the image. To achieve this goal, we designed a top-down, multi-level hierarchical segmentation process. Within this environment, input parameters were set by the following conditions:

- an algorithm, for which three options are provided – chessboard segmentation, quad-tree based segmentation and multi-resolution segmentation. In this research, a multi-resolution segmentation algorithm was selected to segment building and other objects.
- image layer weight: We were able to set weights for each image layer.
- thematic layer usage: We were able to consider any thematic vector data available to make classification process easier or better.

All input parameters were applied based on our goal to define the range of homogeneity or the differentiation between neighbouring regions (heterogeneity). In other words, this task should be performed with the strong understanding of principles of neighbourhood and similarity. There are four approaches for segmenting an image into objects, including point-based, edge-based, region-based and combined. In this research, the segmentation process was performed by using a so called region-merging approach. This approach is regarded as the most reliable compared to other approaches (see Baatz and Schäpe, 2000). In this algorithm, after each pixel forms one object, object pairs are continuously merged into a larger object based on local homogeneity criteria until there are no more possible merges.

One of the problems that often arise in the segmentation process within the framework of building detection is the heterogeneity of roof colour in a single building. This leads to the difficulty of segmenting building edges accurately. To solve this problem, we filtered the image before the segmentation process. We applied both

adaptive local sigma and morphological opening filter algorithms. According to Eliason et al. (1990), adaptive box-filtering algorithms were designed to remove random bit errors and to smooth noisy data. In the adaptive filtering procedure, the standard deviation of those pixels within a local box surrounding each pixel was used. A series of two or three filters with decreasing box sizes was run to clean up extremely noisy images and to remove bit errors near sharp edges. A morphological opening filter smoothed the contours, broke narrow isthmuses, and eliminated small islands and sharpened peaks or capes in the image. The opening of the image was defined as the erosion of the image, followed by subsequent dilation using the same structural element (Haralick et al., 1987). Figure 5.6 demonstrates the result of the filtering techniques, an image in which the building objects as well as other objects are smoother than their appearance in the original image. The smoothness of the objects did not reduce the sharpness of the building and other object edges. This can be seen in the spectral profile shown in Figure 5.7.

Figure 5.7 shows how filtering techniques adjusted sharper edges by smoothing those pixels inside the bounding edges of objects. This was demonstrated by the changing of pixel profiles before (a) and after the image filtering (b) process. In a horizontal spectral profile, an object was indicated by two steep slopes and a relative-flat area in between. The steep slopes indicate the contrast level of the spectral value of an object to its neighbour. In many cases, the filtered image displays the abrupt transition zones of the image pixel profile more sharply than the unfiltered image does. On the contrary, the filtered image shows a flatter profile in the area between two steep slopes of the abrupt transition zones (see Figure 7.7). The flat zones of the pixel profile indicate that pixel values in these areas became relatively homogeneous, owing to the image filtering treatment. It means that, relatively speaking, pixel values in an object were adjusted more homogeneously.

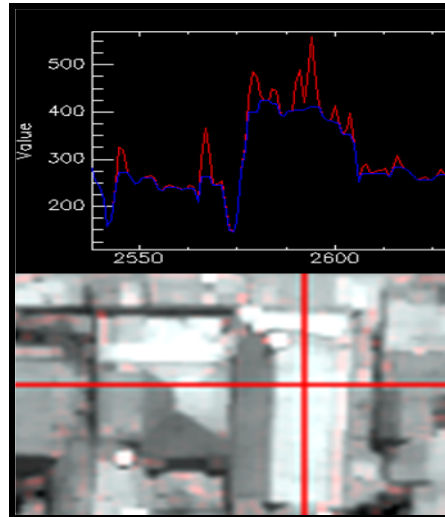


Figure 7.7. Comparison of two adjacent building profiles before (red) and after filtering (blue).

Figure 7.7 illustrates that pixel values in a building are more homogenous after the filtering treatment (see the blue profile) compared to the pixel values before the filtering treatment (see the red profile). This smoothing technique does, however, preserve the edge sharpness. The pixel profile shows that between two building profiles (indicated by two flat zones), there is still a gap with steep slopes separating both building profiles. The low pixel value between two building profiles is a dark area, clearly recognized as a shadow. The blue profile clearly defines the building zone and its edge on the left and the right side of the zone. Contrarily, the red profile shows a random behaviour of peak and cliff transition and does not demonstrate a clear building zone and its edge.

This led to differing results of segmentation. Because there was neither a clear building pixel profile zone, nor a sharp edge of the building, the unfiltered image was not accurately segmented. Figure 7.8 demonstrates the segmentation results of both the filtered image and the unfiltered image.

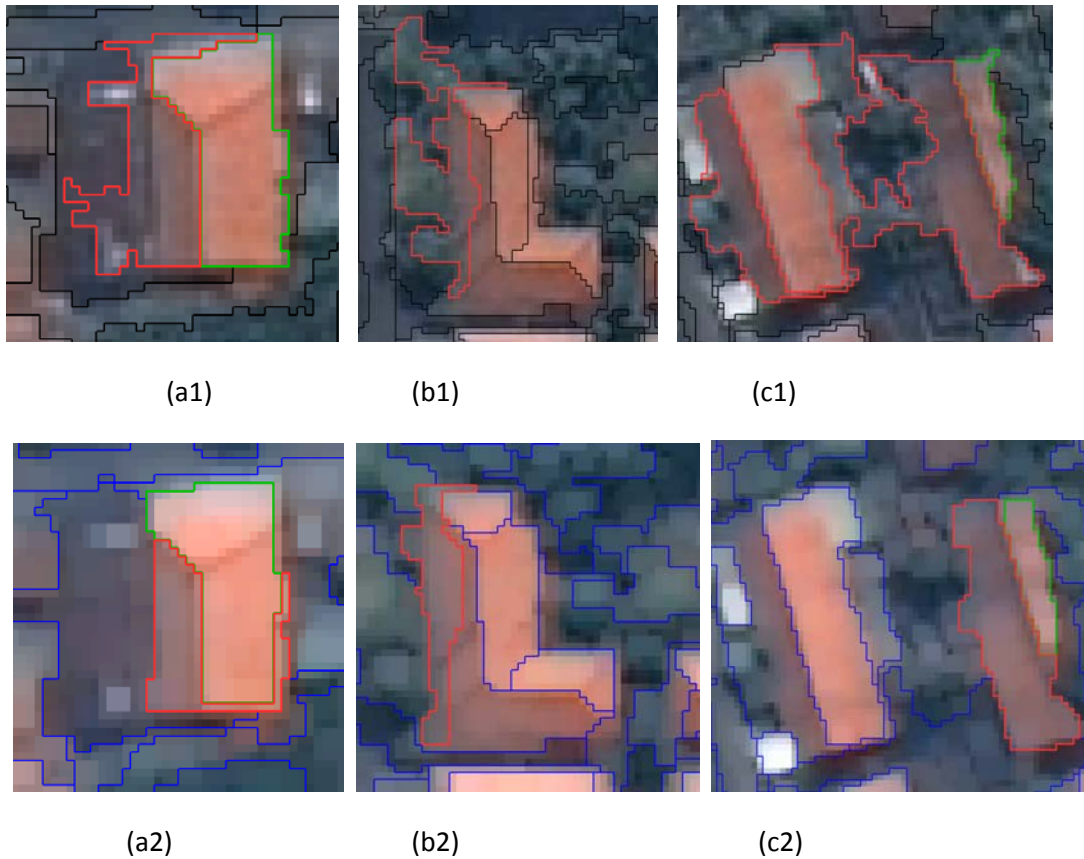


Figure 7.8. Comparison of image segmentation results before filtering (a1, b1 and c1) and after filtering (a2, b2, c2).

Figure 7.8 shows the comparative results of the same image segmentation process before filtering (see a1, b1 and c1) and after filtering (see a2, b2 and c2). Figure 7.8 (a2), (b2) and (c2) show much better quality of segmentation results than (a1), (b1) and (c1). In comparing b1 and b2, it is clear that b2 demonstrates a higher accuracy in the edge detection of buildings than b1. The segmentation process in b1 failed to delineate the edges of the building owing to lower building edge sharpness compared with that of the adjacent object (in this case vegetation). This is the so-called under-segmentation (Schiewe, 2002), for which the number of segments is low and the dimension of the segments is large. Under-segmentation is regarded as a less satisfactory segmentation compared to over-segmentation, although both of them are not optimal segmentation processes. Under-segmentation often produces inaccurate edge detection, as demonstrated in Figure 7.8 (a1), (b1) and (c1).

7.3. Building Detection

After the segmentation of remotely-sensed data scenes into smaller segments (objects) is performed, the building detection process begins. Each object carries attributes, so-called features, a set of information that represents such object characteristics as layer mean value, maximum, minimum, standard deviation, area, shape, etc. Such object features are the key parameters in building detection analysis. The crucial step in building detection analysis is the selection of object features that represent the similarity of the objects, which then allows them to be put into their various classes. This step is tricky, because there are literally hundreds of features that can be attributed to the objects. We had to make sure to select the most distinctive features for grouping objects with other, similar objects, whilst taking great care not to let any end up with dissimilar objects. Furthermore, in many cases, customized features were needed because the features available were not as well-suited for grouping objects. This made things more complicated. Customized features are features derived from available features by using mathematical operations such as multiplication, division, addition, subtraction, etc. Table 4.6 lists selected features utilized for building detection analysis including customized features.

In this research, we found that available object features calculated automatically by the image analysis machine were not sufficient to group the objects into desired classes. The low value of separability between the object features is to blame for this. Separability was calculated based on a statistical approach (see section 4.3.2.2). The complexity and the variety of building types in the research area and the absence of elevation data with an equal resolution to the optical data used (QuickBird) triggered a need for additional customized features. The best parameter used to detect individual buildings is roof colour.

This research employed two different methods of feature separability analysis i.e. feature range adapter and statistical analysis so-called Bhattacharyya distance. Each of the method has typical strengths and weaknesses and was used in different condition accordingly. Feature range adapter is easy to use and gives a good accuracy in the case

of analyzing a particular object with at least one unique object feature that easily separates it from other objects. A good example of this is the case of vegetation analysis. Vegetation usually demonstrates a good separability in the red and near infrared object feature. By using e.g. the NDVI customized object feature, feature range adapter can separate vegetation objects from other objects. In the case of building extraction in this research, white-roof buildings were easily separated from other objects by using a so-called Band Ratio 10 customized object (see section 4.3.2.2). The problem of using feature range updater was one of time, because feature tests had to be performed one by one until the desired feature was met. In addition, in the case of multi-classes classification in the same level of segmentation with low separability, it was difficult to find appropriate object features. In this case, Bhattacharyya distance statistical analysis provides a powerful approach to solve the problem. Therefore, feature range adapter technique was used for vegetation, water and white-roof buildings classification. Bhattacharyya distance analysis was well-suited in classifying other types of buildings.

7.4. Comparison of Building Detection Methods

In the field of building detection analysis, many researchers have done their analysis using object-based image analysis (Durieux, et.al., 2008; Nussbaum, et.al., 2007; Dutta and Serker, 2004; Marongoz, et.al., 2006; Mueller et.al., München et.al., 2006; 2006; Hoffmann, 2001; Liu, 2005; Taubenboeck, 2006; Teo, 2004; Vu, 2005). Compared with their studies, this research introduced a new approach: A combination of filtering technique use, separability analysis, feature range updaters and fuzzy logic approaches. This combination was required, because of the complexity of Cilacap city conditions: the high density of buildings, crowded building roofs without interval spaces, heterogeneous roof colours in a single building, low-contrast of buildings and surrounding objects and the absence of elevation data with QuickBird spatial resolution-like quality. The selection of the filtering algorithms was done with this complexity in mind. Some studies employed other types of filtering techniques appropriate for solving their specific problems. Some other researchers did not

perform any filtering techniques because the building spectral was well-contrasted in comparison to their surroundings.

7.5. Transferability Analysis

The rule-set of OBIA developed for Cilacap data has been successfully used to classify IKONOS data of Padang city area. Non-building objects such as water, vegetation and ground were well classified without any adaptation of object feature inputs. The customized features which were developed for non-building classification in Cilacap datasets were transferable to the Padang datasets. Some minor adaptation was performed especially in the process of building extraction inputs due to the different conditions of available buildings. Roof materials and colours of buildings in Padang area are different from buildings in Cilacap. Roof of buildings in Padang are mostly made of metal (zinc) and roof of buildings in Cilacap are mostly made of ceramic. Such the different materials definitely reflect different colour and spectral characteristics. This condition most likely will be applicable for other areas with different characteristics of buildings. In the case of areas with similar conditions of buildings available in Cilacap, most likely the rule-set will be applicable without any adaptation. This has been tested in different subset areas of Cilacap and the test confirmed that the rule-set was transferable without any adaptation. According to our observation during field survey, buildings in Java Island mostly characterize similar condition with buildings in Cilacap. Thus, the rule-set is expected to be transferable for all area of Java Island.

In the part of building vulnerability classification, the rule-set was completely transferable without any adaptation. It means that the selected spatial parameters which are regarded as the key factors of the classification are valid for both Cilacap and Padang datasets. This rule-set is expected to be also transferable to other areas of Indonesia, probably also to comparable areas in Asia. However, this rule-set is not expected to be transferable e.g. to European countries area due to the different characteristics of buildings.

7.6. Research Application: Tsunami Evacuation Modelling

In the case of tsunami evacuation modelling the role of the vertical evacuation shelters is of high importance for Cilacap. Because of the absence of horizontal evacuation shelters that provide high capacity and are accessible by most people in due time vertical evacuation shelters play a vital role in tsunami evacuation planning. The topographical condition of the city is relatively flat: There is no elevated ground and it is surrounded by water (sea and river water bodies).

As discussed in the previous chapter, the evacuation target points to access shelter areas in the event of a major tsunami warning are not sufficient to serve the whole population of the urban area within the given evacuation time for the study area (about 30 minutes). Not only because of the far distance from the city, but also because of the limited capacity of shelters in accommodating a huge number of people in danger. Thus, vertical evacuation in the tsunami-inundated zone is considered to be the most effective measure to evacuate people from tsunami impacts when there isn't time to evacuate horizontally out of the inundation zone.

The determination of shelter capacity and time area requires the analysis of the population number that can reach the evacuation shelter in a given time period and the population number that can be sheltered in the evacuation shelter in terms of capacity. As previously illustrated, there were only a limited number of vertical evacuation buildings available in the study area, whereas the whole urban area is far from safe areas and would be inundated by a tsunami. Consequently, the determination of evacuation shelter capacity and time area must be implemented for each potential evacuation building. From the calculation result, as seen in Figure 6.8, it becomes evident that the capacity of each building (L2) is inadequate to serve the population within a 30-minutes time area (L1).

Each of the evacuation shelters and time areas has a different shape. This is because each of evacuation building capacity and time area figures in this research is based on tsunami impact probabilities. It means the status of each evacuation shelter capacity

and time area is determined by the direction of the tsunami waves when they arrive. This approach is applied to give evacuation shelter building access priority to people on the most dangerous sides of the building in which they are located at the time the tsunami warning is announced.

By deriving the ratio of evacuation shelter capacity and time area, the capability of available evacuation shelters according to population number in a defined area was analysed. In a case where the available evacuation shelters are not sufficient to serve all the population in danger, the necessary number of evacuation shelters should be calculated. Their spatial distribution can be derived by identifying the areas where people cannot be sheltered in any evacuation shelter building.

As described in the previous chapter, the process of evacuation modelling using GIS also aims to identify suitable evacuation routes in the study area. Interactive evacuation routes generated in this research provide the fastest route to reach the nearest shelter from any source point. It allows people to use passable and respectively suitable land surfaces (not only roads) during an evacuation process. According to this model, for each point in the study area the ideal route to reach the nearest shelter can be calculated.

CHAPTER 8

CONCLUSIONS

A new concept and methodology for assessing building vulnerability to tsunami hazard has been successfully developed in this research as one of the crucial key components of risk and vulnerability assessment in the framework of German-Indonesia Tsunami Early Warning System (GITEWS) project. The concept and methodology have been successfully applied to assess building vulnerability to tsunami hazard in one of pilot areas of GITEWS project, namely the City of Cilacap city in Indonesia. The methodology has also been successfully transferred to assess building vulnerability in another pilot area of GITEWS project, i.e. Padang city. This research is integrated in the scientific framework adopted by GITEWS project. Further details of the research achievements are summarized below.

A combined approach using in-situ surveys and remote sensing techniques has been developed as bottom-up approach. The vulnerability assessment was categorized into three components: building stability, tsunami and accessibility components. Building stability components refer to structural stability parameters, tsunami components refer to geometric parameters such as shape and orientation, and accessibility components refer to the suitability of a building for evacuation shelter. The link between in-situ assessment and remote sensing approach was established by spatial parameters and their threshold values which were derived from in-situ building surveys. In the case of Cilacap city and Padang city, the crucial spatial parameters for classifying building vulnerability to tsunami hazard consist of building size, height, shape, regularity, orientation and accessibility. By modelling these parameters and their respective threshold values in a decision tree analysis, buildings in the study area were successfully classified into 4 classes: class A, B, C and VE. Class A is regarded as the most vulnerable and class VE is regarded as the least vulnerable building and dedicated as potential tsunami vertical evacuation shelter.

An object-based image analysis (OBIA) was chosen for the remote sensing based building vulnerability assessment. OBIA technique provides capability to incorporate all important spatial parameters that is not provided by pixel-based image analysis. Sophisticated rule-sets were developed for the building vulnerability classification and the transferability of the approach could be successfully shown by applying the methodology to Cilacap and to Padang city.. The classification rule-set was developed as a rule-based semantic network presented in chronological procedural steps as the representation of knowledge.

To achieve high-quality segmentation results, image pan-sharpening and filtering were applied as pre-processing steps before image segmentation. Adaptive Local Sigma and Morphological Opening image filtering were applied and adapted for the purpose of optimized building edge detection analysis. Feature analysis and selection played a central role in the process of image classification.

One important results of this research in respect to tsunami evacuation modelling is the identification of buildings that are potentially suitable for vertical evacuation. This information has been applied successfully for tsunami evacuation modelling in Cilacap city. Tsunami evacuation modelling was developed by incorporating the positions of the VE buildings resulted from this study. In the case of Cilacap city, vertical evacuation targets are very important because horizontal evacuation target points are located far away from the centre of the city. Tsunami evacuation modelling has been developed for Cilacap city and its surrounding area. The modelling method comprises three parts: 1) determination of evacuation target point distribution derived from a building vulnerability map, a tsunami hazard zone map and elevation data, 2) evacuation modelling and 3) evacuation plan optimization by taking into account local planning policies.

The results of this research reveal that class A buildings cover the biggest portion of area in Cilacap City (63 percent), followed by class C (28 percent), class VE (6 percent) and class B (3 percent). This information indicates that Cilacap City is very vulnerable to tsunami hazard. This information is very important for disaster management,

especially in managing disaster risk reduction and vertical evacuation planning. Since class A and class B are expected to be collapsed or severely damaged if earthquake and tsunami hits the land, preventive measures can be carried out for the purpose of disaster risk reduction, especially for people living in such the most vulnerable buildings. Furthermore, the number, location and capacity of class VE buildings provide vital information for a tsunami vertical evacuation planning as a strategic measure for tsunami risk reduction.

In referring to the research objectives and research questions given in the introduction chapter, this research has met the research objectives and answered the research questions by the following achievements:

- This research demonstrated the capability of the integrative remote sensing, GIS and in-situ survey approaches in vulnerability assessment of buildings to tsunami hazard
- This research revealed relevant information from very high resolution satellite image for the purpose of vulnerability analysis
- Potentially affected buildings by tsunami hazard are well recognized by classifying buildings into class A and B.
- Potential locations for vertical evacuation are well recognized by classifying buildings into class VE
- The building vulnerability assessment method developed for Cilacap City has been successfully transferred to other area (Padang City)
- The result of building vulnerability assessment has been applied in the development of tsunami vertical evacuation modelling.

REFERENCES

- Alkema, D. 2007. Simulating Floods: On the Application of a 2D-Hydrolic Model for Flood Hazard and Risk Assessment. Ph.D. Thesis. International Institute for Geo-information Science and Earth Observation (ITC). Enschede, The Netherlands.
- Anderson, M.B. 1995. Vulnerability to Disaster and Sustainable Development: A General Framework for Assessing Vulnerability. in: Munasinghe, M., Clarke, C. (Eds.). Disaster Prevention for Sustainable Development: Economic and Policy Issues. The International Bank for Reconstruction and Development. Washington, D.C. U.S.A. pp. 41-56.
- Augusti, G., Ciampoli, M., Giovenale, P. 2001. Seismic vulnerability of monumental buildings. *Structural Safety*, 23 (6), 252-274.
- Baatz, M.; Schäpe, A. (2000): Multiresolution Segmentation – an optimization approach for high quality multi-scale image segmentation. In Strobl, J. et al. (Hrsg.): *Angewandte Geographische Informationsverarbeitung XII*. Wichmann, S.12-23.
- BAKORNAS PBP. 2006. Laporan Perkembangan Penanganan Bencana Gempa Bumi dan Tsunami di Jawa Barat, Jawa Tengah dan D.I. Jogjakarta, 1 Agustus 2006.
- Bappenas, 2005. Indonesia: Preliminary Damage and Loss Assessment, The December 26, 2004 Natural Disaster. A Technical Report prepared by Bappenas and The International Donor Community. Jakarta.
- Benz, U.C., Hofmann, P., Willhauck, G., Lingenfelder, I., Heynen, M., 2004. Multiresolution, object-oriented fuzzy analysis of remote sensing data for GIS-ready information. *ISPRS Journal of Photogrammetry and Remote Sensing* 58 (3-4), 239-258.
- Birkmann, J. (Editor) 2006. *Measuring Vulnerability to Hazards of Natural Origin-Towards Disaster- Resilient Societies*. UNU press, Tokyo.
- Birkmann, J. and Wisner, B., 2005. *Measuring the Un-measurable - The challenge of Vulnerability*, Tokyo.
- Birkmann, J., Fernando, N. and Hettige, S. (2007): *Rapid Vulnerability Assessment in SriLanka*. Publication Series of UNU-EHS 7. Bonn, Germany. p.84
- Bitelli, G., Camassi, R., Gusella, L., Mognol, A. 2004. Image change detection on urban area: The earthquake case. Unpublished paper.

- Budiarjo, A. (2006). Evacuation Shelter Building Planning for Tsunami Prone Area, a Case Study of Meulaboh City, Indonesia. Master Thesis. International Institute for Geo-information Science and Earth Observation (ITC). Enschede, The Netherlands.
- Blaschke, T., Strobl, J. 2001. What's wrong with pixels? Some recent developments interfacing remote sensing and GIS. *GIS Journal*, 6, 12-17.
- Blaschke, T., Lang, S., Lorup, E., Strobl, J., Zeil, P., 2000. Object-oriented image processing in an integrated GIS/remote sensing environment and perspectives for environmental applications. In: Cremers, A., Greve, K. (Eds.). *Environmental Information for Planning, Politics and the Public*, 2. Metropolis Verlag, Marburg, pp. 555-570.
- Blaschke, T. 2009. Object -based image analysis for remote sensing. *ISPRS Journal of Photogrammetry and Remote Sensing*.
- Bogardi, J.J. 2006. Measuring Vulnerability to Natural Hazards: Introduction. In: Birkmann, J. (Editor) 2006. *Measuring Vulnerability to Hazards of Natural Origin- Towards Disaster- Resilient Societies*. UNU press, Tokyo.
- Bogardi, J. and Birkmann, J., 2004. Vulnerability Assessment: The First Step Towards Sustainable Risk Reduction. In: D. Malzahn and T. Plapp (Editor), *Disasters and Society - From Hazard Assessment to Risk Reduction*, Berlin, p.82.
- Bou-Rabee, F. and Van Marcke, E. 2001. Seismic vulnerability of Kuwait and other Arabian Gulf Countries: Information base and research needs. *Soil Dynamics and Earthquake Engineering*, 21, 181-186.
- Brooks, N. (2003). *Vulnerability, risk and adaptation: A conceptual framework*. Tyndall Center for Climate Change Research, Norwich. Working Paper No.38.
- Büchle, B., Kreibich, H., Kron, A., Thielen, A., Ihringer, J., Oberle, P., Merz, B. Nestmann, F. 2006. Flood-risk mapping: Contributions towards an enhanced assessment of extreme events and associated risks. 2006. *Natural Hazards and Earth System Sciences*, 6, 485-503.
- Bunting, P.J., Lucas, R.M., 2006. The delineation of tree crowns in Australian mixed species forests using hyperspectral Compact Airborne Spectrographic Imager (CASI) data. *Remote Sensing of Environment* , 101, 230_248.
- Burnett, C., Blaschke, T., 2003. A multi-scale segmentation/object relationship modelling methodology for landscape analysis. *Ecological Modelling*, 168 (3) , 233_249.

- Cabinet Office. 2005. Tsunami Mitigation Guidelines for Evacuation Building, Review Committee on Tsunami Mitigation Guidelines for Evacuation Buildings, Directorate General for Disaster Management. Japan.
- Caliskan S, Taubenböck H, Hinz S and Roth A. 2006. Earthquake vulnerability indicators and vulnerability assessment using remote sensing, Istanbul. 1st EARSeL Workshop of the SIG Urban Remote Sensing Humboldt-Universität zu Berlin.
- Cannon, T., Twigg, J., Rowell, J. 2004. Social Vulnerability, Sustainable Livelihoods and Disasters. Report to DFID Conflict and Humanitarian Assistance Department (CHAD) and sustainable livelihoods support office. University of Greenwich.
- Cardona, O.D., 2001. Estimation Holística del Riesgo Sísmico. Utilizando Sistemas Dinámicos Complejos, Technical University of Catalonia, Barcelona.
- Cardona, O.D. 2004. "The Need for Rethinking the Concepts of Vulnerability and Risk from a Holistic Perspective: A Necessary Review and Criticism for Effective Risk Management". In Bankoff G., G. Frerks and D. Hilhorst, eds, Mapping Vulnerability: Disasters, Development and People, London: Earthscan, Chapter 3.
- Cardona, O. D. 2005. Indicators of Disaster Risk and Risk Management - Program for Latin America and the Caribbean. Inter-American Development Bank Sustainable Development Department. p.53.
- Chambers, R., 1989. Vulnerability, coping and policy. IDS Bulletin, 20, 1-7.
- Christine, S., Markus, M. 2006. Classification of Collapsed Buildings for Fast Damage and Loss Assessment. Bulletin of Earthquake Engineering, 4, 177-192.
- Chubey, M.S., Franklin, S.E., Wulder, M.A., 2006. Object-based analysis of IKONOS-2 imagery for extraction of forest inventory parameters. Photogrammetric Engineering & Remote Sensing, 72 (4), 383_394.
- Clark, G. E., Moser, S. C., Ratick, S. J., Dow, K., Meyer, W. B., Emani, S., Jin, W., Kasperson, J. X., Kasperson, R. E., Schwarz, H. E. 1998. Assessing the Vulnerability of Coastal Communities to Extreme Storms: The Case of Revere, MA., USA. Mitigation and Adaptation Strategies for Global Change, 3, 59-82.
- Coburn, A.W., R.J.S. Spence and A. Pomonis. 1994. Vulnerability and Risk Assessment. Cambridge Architectural Research Limited. The Oast House, Malting Lane, Cambridge, United Kingdom. p.40.
- Conchedda, G., Durieux, L., Mayaux, P., 2008. An object-based method for mapping and change analysis in mangrove ecosystems. ISPRS Journal of Photogrammetry & Remote Sensing 63 (5), 578-589.

- Congalton, R.G. 1991. A review of assessing the accuracy of classifications of remotely sensed data. *Remote Sensing of Environment*, 37, 35-46
- Dall'Osso, F., Gonella, M., Gabbianelli, G., Withycombe, G., Dominey-Howes, D. 2009. A revised (PTVA) model for assessing the vulnerability of buildings to tsunami damage. *Natural Hazards and Earth System Sciences* 9, 1557-1565.
- Definiens. 2007. Definiens Developer 7 Reference Book. Definiens A.G. Muenchen. Germany. Dokument Version. 7.0.2.936. pp. 122-124
- De Kok, R. Wever, T. Fockelmann, R. 2003. Analysis of urban structure and development applying procedures for automatic mapping of large area data. *International Archives of Photogrammetry and Remote Sensing, Remote sensing and spatial information sciences*, 36, 41-46.
- Desclée, B., Bogaert, P., Defourny, P. 2006. Forest change detection by statistical object-based method. *Remote Sensing of Environment*, 102, 1–11
- DFID, 1999. Sustainable Rural Livelihoods: What contribution can we make, Department for International Development (DFID), London.
- Dominey-Howes, D. Papathoma, M. 2007. Validating a Tsunami Vulnerability Assessment Model (the PTVA Model) using field data from the 2004 Indian Ocean tsunami. *Natural Hazards*, 40, 113-136.
- Dorren, L.K., Maier, B., Seijmonsbergen, A.C., 2003. Improved Landsat-based forest mapping in steep mountainous terrain using object-based classification. *Forest Ecology and Management* 183 (1_3), 31_46.
- Downing, T., Soussan, J., Barthelemy, O., Bharwani, S., Hinkel, J., Ionescu, C., Klein, R. J. T., Mata, L. J., Matin, N., Moss, S., Purkey, D., Ziervogel, G. 2005. Integrating social vulnerability into water management. Stockholm Environment Institute. NeWater Working Paper No. 5.
- Durieux, L., Lagabrielle, E., Nelson, A., 2008. A method for monitoring building construction in urban sprawl areas using object-based analysis of Spot 5 images and existing GIS data. *ISPRS Journal of Photogrammetry and Remote Sensing* 63 (4), 399-408
- Dutta, D. and Serker, N.H.M.K. 2004. Urban building Inventory for Bangkok City with very high-resolution remote sensing data. *Seisan-Kenkyu*, 56 (3), 203-206
- Duveiller, G., Defourny, P., Desclée, B., Mayaux P. 2008. Deforestation in Central Africa: Estimates at regional, national and landscape levels by advanced processing

- of systematically-distributed Landsat extracts. *Remote Sensing of Environment*, 112, 1969–1981
- Du Y. 2008. Verification of Tsunami Reconstruction Projects by Object-Oriented Building Extraction from High Resolution Satellite Imagery. Master of Science Thesis. International Institute for Geo-information Science and Earth Observation (ITC). Enschede, The Netherlands.
- Dwyer, A., Zoppou, C., Nielsen, O., Day, S., Roberts, S. 2004. Quantifying Social Vulnerability: A methodology for identifying those at risk to natural hazards. *Geoscience Australia Record* 2004/14.
- EEA. 2004. Impacts of Europe's changing climate - An indicator-based assessment. EEA Report for European Environment Agency, Copenhagen, No 2/2004
- EEA. 2005. Vulnerability and Adaptation to Climate Change in Europe. EEA Technical report for European Environment Agency. Copenhagen.
- Ehlers, M., Gaehler, M., Janowsky, R. 2003. Automated analysis of ultra high resolution remote sensing data for biotope type mapping: new possibilities and challenges. *ISPRS Journal of Photogrammetry & Remote Sensing*, 57, 315– 326
- Eliason, Eric M. and McEwen, Alfred S., "Adaptive Box Filters for removal of random noise from digital images," *Photogrammetric Engineering & Remote Sensing*, April, 1990, 56, 4, p. 453.
- El-Raey M. 1997. Vulnerability assessment of the coastal zone of the Nile delta of Egypt, to the impacts of sea level rise. *Ocean & Coastal Management*, 37 (1), 29-40.
- Evgueni, A., Kulikov, Rabinovich, A.B, Thomson, R.E. 2005. Estimation of tsunami risk for the coasts of Peru and Northern Chile. *Natural Hazards*, 35, 185-209.
- Fernandez, V.B. 2009. Geo-information for Measuring Vulnerability to Earthquakes: a Fitness for Use Approach. Ph.D. Thesis. International Institute for Geo-information Science and Earth Observation (ITC). Enschede, The Netherlands.
- Fischer, T., Alvarez, M., De la Lliera, J.C., Riddel, R. 2002. An integrated model for earthquake risk assessment of buildings. *Engineering Structures*, 24, 979-998
- Forte, F., Strobl, R.O., Pennetta, L. 2006. A methodology using GIS, aerial photos and remote sensing for loss estimation and flood vulnerability analysis in the Supersano-Ruffano-Nociglia Graben, southern Italy. *Environmental Geology*, 50 , 581-594.

- Freeman, P., Warner, K. 2001. Vulnerability of Infrastructure to Climate Variability: How Does this Affect Infrastructure Lending Policies? World Bank, Disaster Management Facility, ProVention Consortium. Washington
- Füssel, H. M. 2005. Vulnerability in Climate Change Research: A Comprehensive Conceptual Framework. Breslauer Symposium, University of California.
- Füssel, H. M., Klein, R. J. T. 2006. Climate change vulnerability assessments: An evolution of conceptual thinking. *Climatic Change*, 75, 301-329.
- Gallopín, G. C. 2006. Linkages between vulnerability, resilience, and adaptive capacity. *Global Environmental Change*, 16, 293.
- Gambolati, G. And Teatini, P. 2002. GIS simulations of the inundation risk in the coastal lowlands of the Northern Adriatic Sea. *Mathematical and Computer Modelling*, 35, 963-972.
- Giakoumakis, M. N., Gitas, I. Z., San-Miguel, J. 2002. Object-oriented classification modelling for fuel type mapping in the Mediterranean, using LANDSAT TM and IKONOS imagery-preliminary results. *Forest Fire Research & Wildland Fire Safety*, 1-13.
- Gomez, A., Gaspar, J.L., Queiroz, G. 2006. Seismic vulnerability of dwellings at Sete Cidades Volcano. *Natural Hazards and Earth System Sciences*, 6, 41–48
- Grothmann, T. And Reusswig, F. 2006. People at risk of flooding: Why some residents take precautionary action while others do not. *Natural Hazards*, 38 , 101–120
- Grünthal, G., Musson, R., Schwarz, J., Stucchi, M. 1998. European Macroseismic Scale 1998. *Cahiers du Centre Européen de Geodynamique et de Seismologie*, Volume 15, Luxembourg 1998.
- Grünthal, G., Thieken, A.H., Schwarz, J., Radtke, K.S., Smolka, A., Merz, B. 2006. Comparative risk assessments for the city of Cologne – Storms, Floods, Earthquakes. *Natural Hazards*, 38 (1), 21-44.
- GTZ-IS. (2007). Capacity Building in Local Communities. German- Indonesian Cooperation for Tsunami Early Warning System. Newsletter No.4, p.12, October-December 2007. Eschborn, Germany.
- Guarin, G.P. 2008. Integrating Local Knowledge into GIS-Based Flood Risk Assessment: The Case of Triangulo and Mabolo Communities in Naga City – The Philippines. Ph.D. Thesis. International Institute for Geo-information Science and Earth Observation (ITC). Enschede, The Netherlands.

- Günter, B.H. 2005. Threats Challenges, Vulnerabilities and Risk in Environmental and Human Security. SOURCE - Publication Series of UNU-EHS. Bonn
- Gwilliam, J., Fedeski, M., Lindley, S., Theuray, N., Handley, J. 2006. Methods for assessing risk from climate hazards in urban areas. *Municipal Engineer*, 159 , 245-255.
- Hahn, H. 2003. Indicators and Other Instruments for Local Risk Management for Communities and Local Governments. Document prepared as part of the documents related to the Project: Local Risk Management for Communities and Local Governments. The German Technical Cooperation Agency, GTZ, for IADB.
- Haralick, Sternberg, and Zhuang, 1987. Image analysis using mathematical morphology, *IEEE Transactions on Pattern Analysis and Machine Intelligence*, PAMI-9 (4), 532-550.
- Heiko, A., Thielen, A.H., Merz, B. Bloesch, G. 2006. A probabilistic modelling system for assessing flood risks. *Natural Hazards*, 38, 79–100.
- Herold, M., Roberts, D.A., Gardner, M. E., Dennison, P. E. 2004. Spectrometry for urban area remote sensing--development and analysis of a spectral library from 350 to 2400 nm. *Remote Sensing of Environment*, 91 (3-4). 304-319.
- Hofmann, P. 2001. Detecting buildings and roads from IKONOS data using additional elevation information. *GIS Journal*, 6 (1), 28-33.
- Hwang, G. Francis, M., Choi, B.H., Singh, J.P., Stein, S. Borrero, J., Thio, H.K., Ratti, C., Bergado, D. 2005. Mitigating the Risk from Coastal Hazards: Strategies & Concepts for Recovery from the December 26, 2004 Tsunami. Report for Hawaii Department of Land and Natural Resources. Hawaii.
- ISDR, 2004. Living with Risk: A global review of disaster reduction initiatives UNISDR, Geneva.
- ISDR. 2009. Global Assessment Report on Disaster Risk Reduction. United Nations, Geneva, Switzerland.
- Johansen, K., Coops, NC., Gergel, S.E., Stange Y. 2007. Application of high spatial resolution satellite imagery for riparian and forest ecosystem classification. *Remote Sensing of Environment*, 110, 29–44
- Kamagata, N.; Akamatsu, Y.; Mori, M.; Li, Y.Q.; Hoshino, Y.; Hara, K. (2005). Comparison of pixel-based and object-based classifications of high resolution satellite data in urban fringe areas. Scientific Paper of eCognition Resources. URL:

- <http://www.ecognition.com/document/comparison-pixel-based-and-object-based-classifications-high-resolution-satellite-data-urba>. Accessed on June 2009.
- Kaplan, M., Renaud, F.G., Luchters, G. 2009. Vulnerability assessment and protective effects of coastal vegetation during the 2004 Tsunami in Sri Lanka. *Natural Hazards and Earth Sciences*, 9, 1479-1494.
- Kappos, A.J., Styliandis, K.C., Pitolakis, K. 1998. Development of seismic risk scenarios based on a hybrid method of vulnerability assessment. *Natural Hazards*, 17, 177-192.
- Karantoni, F. V., Bouckovalas, G. 1997. Description and analysis of building damage due to Pyrgos, Greece earthquake. *Soil Dynamics and Earthquake Engineering*, 16 (2), 141-150.
- Kasperson, R. 2001. Vulnerability and Global Environmental Change. Newsletter of the International Human Dimensions Programme on Global Environmental Change. Nr. 2. Stockholm.
- Khanduri, A. C., Morrow, G. C. 2003. Vulnerability of buildings to windstorms and insurance loss estimation. *Journal of Wind Engineering and Industrial Aerodynamics*, 91, 455-467.
- Kim, H. O., Lakes, T., Kenneweg, H., Kleinschmit, B. 2005. Different approaches for urban habitat type mapping - The case study of Berlin and Seoul. TU Berlin, Institute for Landscape Architecture and Environmental Planning.
- Kim, H. O., Lakes, T., Kenneweg, H., Kleinschmit, B. 2005. High resolution satellite imagery for analysis of sealing in the Metropolitan area Seoul. *Göttinger Geographische Abhandlungen*, 131, 281-286.
- Kouchi, K., Yamazaki, F. 2005. Damage Detection Based on Object-based Segmentation and Classification from High-resolution Satellite Images for the 2003 Boumerdes, Algeria Earthquake.
- Kong, C., Xu, K., Wu, C. 2006. Classification and extraction of urban land-use information from high-resolution image based on object multi-features. *Journal of China University of Geosciences*, 17 (2), 151-157
- Kropp, J.P., Block, A., Reusswig, F., Zickfeld, K., Schellhuber, H.J. 2006. Semiquantitative assessment of regional climate vulnerability: The North-Rhine Westphalia Study. *Climatic Change*, 76, 265-290.
- Laliberte, A.S., Rango, A., Havstad, K.M., Paris, J.F., Beck, R.F., McNeely, R., Gonzalez, A.L., 2004. Object-oriented image analysis for mapping shrub encroachment from

- 1937 to 2003 in southern New Mexico. *Remote Sensing of Environment* 93 (1-2), 198-210.
- Lamadrid, U.G.R. 2002. *Seismic Hazard and Vulnerability Assessment in Turrialba, Costa Rica*. Master Thesis. International Institute for Geo-information Science and Earth Observation (ITC). Enschede, The Netherlands.
- Lang, K. 2002. *Seismic Vulnerability of Existing Buildings*. Ph.D. Thesis. Swiss Federal Institute of Technology Zurich. Zurich. Swiss.
- Lang, K., Bachmann, H. 2004. On the seismic vulnerability of existing buildings: a case study of the City of Basel. *Earthquake Spectra*, 20 (1), 43-46.
- Langanke, T., Burnett, C., Lang S. 2007. Assessing the mire conservation status of a raised bog site in Salzburg using object-based monitoring and structural analysis *Landscape and Urban Planning*, 79, 160–169
- Lewinski, S. 2006. Applying fused multispectral and panchromatic data of Landsat ETM+ to object oriented classification. *Proceedings of the 26th EARSeL Symposium, New Developments and Challenges in Remote Sensing*. Warsaw, Poland.
- Liu, Z. J., Wang, J., Liu, W. P. 2005. Building extraction from high resolution imagery based on multi-scale object oriented classification and probabilistic Hough transform. *IEEE Journal*, 4.
- Madariaga, R. 2002. The El Salvador earthquakes of January and February 2001: Context, characteristics and Implications for Seismic Risk. *Soil Dynamics and Earthquake Engineering* 22, 389-418.
- Mallinis, G., Koutsias, N., Tsakiri-Strati, M., Karteris, M., 2008. Object-based classification using Quickbird imagery for delineating forest vegetation polygons in a Mediterranean test site. *ISPRS Journal of Photogrammetry and Remote Sensing* 63 (2), 237-250.
- Mann P.S. 1995. *Introductory Statistics*, 2nd Edition. Wiley.
- Marangoz M.A, Karakis, S., Oruc, M., Sahin, H., Sefercik, U.G., Topan, H., Buyuksalih, G., 2006. 3D Cultural heritage documentation of Safranbolu test site using high resolution satellite imagery. 1st EARSeL Workshop of the SIG Urban Remote Sensing. Berlin.
- Marpu, P.R., Niemeyer, I., Nussbaum, S., Gloaguen, R. 2008. A Procedure for Automatic Object-Based Classification. in: Blaschke, T., Lang, S. (Eds.). *Object-*

- Based Image Analysis: Spatial Concepts for Knowledge-Driven Remote Sensing Applications. Springer-Verlag Berlin Heidelberg, pp. 169-184
- Mathieu, R., Freeman, C., Aryal, J., 2007. Mapping private gardens in urban areas using object-oriented techniques and very high-resolution satellite imagery. *Landscape and Urban Planning*, 81 (3), 179_192.
- Meinel, G., Neubert, M., Reder, J., 2001. Pixelorientierte versus segmentorientierte Klassifikation von IKONOS-Satellitenbilddaten - ein Methodenvergleich. *Photogrammetrie, Fernerkundung, Geoinformation* 5 (3), 157-170.
- Metzger, J. M. 2005. European Vulnerability to Global Change a Spatially Explicit and Quantitative Assessment. Ph.D. Thesis. International Institute for Geo-information Science and Earth Observation (ITC). Enschede, The Netherlands.
- Michel, G.W., Becker, M., Angermann, D., Reigber, C., and Reinhart, E. (2000). Crustal Motion in E- and SE-Asia from GPS Measurements. Bundesamt für Kartographie und Geodäsie, Frankfurt am Main and Geoforschungszentrum, Postdam. Germany.
- Minciardi, R., Sacile, R., Taramasso, A.C., Trasforini, E., Traverso, S. 2006. Modeling the vulnerability of complex territorial systems: An application to hydrological risk. *Environmental Modelling & Software*, 21, 949-960.
- Montoya, L. 2003. Geo-data acquisition through mobile GIS and digital video: an urban disaster management perspective. *Environmental Modelling & Software*, 18 (10), 869-876.
- Mueller M, Segl K, Heiden U, and Kauffman H. 2006. Potential of high-resolution satellite data in the context of vulnerability of buildings. *Natural Hazards*, 38, 247-258.
- Münich JC, Taubenböck H, Stempniewski L, Dech S, Roth A. 2006. Remote sensing and engineering: An Interdisciplinary approach to assess vulnerability in urban areas. First European Conference on Earthquake Engineering and Seismology. Geneva. Paper : 1412.
- Myint, S.W., May Yuan, Randall S.C., Chandra, P.G. 2008. Comparison of remote sensing image processing techniques to identify tornado damage areas from Landsat TM Data. *Sensors*, 8, 1128-1156.
- Nussbaum, S., Niemeyer, I., Canty, M.J. 2007. Feature recognition in the context of automated object-oriented analysis of remote sensing data monitoring the Iranian nuclear sites. *Proc. of SPIE*, 5988 598805, 1-9.

- O'Brien, K., Leichenko, R., Kelkar, U., Venema, H., Aandahl, G., Tompkins, H., Javed, A., Bhadwal, S., Barg, S. Nygaard, L., West, J. 2004. Mapping vulnerability to multiple stressors: climate change and globalization in India. *Global Environmental Change Part A*, 14, 303-313.
- Oliveira, C. S.; Roca, A.; Goula, X. (2006): *Assessing and Managing Earthquake Risk: Geo-scientific and Engineering Knowledge for Earthquake Risk Mitigation: developments, tools, techniques*. Berlin: Springer. p. 543
- Papathoma, M., Howes, D.D., Zong, Y. and Smith D. 2003. Assessing tsunami vulnerability, an example from Heracleio, Crete. *European Geosciences Union. Natural Hazards and Earth System Sciences*, 3, 377-389.
- Papathoma, M and Howes, D.D. 2003. Tsunami vulnerability assessment and its implications for coastal hazard analysis and disaster management planning, Gulf of Corinth, Greece. *Natural Hazards and Earth System Sciences* 3, 733-747.
- Pareschi, M.T., Cavarra, L., Favalli, M., Giannini, F., Meriggi, A. 2000. GIS and volcanic risk management. *Natural Hazards*, 21, 361-379.
- Paris, R., 2008. Tsunami Hazard Map of Indonesia. GEOLAB UMR 6042 CNRS - UBP – MSH Clermont-Ferrand, France. URL : [http://www.reliefweb.int/rw/fullMaps_Wd.nsf/luFullMap/644323E1F93E4387C125761C004A5D7C/\\$File/map.pdf?OpenElement](http://www.reliefweb.int/rw/fullMaps_Wd.nsf/luFullMap/644323E1F93E4387C125761C004A5D7C/$File/map.pdf?OpenElement). Accessed on July, 2009.
- Park, N.-W., Chi, K.-H., 2008. Quantitative assessment of landslide susceptibility using high-resolution remote sensing data and a generalized additive model. *International Journal of Remote Sensing* 29 (1), 247-264
- Peduzzi, P., Dao, H., and Herold, C. 2005. Mapping disastrous natural hazards using global datasets. *Natural hazards* (2005) 35:266. Springer.
- Pelling, M., Uitto, J.I. 2001. Small island developing states: natural disaster vulnerability and global change. *Environmental Hazards*, 3, 49-62.
- Petrazzuoli, S. M., Zuccaro, G. 2004. Structural resistance of reinforced concrete buildings under pyroclastic flows: a study of the Vesuvian area. *Journal of Volcanology and Geothermal Research*, 133, 353-367.
- Polsky, C., Schröter, D., Patt, A., Gaffin, S., Martello, M.L., Neff, R., Pulsipher, A., Selin, H. 2003. *Assessing Vulnerabilities to the Effects of Global Change: An Eight-Step Approach*. Research and Assessment Systems for Sustainability Program Discussion Paper 2003-05. Cambridge, MA: Environment and Natural Resources Program, Belfer Center for Science and International Affairs, Kennedy School of Government, Harvard University.

- Pomonis, A., Spence, R., Baxter, P. 1999. Risk assessment of residential buildings for an eruption of Furnas Volcano, Sao Miguel, the Azores. *Journal of Volcanology and Geothermal Research*, 93, 107-131.
- Radoux, J., Defourny, P., 2007. A quantitative assessment of boundaries in automated forest stand delineation using very high resolution imagery. *Remote Sensing of Environment* 110 (4), 468-475.
- Rashed T and Weeks J. 2003. Exploring the Spatial Association Between Measures from Satellite Imagery and Patterns of Urban Vulnerability to Earthquake Hazards. University of Redlands. USA
- Roca, A.; Goula, X.; Susagna, T.; Cavez, J.; Gonzalez, M. (2006): A simplified method for vulnerability assessment of dwelling buildings and estimation of damage scenarios in Catalonia, Spain. *Bulletin of Earthquake Engineering* 4(2), 141-158.
- Sato, H., Murakami, H., Kozuki, Y., Yamamoto, N. 2003. Study on a simplified method of tsunami risk assessment. *Natural Hazards*, 29, 325-340.
- Schiewe, J. 2002. Segmentation of high-resolution remotely sensed data concepts, applications and problems. Symposium on Geospatial Theory, Processing and Applications. Ottawa. p.1
- Schlerf, M. 2000. Flood Hazard Modelling and Risk Assessment of Tieler-Culembergerwaard Polder, Netherlands. Final Assignment. International Institute for Geo-information Science and Earth Observation (ITC). Enschede, The Netherlands.
- Schmidt-Thome, P., Greiving, S., Kallio, H., Fleischhauer, M. and Jarva, J. 2006. Economic Risk Maps of Flood and Earthquakes for European Regions. *Quaternary International*, pp. 103-112
- Schröter, D., Colin, P., Anthony, G.P. 2005. Assessing vulnerabilities to the effects of global change: an eight step approach. *Mitigation and Adaptation Strategies for Global Change*, 10, 573-595.
- Smith, D.I. 1994. Flood damage estimation – A review of urban stage -damage curves and loss functions. *Water SA*, 20(3), 231-238.
- Spence, R. J. S., Baxter, P. J., Zuccaro, G. 2004. Building vulnerability and human casualty estimation for a pyroclastic flow: a model and its application to Vesuvius. *Journal of Volcanology and Geothermal Research*, 133, 321-343.
- Stewart, M. G. 2003. Cyclone damage and temporal changes to building vulnerability and economic risks for residential construction. *Journal of Wind Engineering and Industrial Aerodynamics*, 91, 671-691.

- Stow, D., Hamada, Y., Coulter, L., Anguelova, Z., 2008. Monitoring shrubland habitat changes through object-based change identification with airborne multispectral imagery. *Remote Sensing of Environment*, 112 (3), 1051_1061
- Strunz, G., Post, J. and Zoßeder, K. (2008). Draft Guidelines Hazard Assessment. UNESCO IOC ICG WG 3: Risk Assessment, Version 0.5. Unpublished Working paper, German Remote Sensing Data Centre (DFD). Germany.
- Sutherst, R. W., Maywald, G. F., Russell, B. L. 2000. Estimating vulnerability under global change: modular modelling of pests. *Agriculture, Ecosystems and Environment*, 82, 303-319.
- Taubenböck, H.; Esch, T.; Roth, A. (2006): An urban classification approach based on an object-oriented analysis of high resolution satellite imagery for a spatial structuring within urban areas. First Workshop of the EARSeL Special Interest Group on Urban Remote Sensing "Challenges and Solutions".
- Taubenböck, H.; Habermeyer, M.; Roth, A.; Dech, S. 2006. Automated allocation of highly structured urban areas in homogeneous zones from remote sensing data by Savitzky-Golay Filtering and Curve Sketching. *IEEE Geoscience and Remote Sensing Letters*, 3 (4), 532-536.
- Taubenböck, H.; Kemper, T.; Roth, A.; Voigt, S. (2006): Assessing vulnerability in Istanbul: An example to support disaster management with remote sensing at ZKI-DLR. In: Technical University Berlin [Hrsg.]: Fifth International Symposium - German Turkish Joint Geodetic Days, S. 1 - 9, Fifth International Symposium - German Turkish Joint Geodetic Days, Berlin.
- Teo, T. A., Chen, L. C. 2004. Object-based building detection from LIDAR data and high resolution satellite imagery. 25th ACRS, Chiang Mai, Thailand.
- Theodoridis, S. and Koutroumbas, K. 2006. *Pattern Recognition*, Third Edition. Academic Press. San Diego, USA, p. 227.
- The World Bank. 2006. *Hazards of Nature, Risks to Development. An IEG Evaluation of World Bank Assistance for Natural Disasters*. Washington, D.C.
- Thomalla, F., Downing, T., Spanger-Siegfried, E., Han, G. and Rockstrom, J., 2006. Reducing hazard vulnerability: towards a common approach between disaster risk reduction and climate adaptation. *Disasters*, 30, 39-48.
- Turker, M., Sumer, E., 2008. Building-based damage detection due to earthquake using the watershed segmentation of the post-event aerial images. *International Journal of Remote Sensing* 29 (11), 3073_3089.

- Turner, B. L., Kasperson, R. E., Matson, P. A., McCarthy, J. J., Corell, R. W., Christensen, L., Eckley, N., Kasperson, J. X., Luers, A., Martello, M. L. 2003. A framework for vulnerability analysis in sustainability science. *Proceedings of the National Academy of Sciences*, 100, 8074-8079.
- Turner, B. L., Matson, P. A., McCarthy, J. J., Corell, R. W., Christensen, L., Eckley, N., Hovelsrud-Broda, G. K., Kasperson, J. X., Kasperson, R. E., Luers, A. 2003. Illustrating the coupled human-environment system for vulnerability analysis: Three case studies. *Proceedings of the National Academy of Sciences*, 100, 8080-8085.
- Thywissen, K. 2006. *Components of Risk, A Comparative Glossary*. United Nations University, Institute for Environment and Human Security. Bonn
- USGS. (2006): Magnitude 7.7-South of Java, Indonesia. Earthquake Hazard Program. URL: <http://earthquake.usgs.gov/eqcenter/eqinthenews/2006/usqgaf/#details>. Accessed on June 2009.
- UNCHS. 2001. *Assessment of Vulnerability to Flood Impacts and Damages*. Report of the Flood Hazard Research Centre.
- UNEP. 2009. GIS Analysis NGI Cartography UNEP/GRID-Europe. URL: [http://www.reliefweb.int/rw/fullMaps_Wd.nsf/luFullMap/644323E1F93E4387C125761C004A5D7C/\\$File/map.pdf?OpenElement](http://www.reliefweb.int/rw/fullMaps_Wd.nsf/luFullMap/644323E1F93E4387C125761C004A5D7C/$File/map.pdf?OpenElement). Accessed on June 2009
- Van der Sande, C. J., de Jong, S. M., de Roo, A. P. J. 2003. A segmentation and classification approach of IKONOS-2 imagery for land cover mapping to assist flood risk and flood damage assessment. *International Journal of Applied Earth Observation and Geoinformation*, 4, 217-229.
- Van Westen, C.J., Montoya, L. Boerboom, L. 2002. Multi-hazard risk assessment using GIS in urban areas: A case study for the city of Turrialba, Costa Rica. *The Regional Workshop on Best Practices in Disaster Mitigation*. Bali. Indonesia.
- Villagran de-Leon, J.C. (2006). *Vulnerability: A Conceptual and Methodological Review*, United Nations University, Institute for Environment and Human Security. Bonn
- Vu, T. T., Matsuoka, M., Yamazaki, F. 2006. Object-based image analysis for mapping tsunami-affected areas. *Proceedings. 8th U.S. National Conference on Earthquake Engineering*, April 18-22, 2006. San Francisco, California

- Walker, J.S., Blaschke, T., 2008. Object-based land cover classification for the Phoenix metropolitan area: Optimization vs. transportability. *International Journal of Remote Sensing* 29 (7), 2021-2040.
- Walter, V., 2004. Object-based classification of remote sensing data for change detection. *ISPRS Journal of Photogrammetry and Remote Sensing*, 58 (3_4), 225_238.
- Wei, W., Chen, X., Ma, A. 2005. Object-oriented information extraction and application in high-resolution remote sensing image. *Geoscience and Remote Sensing Symposium*.
- Wen, Z.P., Hu, Y.X., Chau, K.T. 2002. Site effect on vulnerability of high-rise shear wall buildings under near and far field earthquakes. *Soil Dynamics and Earthquake Engineering*, 22, 1175–1182.
- Whiteside, T., Ahmad, W. 2005. A comparison of object-oriented and pixel-based classification methods for mapping land cover in northern Australia. *Proceedings of SSC2005 Spatial intelligence, innovation and praxis: The national biennial Conference of the Spatial Sciences Institute*, 0-9581366-2-9, 1255–1231
- Wiseman, G., Kort, J., Walker, D., 2009. Quantification of shelterbelt characteristics using high-resolution imagery. *Agriculture, Ecosystems and Environment* 131 (1-2), 111-117.
- Wisner, B., P. Blaikie, T. Cannon and I. Davis. 2005. *At Risk: Natural Hazards, People's Vulnerability and Disasters*. Routledge. London. p.11.
- Wood, N. and Stein, D. 2001. A GIS-based vulnerability assessment of Pacific northwest ports and harbors to tsunami hazards. *ITS 2001 Proceedings, Session 1, Number 1-13*.
- Wu, J., David, J.L., 2002. A spatially explicit hierarchical approach to modeling complex ecological systems: Theory and applications. *Ecological Modelling* 153 (1-2), 7-26.
- Xiaoxia, S., Jixian, Z., Zhengjun, L., Caof, M. 2004. An object-oriented classification method on high resolution satellite data. *25th ACRS*. Chiang Mai, Thailand.
- Yan, G., Mas, J.F., Maathuis, B.H.P., Xiangmin, Z., Van Dijk, P.M. 2006. Comparison of pixel-based and object-oriented image classification approaches-a case study in a coal fire area, Wuda, Inner Mongolia, China. *International Journal of Remote Sensing*, 27 (18, 20), 4039–4055

- Yohe, G., Tol, R. S. J. 2002. Indicators for social and economic coping capacity-moving toward a working definition of adaptive capacity. *Global Environmental Change*, 12, 25-40.
- Zebisch, M., Grothmann, T., Schröter, D., Hasse, C., Fritsch, U., Cramer, W. 2005. Vulnerability mapping of climate sensitive systems in Germany. AVEC Summer School.
- Zhang, Q., Pavlic G., Chen W., Fraser, R., Leblanc, S., Cihlar J. 2005. A semi-automatic segmentation procedure for feature extraction in remotely sensed imagery. *Computers & Geosciences*, 31, 289–296.
- Zhang, Y. 2002. Problems in the fusion of commercial high-resolution satellite as well as Landsat 7 images and initial solutions. *ISPRS*, 34 (4), “Geospatial Theory, Processing and Applications”. Ottawa.

9 Building Foundation material :

River stone Well Foot
 Pile

10 Describe Type of Wood and its quality

DIMENSION OF MAIN STRUCTURE

- 11 Foundation :** **cm x** **cm**
- 12 Sloof :** **mm x** **mm**
 Main reinforcement diameter : **mm**
 Stirrups
 diameter : **mm**
 length : **mm**
- 13 Columns :** 100 **mm x** 100 **mm**
 Main reinforcement diameter : **mm**
 Stirrups
 Diameter : **mm**
 length : **mm**
- 14 Ring Balk**
 Main reinforcement diameter : **mm**
 Stirrups
 Diameter : **mm**
 length : **mm**
- 15 Truss Beam**
 Available Not Available

CONNECTION BETWEEN STRUCTURAL ELEMENTS

- 16 Column reinforcement anchored to foundation :** **cm**
- 17 Wall with anchorage to the column :**
 Diameter / length : **mm /** **mm**
 Not Available
- 18 Truss roof anchorage to the column :**
 Available Not Available

19 Truss Roof Brace

Available Not Available

20 Is there enough development length for the reinforcement ?

Yes No

21 Roof Material

zinc Color :

Concrete Color :

Metal Color :

Asbestos Color :

Ceramic Color :

Clay Color :

..... Color :

22 Building damage due to previous earthquake

Hard Moderate Minor

No damage

23 Developer

Contractor Skilled Labour

Self Built

24 Built Year (Building Age) :

25 Building Class of Susceptibility

Class A (high susceptible, 1 m wave height)

Class B (medium susceptible, 3 m wave height)

Class C (Low susceptible, 5 m wave height)

VE (Vertical Evacuation, 10 m wave height)

26 Photo Code :

Identification :

Perspective (exterior) :

Column / Wall :

Sloof / Foundation :

Roof :

Interior :

27 Width of main road : m

28 Building Accessibility

All directions

3 directions

2 directions

1 directions

29 Number of staff (all sectors, except residential)

morning

afternoon

night

30 Is the building accessible at any time ? (all sectors, except residential)

Yes

No

31 Ability to receive warning (all sectors)

Yes

No

32 availability of a tsunami evacuation plan (all sectors, except residential)

Yes

No

33 amount of people (number) (all sectors)

During the day

During the night

34 Space for temporary evacuation (all sectors)

Available

Not Available

In storey (if available)

1

2

3

4

5

35 Accessibility to space for temporary evacuation :
(regarding to Question 26)

Stairs Elevator

36 Occupation rate (in percent)
(if sector = hotel)

Jan Feb Mar Apr Mai Jun

Jul Aug Sep Oct Nov Dec

FORM OF HAMMER TEST

TEST : **REBOUND SCHMIDT HAMMER**
No. Building : _____

No.Hammer :
Address :

No	Structure Element	Hammer Value										Avg.
		1	2	3	4	5	6	7	8	9	10	
1	Sloof											
2	Column											
3	Ring Balk											

CURRICULUM VITAE

Personal

Name	Sumaryono
Date of Birth	09 September 1967
Place of Birth	Demak, Inonesia
Sex	Male
Nationality	Indonesian
Degree	Master of Science in Information Technology for Natural Resources Management
Email	sumaryono99@gmail.com Sumaryono.Sumaryono@dlr.de

Formal Education

2007-2010	Ph.D-studies, Ludwig-Maximilians-Universität (LMU) Munich –Germany
2006	Degree in Master of Science in Information Technology for Natural Resources Management, Bogor Agricultural University (IPB), Bogor, Indonesia
2006	Master Thesis: Spatial Decision Support System for Land Use Planning
1986-1991	Faculty of Forestry, Bogor Agricultural University (IPB), Bogor, Indonesia
1983-1986	Senior High School, SMA Negeri 1 Demak, Indonesia
1980-1983	Junior High School, SMP Negeri 2 Demak, Indonesia
1974-1980	Elementary School, SD Negeri Bintoro 6 Demak, Indonesia

Training Course

1994	Research Methodology, Bogor, Indonesia
1995	Application of Radar for Coastal and Marine Management, EC-ASEAN, Kuala Lumpur, Malaysia
1997	Fundamental of Remote Sensing Technology, RESTEC, Tokyo, Japan

1998	Remote Sensing Technology for Coastal and Marine Monitoring, Bogor, Indonesia
1998	GIS for Environmental Management, Oslo, Norway
2001	Wetland Ecosystem and Biodiversity, JICA, Hokkaido, Japan
2004	Remote Sensing and GIS for Development, AIT, Bangkok, Thailand
2007	Risk and Vulnerability, Bonn, Germany
2009	Remote Sensing Techniques, Freiberg, Germany
2009	Peer Reviewed Publishing, DLR Oberpfaffenhofen, Germany

**Current
Appointment**

1992-present	Remote Sensing and GIS Researcher of Bakosurtanal (National Coordinating Agency for Surveys and Mapping)
--------------	--